CAPRAM2.3: A Chemical Aqueous Phase Radical Mechanism for Tropospheric Chemistry

H. HERRMANN [1], B. ERVENS [1], H.-W. JACOBI [2][*], R. WOLKE [1],
P. NOWACKI [1] and R. ZELLNER [2]

[1]*Institut für Troposphärenforschung, Permoserstr. 15, 04303 Leipzig, Germany*
[2]*Institut für Physikalische und Theoretische Chemie, FB 8, Universität GH Essen,
Universitätsstr. 5, 45117 Essen, Germany*

Abstract. A Chemical Aqueous Phase Radical Mechanism (CAPRAM) for modelling tropospheric multiphase chemistry is described. CAPRAM contains (1) a detailed treatment of the oxidation of organic compounds with one and two carbon atoms, (2) an explicit description of S(IV)-oxidation by radicals and iron(III), as well as by peroxides and ozone, (3) the reactions of OH, NO_3, Cl_2^-, Br_2^-, and CO_3^- radicals, as well as reactions of the transition metal ions (TMI) iron, manganese and copper. A modelling study using a simple box model was performed for three different tropospheric conditions (marine, rural and urban) using CAPRAM coupled to the RADM2-mechanism (Stockwell *et al.*, 1990) for liquid and gas phase chemistry, respectively. In the main calculations the droplets are assumed as monodispersed with a radius of 1 μm and a liquid water content of 0.3 g m^{-3}. In the coupled mechanism the phase transfer of 34 substances is treated by the resistance model of Schwartz (1989). Results are presented for the concentration levels of the radicals in both phases under variation of cloud duration and droplet radius.

The effects of the multiphase processes are shown in the loss fluxes of the radicals OH, NO_3 and HO_2 into the cloud droplets. From calculations under urban conditions considering gas phase chemistry only the OH maximum concentration level is found to be $5.5 \cdot 10^6$ cm^{-3}. In the presence of the aqueous phase ($r = 1$ μm, LWC = 0.3 g m^{-3}) the phase transfer constitutes the most important sink (58%) reducing the OH level to $1.0 \cdot 10^6$ cm^{-3}. The significance of the phase transfer during night time is more important for the NO_3 radical (90%). Its concentration level in the gas phase ($1.9 \cdot 10^9$ cm^{-3}) is reduced to $1.4 \cdot 10^6$ cm^{-3} with liquid water present. In the case of the HO_2 radical the phase transfer from the gas phase is nearly the only sink (99.8%). The concentration levels calculated in the absence and presence of the liquid phase again differ by three orders of magnitude, $6 \cdot 10^8$ cm^{-3} and $4.9 \cdot 10^5$ cm^{-3}, respectively. Effects of smaller duration of cloud occurrence and of droplet size variation are assessed.

Furthermore, in the present study a detailed description of a radical oxidation chain for sulfur is presented. The most important reaction chain is the oxidation of (hydrogen) sulphite by OH and the subsequent conversion of SO_3^- to SO_5^- followed by the interaction with TMI (notably Fe^{2+}) and chloride to produce sulphate. After 36 h of simulation ($[H_2O_2]_0 = 1$ ppb; $[SO_2]_0 = 10$ ppb) the direct oxidation pathway from sulfur(IV) by H_2O_2 and ozone contributes only to 8% ($2.9 \cdot 10^{-10}$ M s^{-1}) of the total loss flux of S(IV) ($3.7 \cdot 10^{-9}$ M s^{-1}).

Key words: multiphase, modelling, radical chemistry, cloud chemistry.

Introduction

Several modelling studies have shown that the concentration levels of important trace gases in the troposphere are influenced by reactions in the tropospheric aqueous phase (e.g., Jacob, 1986; Lelieveld and Crutzen, 1991; Möller and Mauersberger, 1995; Sander and Crutzen, 1996; Walcek *et al.*, 1997). Among the most important processes are the oxidation of sulphur(IV), the possible reaction of ozone with superoxide radical anions and the oxidation of organic compounds. Several aspects of these processes, however, are still unresolved.

S(IV) compounds may be oxidised in the aqueous phase via different pathways. The reactions of bisulfite and sulphite with oxidants such as ozone, hydrogen peroxide, methyl hydroperoxide and peroxy acetic acid are well established. The rate constants for the peroxide reactions show a strong pH-dependence (Lind *et al.*, 1987; Möller *et al.*, 1992). An additional alternative is the free radical driven chain mechanism, in which several oxysulfur radicals act as intermediates (Deister and Warneck, 1990). This chain mechanism may be initiated by reactions of HSO_3^-, SO_3^{2-} with radicals and radical anions or by the iron-catalysed oxidation of S(IV)-compounds (see e.g., Ziajka *et al.*, 1994).

The influence of aqueous droplets on the gas phase concentration of ozone is still controversial. Using a box model, Lelieveld and Crutzen (1991) calculated reduced ozone concentrations when cloud chemistry was included. This effect was mainly due to lower production rates in the gas phase. In addition, the decomposition of ozone in the liquid phase via the reaction with O_2^- was identified as a direct loss process. Dentener and Crutzen (1993) also obtained comparable results in a consideration of aerosol chemistry, however, with smaller ozone reductions. More recently, Matthijsen *et al.* (1995) showed that the destruction of ozone within the droplets is further reduced, when transition metal ions (TMI) such as iron and copper are included in the aqueous phase chemical mechanism, because HO_2/O_2^--concentrations are strongly decreased in reactions with dissolved TMI.

The most recent aqueous phase chemical models usually consider the oxidation of organic compounds with only one carbon atom. In the present study organic compounds with two carbon atoms, including alcohols, aldehydes and acids are treated. Each oxidation step can be initiated by radicals or radical anions such as OH, NO_3, SO_4^-, Cl_2^-, Br_2^- or CO_3^-, which are all considered here.

Radicals and radical anions may be key species for the chemical transformation of tropospheric constituents in the aqueous phase. Not only the highly reactive radicals OH and NO_3, which may be transferred from the gas phase into the aqueous phase, but also the radical anions SO_4^-, Cl_2^-, Br_2^- and CO_3^- may be involved in each of the above mentioned processes. Recently, new kinetic data for reactions of the radical anions with many constituents of the tropospheric liquid phase in diluted solutions became available (for overviews see Warneck (1996), Zellner and Herrmann (1995), and Herrmann and Zellner (1998), and references therein). The chemical aqueous phase radical mechanism (CAPRAM) described here includes an

extended reaction scheme with production and destruction reactions for the radical anions. Moreover, the reaction rates for the mechanism are updated using existing and, where available, revised kinetic data.

In this study, CAPRAM has been coupled to the RADM2-mechanism for gas phase chemistry (Stockwell *et al.*, 1990). The partitioning of 34 species, which exist in both phases, is described by the resistance model of Schwartz (1986). A simple box model has been used to calculate concentrations of radicals and radical anions in the tropospheric aqueous phase. The numerical solution procedure was developed by Wolke and Knoth (1996). Results are presented for two different photochemical regimes applied to continental and marine summer conditions, leading to three different chemical cases (urban, rural and marine).

1. Chemical Mechanism Description

1.1. GAS PHASE CHEMISTRY

The gas phase chemistry described here uses the RADM2 mechanism with about 160 reactions (Stockwell *et al.*, 1990). Apart from an established reaction scheme for the chemistry of nitrogen and sulphur oxides, it includes a description of the oxidation of methane, ethane, ethene, isoprene, formaldehyde, glyoxal, methylglyoxal and formic acid. Higher organic compounds are lumped together in 12 classes. A detailed treatment of reactions between peroxyl radicals is also included.

The species $CH_3OH_{(g)}$, $CH_3CH_2OH_{(g)}$, $NH_{3(g)}$, $HCl_{(g)}$ have been added to the gas phase mechanism. Due to the comparatively low reaction rates, these species have lifetimes of several days. In the presence of a liquid phase they may be rapidly depleted by gas-droplet transfer. Moreover, during the simulations their gas phase concentrations only change by phase transfer. Furthermore, the species $Cl_{2(g)}$ and $Br_{2(g)}$, have been included in the mechanism, because evaporation of these halogens, produced in the liquid phase, represents a possible source of these compounds in the gas phase.

1.2. AQUEOUS PHASE CHEMISTRY

1.2.1. *General*

The mechanism in its basic form, i.e., CAPRAM2.3, includes 70 aqueous-phase species, 34 equilibria for compounds which are stable in both gas and aqueous phase, 6 photolysis reactions, and 199 aqueous-phase reactions. It covers 31 acid-base and metal-complex equilibria. Compared to the mechanism of Jacob (1986) and Jacob *et al.* (1989) the main differences are (1) a revision of the rate constants using more recent literature data and results from our own laboratory studies, (2) addition of the chemistry of ethanol, acetaldehyde and acetic acid, (3) extensive description of production and destruction of radicals and radical anions such as SO_4^-, NO_3, Cl_2^-, Br_2^-, and CO_3^- and (4) the inclusion of C_1 and C_2-peroxyl radical

chemistry. In the present form of CAPRAM, halogen chemistry in the aqueous phase is terminated with the hydrolysis reactions of Cl_2 (R166) and Br_2 (R180), in which HOCl and HOBr are produced.

Although extensive laboratory studies of reactions of small radicals in the aqueous phase have been performed in recent years, many reaction rate constants are still unknown. In the present study, such rate coefficients are estimated based on other kinetic data and reactivity relationships (Zellner and Herrmann, 1995; Herrmann *et al.*, 1995; Herrmann and Zellner, 1998).

To describe the phase transfer of a compound, knowledge of the gas phase diffusion coefficient D_g, the mass accommodation coefficient α and the Henry constant K_H is necessary. For most of the Henry constants recent literature data are available. These data usually show only slight differences compared to the values used by Jacob (1986) and Jacob *et al.* (1989). One important exception, however, is the Henry constant of NO_3 which has recently been shown to be several orders of magnitude smaller than estimated by Jacob (Rudich *et al.*, 1996; Thomas *et al.*, 1998). Furthermore, phase equilibria for peroxyl radicals with 2 carbon atoms, ethylperoxyl radicals (ETHP) and acetylperoxyl radicals (ACO$_3$), and molecular halogens Cl_2 and Br_2 are added to the mechanism. Because no literature data are available for the Henry constants of C_2-peroxyl radicals, these have been estimated as being equal to that of the methylperoxyl radical (MO_2).

Only few gas phase diffusion coefficients are available in the literature from direct measurements. However, those which are not available may be estimated using the method of Fuller (1989). A similar situation applies to mass accommodation coefficients. Some of the values have been measured as a function of temperature (cf. Davidovits *et al.* (1995) for an overview). For organic species, however, such data are not available. These parameters are derived here from existing data for similar species. For example, the mass accommodation coefficients of the peroxyl radicals are taken to be equal to those of the corresponding hydroperoxides or alcohols. Jacob (1986) estimated a value of $\alpha = 0.1$ for many species. It is now evident that by the use of this value the phase transfer is generally overestimated, because all organic species have mass accommodation coefficients in the order of 10^{-2} or 10^{-3}.

The description of chemical equilibria is included in the reaction scheme applied here with their respective equilibrium constants. For a given equilibrium the obtained fluxes in either direction may not be identical when a product is removed from the equilibrium by consecutive reactions. This is the case for the dissociation reactions of species like HCl, HNO_3 or Cl_2^-, where the dissociation products may undergo further reactions. The formation of dibromide radical anions, Br_2^-, is considered by the equilibrium (E24). Their reactivity is somewhat smaller than that of Cl_2^- and due to a slower decomposition reaction, the equilibrium is shifted towards the Br_2^- species. The dissociation of H_2O_2 is neglected because with the pK_s value of 11.8 it may be calculated that under typical tropospheric conditions

the dissociation does not significantly influence the total hydrogen peroxide content (Jacob, 1986).

For the reactions included in the CAPRAM mechanism only a few temperature dependencies are available in the literature. In the case of missing experimental data for such dependencies, calculations were performed here with rate constants for T = 298 K. The estimation of E_a from the rate constant at 298 K and a typical value for the preexponential factor in the Arrhenius expression of $A = 1 \cdot 10^{10}$ M^{-1} s^{-1} (Jacob, 1986) is not satisfactory, since several temperature dependent studies (e.g., Zellner *et al.*, 1996) show that the assumption of a constant preexponential factor is not valid, especially when different radicals and reaction mechanisms are considered. The calculations in the present study have been performed for a mean air parcel temperature of T = 288.15 K using the available data mentioned as above. No diurnal variation of the temperature is considered.

Photolysis rates at ground level are calculated using a solar radiation flux model (after Röth, 1992). This model includes the effects of absorption due to ozone and nitrogen dioxide and scattering by aerosols. Therefore, the photolysis rates are different for continental and marine conditions. For all regimes a surface albedo of 0.1 is assumed. The calculations are performed for a geographical latitude of 51° N. Further input parameters, e.g., wavelength-dependent absorption coefficients and quantum yields for aqueous phase species, are taken from Ruggaber *et al.*, 1997.

1.2.2. *Radical Sources*

Within CAPRAM the radicals and radical anions OH, NO$_3$ and SO$_4^-$, Cl$_2^-$, Br$_2^-$, and CO$_3^-$ are considered in solution. In principle, there are two possible sources for these species in the liquid phase. They are either formed *in situ* by photolysis reactions (P1) to (P6) of dissolved precursor compounds or they result from reactions of these radicals within the droplet. These reactions mainly generate OH radicals. Only in reaction (P4), by photolysis of the iron(III)-sulfato-complex [Fe(SO$_4$)]$^+$, sulphate radical anions are produced. The other source for OH and NO$_3$ is direct transfer from the gas phase into aqueous droplets. Depending on the conditions in the tropospheric liquid phase, the so-called primary radicals, OH and NO$_3$ are converted into secondary radical anions with different reactivity patterns.

For example, Cl$_2^-$ is generated in reactions of chloride with SO$_4^-$ (R153) and NO$_3$ (R154). The reaction of chloride with OH produces ClOH$^-$ (E26) as an intermediate (Jacobi *et al.*, 1998). In a subsequent step, the reaction of ClOH$^-$ with H$^+$ generates Cl atoms (E27). Hence, the formation of Cl is pH-dependent and as a consequence no Cl is produced at higher pH-values. The equilibrium (E28) between chlorine atoms and chloride leads to Cl$_2^-$. A similar sequence applies the reaction of Br$^-$ with OH (E29–E31). Because of their relatively low one-electron reduction potential in aqueous solution, OH radicals cannot oxidise sulphate anions (SO$_4^{2-}$) directly. The SO$_4^-$ radical, therefore, mainly results from the H-atom abstraction reaction (R86) of OH with HSO$_4^-$.

1.2.3. *Radical Sinks*

Possible destruction reactions for each radical or radical anion with inorganic and organic compounds are included in the scheme. Reactants are inorganic anions like OH^-, NO_2^-, HSO_3^- and SO_3^{2-} and transition metal ions in their reduced forms (e.g., Fe^{2+}, Mn^{2+}, and Cu^+). Reactions with peroxides such as H_2O_2 and CH_3OOH and with the hydroperoxyl radical (HO_2) and the superoxide radical anion (O_2^-) are also considered. Several of the rate constants for the reactions of NO_3, Cl_2^- and Br_2^- with these species have recently been determined in our laboratory (Jacobi *et al.*, 1996; Zellner *et al.*, 1996; Jacobi, 1996; Reese, 1997). However, rate constants for various reactions of the carbonate radical anion are still not known. These data are estimated on the basis of comparable reactions and correlations between rate constants and thermodynamic data. For example, for the electron transfer reaction of NO_3, rate coefficients k_{NO_3} are correlated with the reactant's redox potential E_0 (Exner, 1992):

$$\log(k_{NO_3}) = (10 \pm 1) - (1.5 \pm 0.6) \cdot (E_0/V). \tag{1}$$

With a redox potential of $E_0(CO_3^{2-}/CO_3^-) = 1.59V$ (Huie and Neta, 1991), a rate constant of $k_{R185} = 4.1 \cdot 10^7$ M^{-1} s^{-1} can be estimated. Similar procedures have been applied for other reactions where rate constants are not directly available.

Many of the rate coefficients of the reactions of the HO_2/O_2^- couple with other radicals are not available. For a given radical usually only one reaction with either HO_2 or O_2^- has been investigated. In these cases, the available rate constant was used for both reactions.

1.2.4. *Chemistry of Organic Species*

An almost complete oxidation chain is included for organic compounds with one or two carbon atoms. The most reduced compounds are the alcohols CH_3OH and C_2H_5OH. They can be oxidised by reactions with radicals or radical anions. The rate-determining step is an H-atom abstraction forming the α-hydroxy-alkyl radicals, CH_2OH or CH_3CHOH, respectively. Subsequently reactions with molecular oxygen lead to the formation of the respective peroxyl radicals which rearrange to yield HO_2 as well as formaldehyde and acetaldehyde (Graedel and Weschler, 1981). In aqueous solution, the aldehydes considered here are in equilibrium (E21, E22) with the corresponding diols, $H_2C(OH)_2$ and $CH_3CH(OH)_2$.

Formaldehyde forms a complex with S(IV) compounds (Hoffmann *et al.*, 1986). The formation of hydroxymethanesulfonate ($CH_2(OH)SO_3^-$, HMS^-) is described by Reaction (E22) and (E23). The adduct formation between acetaldehyde and S(IV) species is not considered, because the equilibrium constant is four orders of magnitude lower than in the case of formaldehyde (Betterton *et al.*, 1988). HMS^- may only be oxidised by free radicals and radical anions, since the reactions with H_2O_2 and O_3 are extremely slow (Hoigné *et al.*, 1985; Kok *et al.*, 1986). On the other hand the attack of OH radicals to HMS^- is a very fast reaction (R60). In

a pulse radiolysis study, Barlow *et al.* (1997) present evidence for the formation of formic acid, because the reaction follows an H-atom abstraction leading to the oxidation of the organic part of HMS^-. However, NO_3, SO_4^-, Cl_2^- and Br_2^- probably react with HMS^- by electron-transfer (R61–R64) (Buxton, 1994; Herrmann *et al.*, 1996; Jacobi, 1996). In these cases, the unstable hydroxymethanesulfonate radical dissociates very rapidly leading to the formation of different species including formaldehyde and SO_3^-/SO_5^- radical anions.

Hydrated formaldehyde and acetaldehyde are further oxidised. H-atom abstraction in the reactions with radicals or radical anions (R115–R127) and elimination of HO_2 in reaction with O_2 (Bothe *et al.*, 1983) leads to the formation of formic and acetic acid, respectively. The acids are in equilibrium with their anions formate (E15) and acetate (E16), depending on pH. Both forms may again be oxidised by radicals (R128–R149) via H-atom-abstraction and electron transfer reactions, respectively. In the case of formic acid, CO_2 is formed in both reaction pathways. The oxidation of acetic acid is more complex. In electron transfer reactions of the acetate anion, the radical CH_3CO_2 is formed which immediately eliminates CO_2 (Norman *et al.*, 1970; Gilbert *et al.*, 1972; Chawla and Fessenden, 1975). The resulting methyl radical adds O_2 yielding methyl peroxyl radicals (MO_2). The reactions of the undissociated acetic acid, however, and also the reaction (R140) of acetate with OH follow an H-atom abstraction mechanism from the methyl group. By reaction with oxygen the carboxyl-methylperoxyl radical O_2CH_2COOH is formed. Both radicals, $CH_3C(O)O_2$ and O_2CH_2COOH, are lumped into the substance group ACO_3 throughout the present study because it is defined in CAPRAM as C_2 peroxyl radicals containing a carbonyl group.

1.2.5. *S(IV) Oxidation*

At higher pH the reaction with ozone dominates the S(IV) oxidation, whereas in acidic solutions the oxidation due to peroxides, and especially H_2O_2, is more important (Hoffmann, 1986; Jacob, 1986). Moreover, several laboratory studies have shown that the oxidation of bisulfite and sulphite is catalysed by transition metal ions (for a review see, e.g., Brandt and van Eldik, 1995). Ziajka *et al.* (1994) proposed a free radical chain mechanism in which several oxysulfur radicals (SO_3^-, SO_4^-, SO_5^-) act as intermediates. A similar mechanism was suggested in the EUROTRAC/HALIPP research activity (Warneck, 1996 and references therein). The oxidation may also be initiated by the thermal decomposition of iron(III)-sulfito-complexes, which decay into Fe^{2+} and SO_3^- radicals (R71). SO_3^- radical anions are also produced in reactions of dissolved S(IV) compounds with free radicals and radical anions such as OH, NO_3, Cl_2^-, Br_2^- and CO_3^- (R33, R34, R43, R164, R165, R178, R179, R196 and R197). For the various reaction steps in the free radical chain mechanism, Ziajka *et al.* (1994) reported rate constants obtained by computer simulations. In contrast, we used available literature data from direct investigations of most of the elementary reactions. An additional and potentially

significant oxidation path for S(IV) is the reaction with HNO_4 (R59) which is transferred from the gas phase (Amels *et al.*, 1996).

2. Model Description

A box model is applied in this study. It forms part of a multidimensional multiphase modelling system (MCCM, Nowacki (1998)) which allows the numerical treatment of the extremely stiff multiphase differential equation systems. Numerically, the multiphase system is treated following the recommendations of Wolke and Knoth (1996). In this context a Gear type solver, taken from the LSODE package is applied (Hindmarch *et al.*, 1980). The box model used allows explicit analysis of both individual reactions as well as individual species. Flexible interchange of chemical reactions or reaction blocks is made possible with a preprocessing tool supplied with the box model. Emissions, deposition, ad- and convectional fluxes are disregarded throughout the present study.

A liquid water content (LWC) of 0.3 g m^{-3} has been assumed. Moreover, all droplets are assumed to have the same composition and radius of 1 μm, so that about $7 \cdot 10^4$ droplets per cm^{-3} exist. Hence, this small droplet radius was chosen to demonstrate the maximal effect of the aqueous phase to tropospheric chemistry. Because the total air volume occupied by cloud droplets is small (10^{-7}–10^{-6}), no significant gradients in the concentrations of gas phase species over the scale of the air parcel are produced due to transfer between gas and aqueous phase. Therefore it may be assumed that gas phase species are well mixed within the air parcel.

In addition to concentration levels the production and loss fluxes of some substances at given times are determined, so that major sources and sinks for a given species could be identified.

2.1. MODEL CONDITIONS

Three different regimes are considered for the simulations: marine, average continental (rural) and polluted continental. They are initialised in the model runs by different concentrations of stable compounds. The initial concentrations for the gas phase are mainly taken from Zimmermann and Poppe (1996) and Graedel and Weschler (1981). The distribution of NMHC (non methane hydrocarbons) and NO_x into several classes of the RADM2 mechanism is taken from Zimmermann and Poppe, 1996. The initial concentration of NO_x for the marine case (40 ppt) was taken from Rohrer and Brüning, 1992, because the value by Zimmermann and Poppe seems to be too low (0.3 ppt). However, the species $CH_3OH_{(g)}$, $CH_3CH_2OH_{(g)}$, $NH_{3(g)}$, $HCl_{(g)}$, $Cl_{2(g)}$ and $Br_{2(g)}$ are added to the gas phase mechanism as a result of possible evaporation from the liquid phase. The input concentrations for the gas and aqueous phase species are summarised in Table I. It has to be noted that these values are initial state conditions which change

Table I. Initial concentrations for three scenarios under polluted continental (urban), unpolluted continental (remote) and marine conditions (gas phase species in ppb, aqueous phase species in M)

Species	Urban	Remote	Marine
Gas phase species:			
NO_2	4.5 [a]	1.5 [a]	0.4 [k]
HNO_3	1 [b]	0.3 [b]	0.15 [g]
CH_4	1700 [a]	1700 [a]	1700 [a]
H_2O_2	1 [d]	0.001 [a]	0.001 [a]
H_2	2000 [a]	2000 [a]	2000 [a]
CO	200 [a]	150 [a]	140 [a]
O_3	90 [a]	60 [a]	40 [a]
HCl	6 [a]	0.7 [b]	0.5 [g]
NH_3	25 [a]	1.5 [b]	0.05 [g]
CO_2	$5 \cdot 10^5$ [a]	$3.3 \cdot 10^5$ [b]	$3.3 \cdot 10^5$ [b]
SO_2	10 [h]	1 [h]	0.1 [h]
HCHO	0.1 [a]	0.1 [a]	0.01 [a]
C_2H_6	2 [a]	1.5 [a]	1 [a]
HC3: Alkanes with OH rate constant between $2.7 \cdot 10^{-13}$ and $3.4 \cdot 10^{-12}$ cm^3 s^{-1} (298 K, 1 atm)	2 [a]	1 [a]	1 [a]
HC5: Alkanes with OH rate constant between $3.4 \cdot 10^{-12}$ and $6.8 \cdot 10^{-12}$ cm^3 s^{-1} (298 K, 1 atm)	1 [a]	0.5 [a]	0 [a]
HC8: Alkanes with OH rate constant greater than $6.8 \cdot 10^{-12}$ cm^3 s^{-1} (298 K, 1 atm)	0.1 [a]	0 [a]	0 [a]
C_2H_4	1 [a]	0.5 [a]	0.1 [a]
OLT: Terminal alkenes	0.1 [a]	0.1 [a]	0.1 [a]
Isoprene	0.1 [a]	0.1 [a]	0.1 [a]
TOL: Toluene and less reactive aromatics	0.1 [a]	0.01 [a]	0 [a]
CSL: Cresol and other OH-substituted aromatics	0.001 [a]	0.001 [a]	0 [a]
XYL: Xylene and more reactive aromatics	0.1 [a]	0.01 [a]	0 [a]
ALD: Acetaldehyde and higher aldehydes	0.1 [a]	0.1 [a]	0.01 [a]
Ketones	0.1 [a]	0.1 [a]	0.01 [a]
Glyoxal	0.1 [a]	0.1 [a]	0.01 [a]
Methylglyoxal	0.1 [a]	0.1 [a]	0.01 [a]
PAN	0.01 [a]	0.01 [a]	0.01 [a]
CH_3OOH	0.01 [a]	0.01 [a]	0.01 [a]
OP2: Higher organic peroxides	0.01 [a]	0.01 [a]	0.01 [a]
$CH_3C(O)OOH$	0.001 [a]	0.001 [a]	0.001 [a]
CH_3OH	5 [a]	2 [f]	0.8 [g]
EtOH	1 [c]	0.24 [f]	$2.4 \cdot 10^{-3}$ [h]
Aqueous phase species:			
$O_{2(aq)}$	$3 \cdot 10^{-4}$ [b]	$3 \cdot 10^{-4}$ [b]	$3 \cdot 10^{-4}$ [b]
OH^-	$3.16 \cdot 10^{-10}$ [b]	$3.16 \cdot 10^{-10}$ [b]	$1.6 \cdot 10^{-9}$ [b]
pH	4.5 [b]	4.5 [b]	5.2 [i]
Cl^-	$1 \cdot 10^{-4}$ [h]	$1 \cdot 10^{-4}$ [h]	$5.6 \cdot 10^{-4}$ [j]
Br^-	$3 \cdot 10^{-6}$ [h]	$3 \cdot 10^{-7}$ [h]	$1.8 \cdot 10^{-6}$ [j]

Table I. (Continued)

Species	Urban	Remote	Marine
Fe^{3+}	$5 \cdot 10^{-6}$ [d]	$5 \cdot 10^{-7}$ [d]	$5 \cdot 10^{-8}$ [d]
Mn^{3+}	$2.5 \cdot 10^{-7}$ [d]	$2.5 \cdot 10^{-8}$ [d]	$1 \cdot 10^{-9}$ [d]
Cu^{+}	$2.5 \cdot 10^{-7}$ [d]	$2.5 \cdot 10^{-8}$ [d]	$1 \cdot 10^{-9}$ [d]
HSO_4^{-}	$3 \cdot 10^{-7}$	$3 \cdot 10^{-7}$	$3 \cdot 10^{-8}$
SO_4^{2-}	$5.97 \cdot 10^{-5}$ [e]	$5.97 \cdot 10^{-5}$ [e]	$5.97 \cdot 10^{-6}$ [i]
Constant during the simulation time [ppb] or [M]:			
$H_2O_{(g)}$	$2 \cdot 10^{7}$	$3 \cdot 10^{7}$	$3 \cdot 10^{7}$
$O_{2(g)}$	$2 \cdot 10^{8}$	$2 \cdot 10^{8}$	$2 \cdot 10^{8}$
$N_{2(g)}$	$7.8 \cdot 10^{8}$	$7.8 \cdot 10^{8}$	$7.8 \cdot 10^{8}$
$H_2O_{(aq)}$	55.5	55.5	55.5

[a] Zimmermann and Poppe (1996); [b] Graedel and Weschler (1981); [c] Saxena and Hildemann (1996); [d] Matthijsen and Builtjes (1995); [e] Weschler *et al.* (1986); [f] Leibrock and Slemr (1996); [g] Jacob (1986); [h] estimated; [i] Chameides (1984); [j] Herrmann *et al.* (1996); [k] Rohrer and Brüning (1992).

during the simulation. Only the concentrations of $N_{2(g)}$, $O_{2(g)}$, $H_2O_{(g)}$ and $H_2O_{(aq)}$ are assumed as being constant.

2.2. PHASE TRANSFER

The transfer of molecules from the gas phase to the aqueous phase and vice versa is treated by the resistance model of Schwartz (1986). In this model gas phase diffusion, mass accommodation and the Henry's Law constants are considered. All parameters used are listed in Tables IIa, b. Liquid phase diffusion in the droplet is neglected here because the characteristic time for this process is in the order of $\tau = 10^{-3}$ s, whilst the characteristic times for aqueous phase chemical production and removal for most species are both much longer (Jacob, 1986). However, future applications considering chemistry within larger aqueous particles should consider solution phase diffusion. The mass transport from the gas phase is described as a first order loss rate constant, viz.:

$$k_t = \left(\frac{r^2}{3 \cdot D_g} + \frac{4 \cdot r}{3 \cdot \bar{c} \cdot \alpha} \right)^{-1} \tag{3}$$

D_g = gas phase diffusion coefficient [m^2 s^{-1}]

α = mass accommodation coefficient

r = droplet radius (1 μm)

$\bar{c}$ = molecular speed (=8 RT/πM)$^{1/2}$ [m s^{-1}]

M = molecular mass [kg mol^{-1}]

R = gas constant [J mol^{-1} K^{-1}]

Table IIa. Henry's law constants

Reaction no.	Species	K_{H298}, M atm^{-1}	ΔH_{298}, kJ mol^{-1}	References
H1	CO_2	$3.11 \cdot 10^{-2}$	–20.14	Chameides, 1984
H2	HCl	1.10	–16.8	Marsh and McElroy, 1985
H3	NH_3	60.7	–32.6	Clegg and Brimblecombe, 1990
H4	O_3	$1.14 \cdot 10^{-2}$	–19.1	Kosak-Channing and Helz, 1983
H5	HO_2	$9 \cdot 10^3$		Weinstein-Lloyd and Schwartz, 1991
H6	OH	25	–43.9	Kläning *et al.*, 1985
				National Bureau of Standards, 1971
H7	H_2O_2	$1.02 \cdot 10^5$	–52.7	Lind and Kok, 1994
H8	HNO_3	$2.1 \cdot 10^5$	–72.3	Lelieveld and Crutzen, 1991
H9	NO_3	0.6		Rudich *et al.*, 1996
H10	N_2O_5	1.4		[i]
H11	NO_2	$1.2 \cdot 10^{-2}$	–10.5	Schwartz and White, 1982
H12	HNO_2	49	–40.6	Park and Lee, 1988
H13	HO_2NO_2	$1 \cdot 10^5$ [d]		$K_{H13} = K_{H7}$
H14	SO_2	1.24	–27	Beilke and Gravenhorst, 1978
H15	HCHO [a]	$3.0 \cdot 10^3$	–60	Betterton and Hoffmann, 1988a
H16	CH_3OOH	6	–44.2	Lind and Kok, 1994
H17	$CH_3C(O)OOH$	$6.69 \cdot 10^2$	–49.0	Lind and Kok, 1994
H18	CH_3OH	$2.2 \cdot 10^2$	–44.8	Betterton, 1992
H19	C_2H_5OH	$1.9 \cdot 10^2$	–52.3	Betterton, 1992
H20	CH_3CHO [b]	11.4	–52	Betterton and Hoffmann, 1988a
H21	HCOOH	$5.53 \cdot 10^3$	–46.8	Khan and Brimblecombe, 1992
H22	CH_3COOH	$5.50 \cdot 10^3$	–49.0	Khan and Brimblecombe, 1992
H23	CH_3O_2	6	–46.9	Jacob, 1986
H24	ETHP [c]	6 [d]	–46.9 [d]	$K_{H24} = K_{H23}$
H25	Cl_2	$9.15 \cdot 10^{-2}$	–20.7	Wilhelm *et al.*, 1977
H26	Br_2	0.758	–31.6	Loomis, 1928
H27	H_2SO_4	$2.1 \cdot 10^5$		$K_{H27} = K_{H8}$
H28	CH_4	$1.46 \cdot 10^{-3}$		Mackay and Shan, 1981
H29	C_2H_6	$1.95 \cdot 10^{-3}$		Mackay and Shan, 1981
H30	C_2H_4	$4.55 \cdot 10^{-3}$		Mackay and Shan, 1981
H31	PAN [e]	5		Holdren *et al.*, 1984
H32	OP2 [f]	837		O'Sullivan *et al.*, 1996
H33	OL2P [g]	6		$K_{H33} = K_{H23}$
H34	ACO_3 [h]	669		$K_{H34} = K_{H17}$

[a] Equilibrium $HCHO_{(g)} \leftrightarrow CH_2(OH)_{2(aq)}$; [b] Equilibrium $CH_3CHO_{(g)} \leftrightarrow CH_3CH(OH)_{2(aq)}$; [c] Peroxy radical with 2 carbon atoms; [d] Estimated value; [e] Peroxy acetyl nitrate; [f] C_2-hydroperoxides; [g] Peroxy radicals of C_2H_4; [h] Acetyl peroxy radical; [i] Estimated $K_{H(N_2O_5)} = K_{H(N_2O_4)}$ (Schwartz and White, 1983).

Table IIb. Mass accommodation coefficients and gas phase diffusion coefficients

Reaction no.	Species	α	References	D_g $[10^5 \ m^2 \ s^{-1}]$	References
H1	CO_2	$2 \cdot 10^{-4}$	Estimated	1.55	McElroy, 1997
H2	HCl	0.064	Davidovits *et al.*, 1995	1.89	Marsh and McElroy, 1985
H3	NH_3	0.04	Bongartz, 1995	2.3	Ponche, 1993
H4	O_3	$5 \cdot 10^{-2}$	Mirabel, 1996	1.48	Schwartz, 1986
H5	HO_2	0.01	Hanson, 1992	1.04	Hanson, 1992
H6	OH	0.05	Estimated	1.53	Hanson, 1992
H7	H_2O_2	0.11	Davidovits *et al.*, 1995	1.46	McElroy, 1997
H8	HNO_3	0.054	Davidovits *et al.*, 1995	1.32	Kirchner, 1990
H9	NO_3	$4 \cdot 10^{-3}$	Kirchner, 1990 Rudich, 1996	1.00	Thomas, 1998
H10	N_2O_5	$3.7 \cdot 10^{-3}$	George *et al.*, 1994	1.10	Kirchner, 1990
H11	NO_2	$1.5 \cdot 10^{-3}$	Estimated	1.92	Ponche, 1993
H12	HNO_2	0.5	Bongartz, 1995	1.30	Kirchner, 1990
H13	HO_2NO_2	0.1	Jacob, 1986	1.30	Schweitzer, 1998
H14	SO_2	$3.5 \cdot 10^{-2}$	Tang and Lee, 1987 Gardner *et al.*, 1987	1.28	McElroy, 1997
H15	HCHO [a]	0.02	Estimated	1.64	Fuller, 1986 [a]
H16	CH_3OOH	$3.8 \cdot 10^{-3}$	Davidovits *et al.*, 1995	1.31	Fuller, 1986 [a]
H17	$CH_3C(O)OOH$	0.019	$\alpha_{17} = \alpha_{31}$	1.02	Fuller, 1986 [a]
H18	CH_3OH	$1.5 \cdot 10^{-2}$	Davidovits *et al.*, 1995	1.16	Schwartz, 1986
H19	C_2H_5OH	$8.2 \cdot 10^{-3}$	Davidovits *et al.*, 1995	0.95	Schwartz, 1986
H20	CH_3CHO [b]	0.03	Estimated	1.22	Fuller, 1986 [a]
H21	HCOOH	0.012	Davidovits *et al.*, 1995	1.53	Schwartz, 1986
H22	CH_3COOH	0.019	Davidovits *et al.*, 1995	1.24	Schwartz, 1986
H23	CH_3O_2	$3.8 \cdot 10^{-3}$	$\alpha_{23} = \alpha_{16}$	1.35	Fuller, 1986[a]
H24	ETHP [c]	$8.2 \cdot 10^{-3}$	Estimated	1.08	Fuller, 1986 [a]
H25	Cl_2	0.03	Estimated	1.28	Schwartz, 1986
H26	Br_2	0.03	Estimated	1.00	Schwartz, 1986
H27	H_2SO_4	0.07	Davidovits *et al.*, 1995	1.30	Schwartz, 1986
H28	CH_4	$5 \cdot 10^{-5}$	Estimated	1.41	Fuller, 1986 [a]
H29	C_2H_6	$1 \cdot 10^{-4}$	Estimated	0.95	Fuller, 1986 [a]
H30	C_2H_4	$1 \cdot 10^{-4}$	Estimated	1.01	Fuller, 1986 [a]
H31	PAN [e]	0.019	$\alpha_{31} = \alpha_{22}$	0.63	Fuller, 1986 [a]
H32	OP2 [f]	0.01	Estimated	0.76	Fuller, 1986 [a]
H33	OL2P [g]	$8.2 \cdot 10^{-3}$	$\alpha_{33} = \alpha_{24}$	0.82	Fuller, 1986 [a]
H34	ACO_3 [h]	0.019	$\alpha_{34} = \alpha_{22}$	1.0	Fuller, 1986 [a]

[a] These values are calculated after the method by Fuller (1986).

This expression shows that the transport depends on two resistances: The first term represents the resistance caused by gas phase diffusion, whereas the second term corresponds to the interfacial mass transport. The uptake of substances which are highly soluble and reactive such as OH, HO_2 and NO_3 is limited by gas phase diffusion. The uptake of nonreactive substances, which are transported from the gas into the aqueous phase on the other hand, is controlled by the Henry equilibrium. Values of the Henry constants K_{H298} at T = 298 K and the enthalpies of solution ΔH are summarised in Table IIa. The Henry constant $K_H(T)$ for the temperature T = 288.15 K can be calculated by equation:

$$K_H(T) = K_{H298} \cdot \exp\left(-\frac{\Delta H}{R} \cdot \left(\frac{1}{T} - \frac{1}{298\,K}\right)\right), \tag{4}$$

where ΔH is the enthalpy of dissolution.

In total, the phase transfer is described by the following equations (Schwartz, 1986):

$$\frac{d[X]_{aq}}{dt} = Q_{aq} - S_{aq} + \left(C_g \cdot k_t - \frac{[X]_{aq} \cdot k_t}{K_H}\right) \cdot \frac{1000}{RT}, \tag{5}$$

$$\frac{dC_g}{dt} = Q_g - S_g - \left(C_g \cdot LWC \cdot k_t - \frac{[X]_{aq} \cdot k_t}{K_H}\right) \cdot \frac{1000}{RT}, \tag{6}$$

$[X]_{aq}$ = aqueous phase concentration [mol l^{-1}],
Q_g = gas phase source rate [cm^{-3} s^{-1}],
C_g = gas phase particle density [cm^{-3}],
S_g = gas phase sink rate [cm^{-3} s^{-1}],
T = temperature [K],
LWC = liquid water content [–],
(fixed to 0.3 g m^{-3} = $3 \cdot 10^{-7}$ vol/vol),
Q_{aq} = aq. phase source reaction rate [mol l^{-1} s^{-1}],
S_{aq} = aq. phase sink reaction rate [mol l^{-1} s^{-1}],
K_H = Henry's Law constant [mol l^{-1} atm^{-1}],
k_t = gas phase transfer coefficient [s^{-1}],
R = gas constant.

Equation (5) describes a flux budget for which the transfer of a given species into the droplets is counted positive. The third term in this equation represents the total transfer flux from the gas phase, expressed by the product of the gas phase transfer coefficient and the partial pressure of a given reagent. To convert this flux into gas phase units it is divided by RT. The fourth term describes a flux in the opposite direction, i.e., from the droplet phase to the gas phase. The combination of

the third and fourth term is the approach to Henry's law equilibrium, expressed as concentration changes per time unit. If P_g and $[X]_{aq}$ reach the values corresponding to the Henry's law constant, i.e.,

$$K_{H(298K)} = \frac{[X]_{aq}}{P_g} [\text{mol l}^{-1} \text{ atm}^{-1}],$$ (7)

$$P_g \quad = \quad \text{gas phase partial pressure [atm]},$$

the third and fourth term in Equation (5) cancel.

Equation (6) describes the kinetics of the interfacial mass transport as the temporal change of a gas phase species partial pressure (P_g). The individual terms correspond to the terms in Equation (5), but they refer to the changes in the gas phase. The outlined description of phase transfer is applied for all compounds in the present study in order to avoid errors in aqueous phase concentrations if only Henry-equilibria are considered. It has been shown explicitly that tropospheric aqueous phase concentrations will significantly differ from Henry equilibrium concentration when compounds are efficiently removed by chemical reaction (Audiffren *et al.*, 1998).

3. Results

3.1. PARTITIONING BETWEEN GAS AND AQUEOUS PHASE

The time scale of the partitioning of the gas phase substances among the two phases is of interest in order to determine the fraction of species existing in the aqueous phase. The partition coefficient as a dimensionless value is independent of the liquid water content if the concentration in the aqueous phase species is converted into the gas phase units:

$$c_{aq}^g [\text{cm}_g^{-3}] = c_{aq} [\text{mol l}_{aq}^{-1}] \cdot N_A \cdot LWC,$$ (8)

$$N_A \quad = \quad \text{Avogadro number } (6.023 \cdot 10^{23} \text{ mol}^{-1}),$$
$$LWC \quad = \quad \text{liquid water content } (3 \cdot 10^{-10} \text{ l}_{aq} \text{ cm}_g^{-3}).$$

With this conversion the partition coefficient ε results as

$$\varepsilon = \frac{c_{aq}^g}{c_{aq}^g + c_g}.$$ (9)

For some selected species the partition coefficient ε was determined 0.009 seconds after starting the calculations and at noon of the second day if the system is in steady state. The values are listed in Table III. In the case of further pH dependent dissociation of the species the concentration of the anion in the aqueous phase was also considered; the aldehydes were considered in their hydrated and unhydrated forms.

Table III. Partitioning coefficients for selected species at 0.009 s and 36 h after beginning of the simulation time. Comparison between modeling results and theoretical values assuming Henry equilibrium at 288.15 K

Species	$[c]_g$ $[cm^{-3}]$	$[c]_g$ $[cm^{-3}]$	$[c]_{aq,model}$ [M]	$[c]_{aq,Henry}$ [M]	$[c]_{aq,model}$ [M]	$[c]_{aq,Henry}$ [M]	ε_{model}	ε_{model}	ε_{Henry}
	t = 0.009 s	t = 36 h	t = 0.009 s	t = 0.009 s	t = 36 h	t = 36 h	t = 0.009 s	t = 36 h	
HNO_3/NO_3^-	$2.2 \cdot 10^9$	$2.3 \cdot 10^6$	$1.4 \cdot 10^{-5}$	0.59	$7.6 \cdot 10^{-4}$	$59.3 \cdot 10^{-3}$	0.53	1	1
$HCHO/CH_2(OH)_2$	$2.4 \cdot 10^9$	$7.3 \cdot 10^6$	$5.7 \cdot 10^{-7}$	$6.8 \cdot 10^{-7}$	$5.2 \cdot 10^{-6}$	$2.0 \cdot 10^{-9}$	0.04	0.99	0.07
H_2O_2	$2.2 \cdot 10^8$	$9.7 \cdot 10^8$	$1.4 \cdot 10^{-5}$	$8.5 \cdot 10^{-5}$	$8.5 \cdot 10^{-6}$	$8.3 \cdot 10^{-5}$	0.92	0.61	0.61
$HCOOH/HCOO^-$	$4.4 \cdot 10^2$	$2.5 \cdot 10^{10}$	$3.8 \cdot 10^{-13}$	$2.1 \cdot 10^{-13}$	$1.1 \cdot 10^{-5}$	$1.2 \cdot 10^{-5}$	0.02	0.08	0.08
CH_3COOH/CH_3COO^-	$1.9 \cdot 10^2$	$1.2 \cdot 10^9$	$3.6 \cdot 10^{-15}$	$9.5 \cdot 10^{-14}$	$5.3 \cdot 10^{-7}$	$6.0 \cdot 10^{-7}$	0.03	0.08	0.07
HO_2/O_2^-	$2.1 \cdot 10^4$	$5.0 \cdot 10^5$	$2.6 \cdot 10^{-10}$	$7.7 \cdot 10^{-12}$	$8.9 \cdot 10^{-11}$	$1.8 \cdot 10^{-10}$	0.69	0.03	0.06
$SO_2/HSO_3^-/SO_3^{2-}$	$2.5 \cdot 10^7$	$1.9 \cdot 10^{11}$	$3.3 \cdot 10^{-6}$	$2.1 \cdot 10^{-12}$	$1.8 \cdot 10^{-7}$	$4.7 \cdot 10^{-8}$	0.96	$1.6 \cdot 10^{-4}$	$1.5 \cdot 10^{-5}$
ACO_3	$1.7 \cdot 10^2$	$7.8 \cdot 10^7$	$4.6 \cdot 10^{-15}$	$9.1 \cdot 10^{-14}$	$4.3 \cdot 10^{-9}$	$2.1 \cdot 10^{-9}$	$9.8 \cdot 10^{-3}$	$8.1 \cdot 10^{-3}$	$9.6 \cdot 10^{-3}$
$CH_3CHO/CH_3CH(OH)_2$	$2.5 \cdot 10^9$	$1.1 \cdot 10^{10}$	$2.4 \cdot 10^{-9}$	$2.3 \cdot 10^{-9}$	$2.5 \cdot 10^{-8}$	$1.1 \cdot 10^{-8}$	$1.7 \cdot 10^{-4}$	$4.2 \cdot 10^{-4}$	$1.7 \cdot 10^{-4}$
OH	$5.9 \cdot 10^3$	$1.0 \cdot 10^6$	$1.8 \cdot 10^{-13}$	$1.1 \cdot 10^{-14}$	$1.4 \cdot 10^{-12}$	$1.9 \cdot 10^{-12}$	$5.5 \cdot 10^{-3}$	$2.5 \cdot 10^{-4}$	$3.4 \cdot 10^{-4}$
CH_3O_2	$2.2 \cdot 10^2$	$2.6 \cdot 10^8$	$1.1 \cdot 10^{-16}$	$1.0 \cdot 10^{-16}$	$1.3 \cdot 10^{-10}$	$1.2 \cdot 10^{-10}$	$8.8 \cdot 10^{-5}$	$9.0 \cdot 10^{-5}$	$8.5 \cdot 10^{-5}$
CH_3OOH	$2.5 \cdot 10^8$	$2.1 \cdot 10^8$	$1.2 \cdot 10^{-10}$	$1.1 \cdot 10^{-10}$	$9.9 \cdot 10^{-11}$	$9.5 \cdot 10^{-11}$	$8.8 \cdot 10^{-5}$	$8.5 \cdot 10^{-5}$	$8.5 \cdot 10^{-5}$
NO_3	$5.3 \cdot 10^4$	$1.9 \cdot 10^5$	$1.3 \cdot 10^{-15}$	$1.3 \cdot 10^{-15}$	$4.7 \cdot 10^{-15}$	$4.6 \cdot 10^{-15}$	$4.4 \cdot 10^{-6}$	$4.5 \cdot 10^{-6}$	$4.4 \cdot 10^{-6}$
O_3	$2.2 \cdot 10^{12}$	$2.1 \cdot 10^{12}$	$1.3 \cdot 10^{-9}$	$1.2 \cdot 10^{-9}$	$1.2 \cdot 10^{-9}$	$1.3 \cdot 10^{-9}$	$1.1 \cdot 10^{-7}$	$1.1 \cdot 10^{-7}$	$9.5 \cdot 10^{-8}$

It is evident from Table III that soluble trace gases are not in steady-state at the first time step presented, because the consecutive hydration or dissociation is not complete. However, the pH value is reduced abruptly in the first time step from 4.5 to 3.2 and is decreased in the following 36 h only by 0.5 units to 2.7 (Figure 8). As a result the extent of the dissociation does not change significantly during this time.

In addition to the partition coefficient from the model the aqueous phase concentrations resulting from given gas phase concentrations and effective Henry constants at 288 K (i.e., considering the further dissociation or hydration, respectively) were calculated. Furthermore, the partition coefficient ε_{Henry} was determined. This value is independent of the gas phase concentration and given by

$$\varepsilon_{Henry} = \frac{c_{aq,Henry}^{g}}{c_{aq,Henry}^{g} + c_g} = \frac{K_H^{eff*} \cdot c_g}{K_H^{eff*} \cdot c_g + c_g} = \frac{K_H^{eff*}}{K_H^{eff*} + 1}, \tag{10}$$

where

$$K_H^{eff*} = \frac{c_{aq}^{g}[cm_g^{-3}]}{c_g[cm_g^{-3}]} = \text{effective Henry's Law constant (dimensionless).} \tag{11}$$

A comparison between the aqueous phase concentration calculated from the model and for the assumption of Henry equilibria shows that the concentrations for some species are significantly higher in the model droplet than predicted by the Henry's Law constant. Because the concentration $c_{aq,Henry}$ is an upper limit for the fraction of the species within the droplet, the difference between $c_{aq,model}$ and $c_{aq,Henry}$ represents the contribution of the species formed in the aqueous phase. This consideration clarifies that the aqueous phase is not only a sink for soluble gas phase species but it can also act as a source because of the production of these species in excess to the equilibrium value. The deviation between the partition coefficients is most evident for formaldehyde for which in the model nearly 100% is present within the droplet whereas only about 7% are predicted by Henry's Law. With this example the importance of the organic cloud chemistry becomes evident since nearly 40% of the total formaldehyde in the droplet is formed from the oxidation of methanol by OH (R103) in solution. For acetaldehyde, a different situation exists. At the given time (12:00, 2nd day) the most important sink process (90%) is the phase transfer to the gas phase ($7.4 \cdot 10^{-10}$ M s^{-1}). In accordance with the formation of the formaldehyde, the oxidation of ethanol by OH is the most effective source for acetaldehyde in the aqueous phase.

The comparison between ε_{model} and ε_{Henry} for OH and HO$_2$ shows that equilibrium conditions are not reached, because for these species their uptake is controlled by the resistances determined by the mass accommodation and diffusion in the gas phase rather than their Henry solubilities. These results clearly demonstrate the importance of the explicit formulation of the uptake considering more parameters than only Henry's Law coefficients. These results are in qualitative accordance
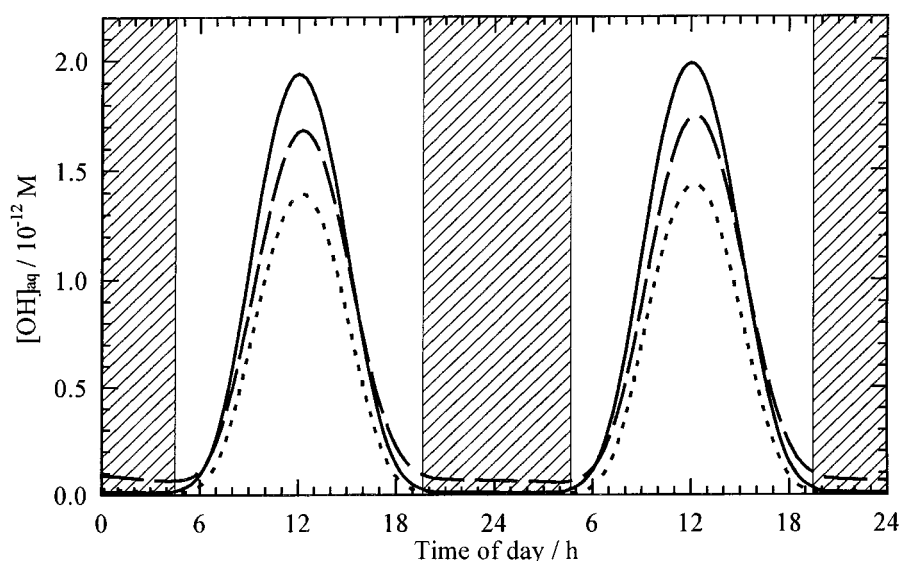
Figure 1. Comparison of model results for $[OH]_{aq}$ for urban (......), remote (- - - - -) and marine(————) conditions.

with the study of the deviation from Henry's Law by Audiffren *et al.* (1998). These authors also present significant differences of the concentrations for moderately soluble species calculated by different approaches to mass transfer description. As can be seen from Table IIb the mass accommodation coefficients for the HO_x radicals are only 0.01 for both species which is small compared to those of the other species listed in Table III. A quantitative comparison with all species considered in the study by Audiffren *et al.* (1998) is not possible because of the very restricted chemical mechanism applied there. From Table III it can also be concluded that soluble species such as nitrous acid, formaldehyde, hydrogen peroxide need some time to achieve the steady state concentration, as can be seen from the comparison of $\varepsilon_{model,t=0.009s}$ and $\varepsilon_{model,t=36h}$.

Less soluble species such as NO_3, CH_3O_2, ACO_3, CH_3OOH and O_3 are in equilibrium with the gas phase and their coefficients ε_{model} and ε_{Henry} are nearly equal. A comparison of the partition coefficients for the radicals and these species for the given times shows that the equilibrium is already reached after some milliseconds. The fractions of these species in the aqueous phase are only in the order of 10^{-4} or less.

3.2. CONCENTRATION LEVELS OF AQUEOUS PHASE RADICALS AND RADICAL ANIONS

3.2.1. *OH and NO$_3$ Radicals*

OH represents the most important radical in both phases. In Figure 1 plots of aqueous phase concentration vs time are shown for the three different environments treated here.

Table IV. HO$_x$- and TMI-chemistry

Reaction no.	Reaction	k_{298}, $M^{-n} s^{-1}$ [a]	E_a/R, K	Reference
R1	$H_2O_2 + Fe^{3+} \rightarrow HO_2 + H^+ + Fe^{2+}$	$2 \cdot 10^{-3}$		Walling and Goosen, 1973
R2	$H_2O_2 + [Fe(OH)]^{2+} \rightarrow HO_2 + H_2O + Fe^{2+}$	$2 \cdot 10^{-3}$		$k_2 = k_1$
R3	$H_2O_2 + [Fe(OH)_2]^+ \rightarrow HO_2 + OH^- + Fe^{2+} + H_2O$	$2 \cdot 10^{-3}$		$k_3 = k_1$
R4	$H_2O_2 + Fe^{2+} \rightarrow OH + OH^- + Fe^{3+}$	76		Walling, 1975
R5	$H_2O_2 + Mn^{3+} \rightarrow HO_2 + H^+ + Mn^{2+}$	$7.3 \cdot 10^4$		Davies *et al.*, 1968
R6	$H_2O_2 + Cu^+ \rightarrow OH + OH^- + Cu^{2+}$	$7.0 \cdot 10^3$		Berdnikov, 1973
R7	$O_2^- + Fe^{3+} \rightarrow O_2 + Fe^{2+}$	$1.5 \cdot 10^8$		Rush and Bielski, 1985
R8	$HO_2 + [Fe(OH)]^{2+} \rightarrow Fe^{2+} + O_2 + H_2O$	$1.3 \cdot 10^5$		Ziajka *et al.*, 1994
R9	$O_2^- + [Fe(OH)]^{2+} \rightarrow O_2 + Fe^{2+} + OH^-$	$1.5 \cdot 10^8$		Rush and Bielski, 1985
R10	$O_2^- + [Fe(OH)_2]^+ \rightarrow O_2 + Fe^{2+} + 2OH^-$	$1.5 \cdot 10^8$		Rush and Bielski, 1985
R11	$O_2^- + Fe^{2+} \xrightarrow{2H^+} H_2O_2 + Fe^{3+}$	$1.0 \cdot 10^7$		Rush and Bielski, 1985
R12	$HO_2 + Fe^{2+} \xrightarrow{H^+} H_2O_2 + Fe^{3+}$	$1.2 \cdot 10^6$	5050	Jayson *et al.*, 1973b
R13	$OH + Fe^{2+} \rightarrow [Fe(OH)]^{2+}$	$4.3 \cdot 10^8$	1100	Christensen and Sehested, 1981
R14	$O_2^- + Mn^{2+} \xrightarrow{2H^+} H_2O_2 + Mn^{3+}$	$1.1 \cdot 10^8$		Pick-Kaplan and Rabani, 1976
R15	$HO_2 + Mn^{2+} \xrightarrow{H^+} H_2O_2 + Mn^{3+}$	$2 \cdot 10^5$		Graedel *et al.*, 1986
R16	$OH + Mn^{2+} \rightarrow OH^- + Mn^{3+}$	$2.6 \cdot 10^7$		Baral *et al.*, 1986
R17	$O_2^- + Cu^+ \xrightarrow{2H^+} H_2O_2 + Cu^{2+}$	$9.4 \cdot 10^9$		von Piechowski *et al.*, 1993
R18	$HO_2 + Cu^+ \xrightarrow{H^+} H_2O_2 + Cu^{2+}$	$2.2 \cdot 10^9$		Kozlov and Berdnikov, 1973
R19	$OH + Cu^+ \rightarrow OH^- + Cu^{2+}$	$3 \cdot 10^9$		Goldstein *et al.*, 1992
R20	$HO_2 + Cu^{2+} \rightarrow O_2 + Cu^+ + H^+$	$1.2 \cdot 10^9$		Cabelli *et al.*, 1987
R21	$O_2^- + Cu^{2+} \rightarrow O_2 + Cu^+$	$1.1 \cdot 10^{10}$		Cabelli *et al.*, 1987
R22	$Fe^{3+} + Cu^+ \rightarrow Fe^{2+} + Cu^{2+}$	$3 \cdot 10^7$		Sedlak and Hoigné, 1993
R23	$[Fe(OH)]^{2+} + Cu^+ \rightarrow Fe^{2+} + Cu^{2+} + OH^-$	$3 \cdot 10^7$		Sedlak and Hoigné, 1993
R24	$[Fe(OH)_2]^+ + Cu^+ \rightarrow Fe^{2+} + Cu^{2+} + 2OH^-$	$3 \cdot 10^7$		Sedlak and Hoigné, 1993
R25	$Fe^{2+} + Mn^{3+} \rightarrow Fe^{3+} + Mn^{2+}$	$1.5 \cdot 10^4$		Diebler and Sutin, 1964
R26	$O_3 + O_2^- \xrightarrow{H^+} 2O_2 + OH$	$1.5 \cdot 10^9$		Sehested *et al.*, 1983
R27	$HO_2 + HO_2 \rightarrow O_2 + H_2O_2$	$8.3 \cdot 10^5$	2720	Bielski *et al.*, 1985
R28	$HO_2 + O_2^- \xrightarrow{H^+} H_2O_2 + O_2$	$9.7 \cdot 10^7$	1060	Bielski *et al.*, 1985
R29	$HO_2 + OH \rightarrow H_2O + O_2$	$1.0 \cdot 10^{10}$		Elliot and Buxton, 1992
R30	$O_2^- + OH \rightarrow OH^- + O_2$	$1.1 \cdot 10^{10}$	2120	Christensen *et al.*, 1989
R31	$H_2O_2 + OH \rightarrow HO_2 + H_2O$	$3.0 \cdot 10^7$	1680	Christensen *et al.*, 1982
R32	$MHP + OH \rightarrow CH_3O_2 + H_2O$	$3.0 \cdot 10^7$	1680 [b]	$k_{R32} = k_{R31}$
R33	$HSO_3^- + OH \rightarrow H_2O + SO_3^-$	$2.7 \cdot 10^9$		Buxton *et al.*, 1996a
R34	$SO_3^{2-} + OH \rightarrow OH^- + SO_3^-$	$4.6 \cdot 10^9$		Buxton *et al.*, 1996a

[a] n = reaction order $- 1$.

As can be seen, the maximum concentrations in the urban and remote continental cases are $1.4 \cdot 10^{-12}$ and $1.7 \cdot 10^{-12}$ M, respectively. Figure 2 summarises the strength of the corresponding source and sink processes for OH for urban conditions. As can be seen the transfer from the gas phase is the most important source for the OH radical which accounts for nearly 80% of the total flux. However, also the Fenton-type reactions of metal ions (Fe^{2+} and Cu^+) with H_2O_2 lead to the production of OH in significant amounts. Comparison of the various sink strengths shows that the oxidation of organic species represents the main sink for the OH radical. The reactions with formic acid and formate contribute about 20% to the destruction of the OH radical. The third important sink is the reaction with the hydrated formaldehyde yielding formic acid (27%).

In the marine case the OH concentration is larger than in the continental environments and has a maximum of $1.9 \cdot 10^{-12}$ M. The difference can be explained with the initial concentrations of organic species in the gas phase, which is about one order of magnitude lower compared to the urban and remote cases. Since the most important sinks for OH in the aqueous phase are the reactions with organics, the concentration of the OH radical in the marine aqueous phase is decreased to a lesser extent.

The results described so far are in general agreement with those obtained by Jacob (1986). In his work, transfer from the gas phase also represented the main source for the OH radical. The other sources, however, are different because in Jacob's work reactions with transition metal ions were not considered. In general the sink strengths for the reactions of OH with $CH_2(OH)_2$, HCOOH and $HCOO^-$ are comparable. However, Jacob (1986) predicted the maximum concentration to be $2.3 \cdot 10^{-13}$ M for a relatively unpolluted environment, a factor of 7 lower than in the present case. Because of this unpolluted scenario, the result of Jacob should be compared with the maximum OH concentration calculated with CAPRAM for the marine case ($1.9 \cdot 10^{-12}$ M), whereupon the difference becomes even larger.

The possible reason for the low concentration of OH in Jacob's work is discussed in the following. In a later publication (Jacob *et al.*, 1989) the production of OH from the transition metal ions was additionally considered. Although no value for the OH aqueous phase concentration is given in that study, the maximum concentration of OH at noon in the gas phase is nearly $2.5 \cdot 10^6$ cm^{-3}, a factor of two higher compared to the one predicted by CAPRAM ($1.2 \cdot 10^6$ cm^{-3}). Therefore the difference cannot be explained by a different uptake rate from the gas phase. Rather, it is suggested that the difference is due to (i) missing reactions involving transition metal ions which produce OH and (ii) the high initial concentration of H_2O_2 used in the calculations of Jacob (1986), i.e., $8.3 \cdot 10^{10}$ cm^{-3}, as compared to only $2.5 \cdot 10^7$ cm^{-3} in CAPRAM. As can be seen from Figure 2, the reaction of OH with H_2O_2 is an important sink (24%) for OH under marine conditions, whereas in the other cases this process is less effective. Hence, the lower OH levels obtained by Jacob (1986) may be due to significantly higher H_2O_2 concentrations in both the gas and the aqueous phase. This conclusion is supported by the fact that the
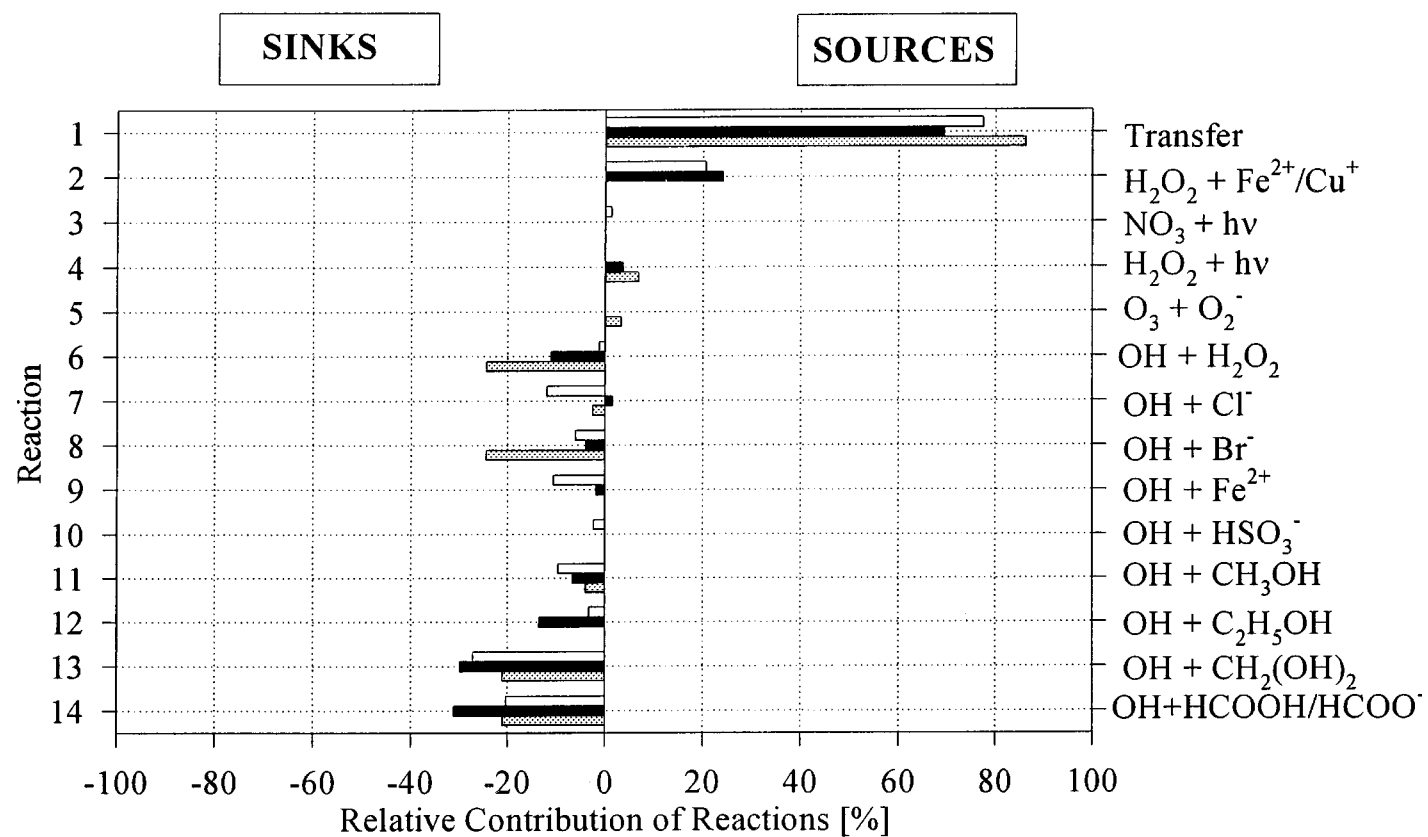
Figure 2. Sinks and sources for $[OH]_{aq}$ for urban $\square$, remote $\blacksquare$ and marine $\boxtimes$ conditions, local time: 12:00, 2nd day, production and loss fluxes $[M \ s^{-1}]$: urban $2.4 \cdot 10^{-8}$, remote $1.7 \cdot 10^{-8}$, marine $1.3 \cdot 10^{-8}$.

Table V. N-chemistry

Reaction no.	Reaction	k_{298}, $M^{-n} s^{-1}$ [a]	E_a/R, K	Reference
R35	$N_2O_5 + H_2O \rightarrow 2H^+ + 2NO_3^-$	$5 \cdot 10^9$		Estimated
R36	$NO_3 + OH^- \rightarrow NO_3^- + OH$	$9.4 \cdot 10^7$	2700	Exner *et al.*, 1992
R37	$NO_3 + Fe^{2+} \rightarrow NO_3^- + Fe^{3+}$	$8 \cdot 10^6$		Pikaev *et al.*, 1974
R38	$NO_3 + Mn^{2+} \rightarrow NO_3^- + Mn^{3+}$	$1.1 \cdot 10^6$		Neta and Huie, 1986
R39	$NO_3 + H_2O_2 \rightarrow NO_3^- + H^+ + HO_2$	$4.9 \cdot 10^6$	2000	Herrmann *et al.*, 1994
R40	$NO_3 + MHP \rightarrow NO_3^- + H^+ + CH_3O_2$	$4.9 \cdot 10^{6 \text{ b}}$	2000^{b}	$k_{R40} = k_{R39}$
R41	$NO_3 + HO_2 \rightarrow NO_3^- + H^+ + O_2$	$3.0 \cdot 10^9$		Sehested *et al.*, 1994
R42	$NO_3 + O_2^- \rightarrow NO_3^- + O_2$	$3 \cdot 10^9$		$k_{R42} = k_{R41}$
R43	$NO_3 + HSO_3^- \rightarrow NO_3^- + H^+ + SO_3^-$	$1.3 \cdot 10^9$	2000	Exner *et al.*, 1992
R44	$NO_3 + SO_3^{2-} \rightarrow NO_3^- + SO_3^-$	$3.0 \cdot 10^8$		Exner *et al.*, 1992
R45	$NO_3 + HSO_4^- \rightarrow NO_3^- + H^+ + SO_4^-$	$2.6 \cdot 10^5$		Raabe, 1996
R46	$NO_3 + SO_4^{2-} \rightarrow NO_3^- + SO_4^-$	$5.6 \cdot 10^3$		Logager *et al.*, 1993
R47	$NO_2 + OH \rightarrow NO_3^- + H^+$	$1.2 \cdot 10^{10}$		Wagner *et al.*, 1980
R48	$NO_2 + O_2^- \rightarrow NO_2^- + O_2$	$1 \cdot 10^8$		Warneck and Wurzinger, 1988
R49	$NO_2 + NO_2 \xrightarrow{H_2O} HNO_2 + NO_3^- + H^+$	$8.4 \cdot 10^7$	-2900	Park and Lee, 1988
R50	$O_2NO_2^- \rightarrow NO_2^- + O_2$	$4.5 \cdot 10^{-2}$		Lammel *et al.*, 1990
R51	$NO_2^- + OH \rightarrow NO_2 + OH^-$	$1.1 \cdot 10^{10}$		Barker *et al.*, 1970
R52	$NO_2^- + SO_4^- \rightarrow SO_4^{2-} + NO_2$	$7.2 \cdot 10^8$		Reese, 1997
R53	$NO_2^- + NO_3 \rightarrow NO_3^- + NO_2$	$1.4 \cdot 10^9$	0	Herrmann and Zellner, 1998
R54	$NO_2^- + Cl_2^- \rightarrow 2Cl^- + NO_2$	$6 \cdot 10^7$		Jacobi, 1996
R55	$NO_2^- + Br_2^- \rightarrow 2Br^- + NO_2$	$1.2 \cdot 10^7$	1720	Shoute *et al.*, 1991
R56	$NO_2^- + CO_3^- \rightarrow CO_3^{2-} + NO_2$	$6.6 \cdot 10^5$	850	Huie *et al.*, 1991a
R57	$NO_2^- + O_3 \rightarrow NO_3^- + O_2$	$5 \cdot 10^5$	7000	Damschen and Martin, 1983
R58	$HNO_2 + OH \rightarrow NO_2 + H_2O$	$1 \cdot 10^9$		Rettich, 1978
R59	$HNO_4 + HSO_3^- \rightarrow HSO_4^- + NO_3$	$3.5 \cdot 10^5$		Amels *et al.*, 1996

[a] n = reaction order – 1.

HO_2 concentrations obtained by Jacob (1986) (i.e., $3 \cdot 10^{-8}$ M) are by the far the highest when compared with other modelling studies (see Zellner and Herrmann, 1995 and references therein).

The analysis of the most important sinks and sources for the $OH_{(aq)}$ in Figure 2 clarifies the importance of the TMI chemistry to the concentration levels of the HO_x radicals. In the study by Matthijsen *et al.*, 1995, a significant decrease of the OH concentration is predicted if the reactions of the metal ions are neglected. Calculations with a modified mechanism of CAPRAM – without initial concentrations for the transition metal ions – lead to a maximum concentration of $OH_{(aq)}$ of $6.7 \cdot 10^{-13}$ M, lower by a factor of 2.1 compared to the concentration in Figure 1. This finding is nearly in accordance with the result from Matthijsen *et al.* who found an increase of about 255% of $OH_{(aq)}$ in the presence of TMI. Whereas in the cited reference, however, the most important source for $OH_{(aq)}$ are the transfer from the gas phase, the photolysis of $H_2O_{2(aq)}$ and the reaction between O_3 and O_2^-,

Table VI. S-chemistry

Reaction no.	Reaction	k_{298}, $M^{-n} s^{-1}$ [a]	E_a/R, K	Reference
R60	$HMS^- + OH \xrightarrow{O_2/H_2O} H_2O + HO_2 + HCOOH + HSO_3^-$	$3 \cdot 10^8$		Buxton, 1994
R61	$HMS^- + SO_4^- \rightarrow SO_4^{2-} + H^+ + HCHO + SO_3^-$	$2.8 \cdot 10^6$		Buxton, 1994
R62	$HMS^- + NO_3 \rightarrow NO_3^- + H^+ + HCHO + SO_3^-$	$4.2 \cdot 10^6$		Herrmann and Zellner, 1998
R63	$HMS^- + Cl_2^- \rightarrow 2Cl^- + H^+ + HCHO + SO_3^-$	$5.0 \cdot 10^5$		Jacobi, 1996
R64	$HMS^- + Br_2^- \rightarrow 2Br^- + H^+ + HCHO + SO_3^-$	$5 \cdot 10^4$		Estimated
R65	$HSO_3^- + H_2O_2 + H^+ \rightarrow SO_4^{2-} + H_2O + 2H^+$	$6.9 \cdot 10^7$	4000	Lind *et al.*, 1987
R66	$HSO_3^- + CH_3OOH + H^+ \rightarrow SO_4^{2-} + 2H^+ + CH_3OH$	$1.8 \cdot 10^7$	3800	Lind *et al.*, 1987
R67	$HSO_3^- + CH_3C(O)OOH + H^+ \rightarrow SO_4^{2-} + 2H^+ + P$	$4.8 \cdot 10^7$	3990	Lind *et al.*, 1987
R68	$SO_2 + O_3 \xrightarrow{H_2O} HSO_4^- + O_2 + H^+$	$2.4 \cdot 10^4$		Hoffmann, 1986
R69	$HSO_3^- + O_3 \rightarrow HSO_4^- + O_2$	$3.7 \cdot 10^5$	5530	Hoffmann, 1986
R70	$SO_3^{2-} + O_3 \rightarrow SO_4^{2-} + O_2$	$1.5 \cdot 10^9$	5280	Hoffmann, 1986
R71	$[Fe(OH)]^{2+} + HSO_3^- \rightarrow Fe^{2+} + SO_3^- + H_2O$	39		Ziajka *et al.*, 1994
R72	$Fe^{2+} + SO_5^- \xrightarrow{H_2O} [Fe(OH)]^{2+} + HSO_5^-$	$4.3 \cdot 10^7$		Herrmann *et al.*, 1996
R73	$Fe^{2+} + HSO_5^- \rightarrow [Fe(OH)]^{2+} + SO_4^-$	$3 \cdot 10^4$		Ziajka *et al.*, 1994
R74	$Mn^{2+} + SO_5^- \xrightarrow{H_2O} Mn^{3+} + HSO_5^- + OH^-$	$4.6 \cdot 10^6$		Herrmann *et al.*, 1996
R75	$Fe^{2+} + SO_4^- \xrightarrow{H_2O} [Fe(OH)]^{2+} + SO_4^{2-} + H^+$	$3.5 \cdot 10^7$		Ziajka *et al.*, 1994
R76	$Fe^{2+} + S_2O_8^{2-} \xrightarrow{H_2O} [Fe(OH)]^{2+} + SO_4^{2-} + SO_4^- + H^+$	17		Buxton *et al.*, 1997
R77	$SO_5^- + SO_5^- \rightarrow S_2O_8^{2-} + O_2$	$1.8 \cdot 10^8$	2600	Herrmann *et al.*, 1995
R78	$SO_5^- + SO_5^- \rightarrow 2SO_4^- + O_2$	$7.2 \cdot 10^6$	2600	Herrmann *et al.*, 1995
R79	$SO_5^- + HO_2 \rightarrow HSO_5^- + O_2$	$1.7 \cdot 10^9$		Buxton *et al.*, 1996b
R80	$SO_5^- + O_2^- \xrightarrow{H_2O} HSO_5^- + OH^- + O_2$	$1.7 \cdot 10^9$		$k_{R80} = k_{R79}$
R81	$SO_3^- + O_2 \rightarrow SO_5^-$	$2.5 \cdot 10^9$		Buxton *et al.*, 1996a
R82	$SO_5^- + HSO_3^- \rightarrow HSO_5^- + SO_3^-$	$8.6 \cdot 10^3$		Buxton *et al.*, 1996a
R83	$SO_5^- + HSO_3^- \rightarrow SO_4^{2-} + SO_4^- + H^+$	$3.6 \cdot 10^2$		Buxton *et al.*, 1996a
R84	$SO_5^- + SO_3^{2-} \xrightarrow{H^+} HSO_5^- + SO_3^-$	$2.13 \cdot 10^5$		Buxton *et al.*, 1996a
R85	$SO_5^- + SO_3^{2-} \rightarrow SO_4^- + SO_4^{2-}$	$5.5 \cdot 10^5$		Buxton *et al.*, 1996a
R86	$OH + HSO_4^- \rightarrow H_2O + SO_4^-$	$3.5 \cdot 10^5$		Tang *et al.*, 1988
R87	$SO_4^- + SO_4^- \rightarrow S_2O_8^{2-}$	$1.6 \cdot 10^8$		Herrmann *et al.*, 1995a
R88	$SO_4^- + HSO_3^- \rightarrow SO_4^{2-} + SO_3^- + H^+$	$3.2 \cdot 10^8$		Reese, 1997
R89	$SO_4^- + SO_3^{2-} \rightarrow SO_4^{2-} + SO_3^-$	$3.2 \cdot 10^8$	1200	Reese, 1997
R90	$SO_4^- + Fe^{2+} \rightarrow [Fe(SO_4)]^+$	$3 \cdot 10^8$		McElroy and Waygood, 1990
R91	$SO_4^- + Mn^{2+} \rightarrow SO_4^{2-} + Mn^{3+}$	$2 \cdot 10^7$		Neta and Huie, 1986
R92	$SO_4^- + Cu^+ \rightarrow SO_4^{2-} + Cu^{2+}$	$3 \cdot 10^8$		$k_{R92} = k_{R90}$
R93	$SO_4^- + H_2O_2 \rightarrow SO_4^{2-} + H^+ + HO_2$	$2.8 \cdot 10^7$		Reese, 1997
R94	$SO_4^- + MHP \rightarrow SO_4^{2-} + H^+ + CH_3O_2$	$2.8 \cdot 10^7$		$k_{R94} = k_{R93}$
R95	$SO_4^- + HO_2 \rightarrow SO_4^{2-} + H^+ + O_2$	$3.5 \cdot 10^9$		$k_{R96} = k_{R95}$
R96	$SO_4^- + O_2^- \rightarrow SO_4^{2-} + O_2$	$3.5 \cdot 10^9$		$k_{R96} = k_{R95}$
R97	$SO_4^- + NO_3^- \rightarrow SO_4^{2-} + NO_3$	$5.0 \cdot 10^4$		Exner *et al.*, 1992
R98	$SO_4^- + OH^- \rightarrow SO_4^{2-} + OH$	$1.4 \cdot 10^7$		Herrmann *et al.*, 1995
R99	$SO_4^- + H_2O \rightarrow SO_4^{2-} + H^+ + OH$	11	1110	Herrmann *et al.*, 1995
R100	$HSO_5^- + HSO_3^- + H^+ \rightarrow 2SO_4^{2-} + 3H^+$	$7.14 \cdot 10^6$		Betterton and Hoffmann, 1988b
R101	$HSO_5^- + SO_3^{2-} + H^+ \rightarrow 2SO_4^{2-} + 2H^+$	$7.14 \cdot 10^6$		Betterton and Hoffmann, 1988b
R102	$HSO_5^- + OH \rightarrow SO_5^- + H_2O$	$1.7 \cdot 10^7$		Maruthamuthu and Neta, 1977

[a] n = reaction order – 1.

Table VII. Organic chemistry

Reaction no.	Reaction	k_{298}, $M^{-n}\,s^{-1\,a}$	E_a/R, K	Reference
R103	$CH_3OH + OH \xrightarrow{O_2} H_2O + HO_2 + HCHO$	$1.0 \cdot 10^9$	580	Elliot and McCracken, 1989
R104	$CH_3OH + SO_4^- \xrightarrow{O_2} SO_4^{2-} + H^+ + HO_2 + HCHO$	$9.0 \cdot 10^6$	2190	Clifton and Huie, 1989
R105	$CH_3OH + NO_3 \xrightarrow{O_2} NO_3^- + H^+ + HO_2 + HCHO$	$5.4 \cdot 10^5$	4300	Herrmann and Zellner, 1998
R106	$CH_3OH + Cl_2^- \xrightarrow{O_2} 2Cl^- + H^+ + HO_2 + HCHO$	1000	5500	Zellner *et al.*, 1996
R107	$CH_3OH + Br_2^- \xrightarrow{O_2} 2Br^- + H^+ + HO_2 + HCHO$	$5.4 \cdot 10^5$		Wicktor *et al.*, 1996
R108	$CH_3OH + CO_3^- \xrightarrow{O_2} CO_3^{2-} + H^+ + HO_2 + HCHO$	$2.6 \cdot 10^3$		Zellner *et al.*, 1996
R109	$ETOH + OH \xrightarrow{O_2} H_2O + HO_2 + CH_3CHO$	$1.9 \cdot 10^9$		Buxton *et al.*, 1988a
R110	$ETOH + SO_4^- \xrightarrow{O_2} SO_4^{2-} + H^+ + HO_2 + CH_3CHO$	$4.1 \cdot 10^7$	1760	Clifton and Huie, 1989
R111	$ETOH + NO_3 \xrightarrow{O_2} NO_3^- + H^+ + HO_2 + CH_3CHO$	$2.2 \cdot 10^6$	3300	Herrmann and Zellner, 1998
R112	$ETOH + Cl_2^- \xrightarrow{O_2} 2Cl^- + H^+ + HO_2 + CH_3CHO$	$1.2 \cdot 10^5$		Zellner *et al.*, 1996
R113	$ETOH + Br_2^- \xrightarrow{O_2} 2Br^- + H^+ + HO_2 + CH_3CHO$	$3.8 \cdot 10^3$		Reese *et al.*, 1999
R114	$ETOH + CO_3^- \xrightarrow{O_2} CO_3^{2-} + H^+ + HO_2 + CH_3CHO$	$1.5 \cdot 10^4$		Khuz'min, 1972
R115	$CH_2(OH)_2 + OH \xrightarrow{O_2} H_2O + HO_2 + HCOOH$	$1.0 \cdot 10^9$	1020	Hart *et al.*, 1964; Chin and Wine, 1994
R116	$CH_2(OH)_2 + SO_4^- \xrightarrow{O_2} SO_4^{2-} + H^+ + HO_2 + HCOOH$	$1.4 \cdot 10^7$	1300	Buxton *et al.*, 1990
R117	$CH_2(OH)_2 + NO_3 \xrightarrow{O_2} NO_3^- + H^+ + HO_2 + HCOOH$	$1.0 \cdot 10^6$	4500	Exner *et al.*, 1993
R118	$CH_2(OH)_2 + Cl_2^- \xrightarrow{O_2} 2Cl^- + H^+ + HO_2 + HCOOH$	$3.1 \cdot 10^4$	4400	Zellner *et al.*, 1996
R119	$CH_2(OH)_2 + Br_2^- \xrightarrow{O_2} 2Br^- + H^+ + HO_2 + HCOOH$	$3 \cdot 10^3$		Estimated
R120	$CH_2(OH)_2 + CO_3^- \xrightarrow{O_2} CO_3^{2-} + H^+ + HO_2 + HCOOH$	$1.3 \cdot 10^4$		Zellner *et al.*, 1996
R121	$CH_3CH(OH)_2 + OH \xrightarrow{O_2} H_2O + HO_2 + HAc$	$1.2 \cdot 10^9$		Schuchmann and von Sonntag, 1988
R122	$CH_3CHO + OH \xrightarrow{H_2O/O_2} H_2O + HO_2 + HAc$	$3.6 \cdot 10^9$		Schuchmann and von Sonntag, 1988
R123	$CH_3CH(OH)_2 + SO_4^- \xrightarrow{O_2} SO_4^{2-} + H^+ + HO_2 + HAc$	$1 \cdot 10^7$		Estimated
R124	$CH_3CH(OH)_2 + NO_3 \xrightarrow{O_2} NO_3^- + H^+ + HO_2 + HAc$	$1.9 \cdot 10^6$		Zellner *et al.*, 1996
R125	$CH_3CH(OH)_2 + Cl_2^- \xrightarrow{O_2} 2Cl^- + H^+ + HO_2 + HAc$	$4 \cdot 10^4$		Jacobi, 1996
R126	$CH_3CH(OH)_2 + Br_2^- \xrightarrow{O_2} 2Br^- + H^+ + HO_2 + HAc$	$4 \cdot 10^4$		Estimated
R127	$CH_3CH(OH)_2 + CO_3^- \xrightarrow{O_2} CO_3^{2-} + H^+ + HO_2 + HAc$	$1 \cdot 10^4$		Estimated
R128	$HCOOH + OH \xrightarrow{O_2} H_2O + HO_2 + CO_2$	$1.3 \cdot 10^8$	1000	Buxton *et al.*, 1988a; Chin and Wine, 1994
R129	$HCOO^- + OH \xrightarrow{O_2} OH^- + HO_2 + CO_2$	$4 \cdot 10^9$	1000	Buxton *et al.*, 1988a; Elliot and Simsons, 1984
R130	$HCOOH + SO_4^- \xrightarrow{O_2} SO_4^{2-} + H^+ + HO_2 + CO_2$	$2.5 \cdot 10^6$		Reese, 1997
R131	$HCOO^- + SO_4^- \xrightarrow{O_2} SO_4^{2-} + HO_2 + CO_2$	$2.1 \cdot 10^7$		Reese, 1997
R132	$HCOOH + NO_3 \xrightarrow{O_2} NO_3^- + H^+ + HO_2 + CO_2$	$3.8 \cdot 10^5$	3400	Exner *et al.*, 1994
R133	$HCOO^- + NO_3 \xrightarrow{O_2} NO_3^- + HO_2 + CO_2$	$5.1 \cdot 10^7$	2200	Exner *et al.*, 1994
R134	$HCOOH + Cl_2^- \xrightarrow{O_2} 2Cl^- + H^+ + HO_2 + CO_2$	5500	4500	Jacobi *et al.*, 1999
R135	$HCOO^- + Cl_2^- \xrightarrow{O_2} 2Cl^- + HO_2 + CO_2$	$1.3 \cdot 10^6$		Jacobi *et al.*, 1996
R136	$HCOOH + Br_2^- \xrightarrow{O_2} 2Br^- + H^+ + HO_2 + CO_2$	$4 \cdot 10^3$		Reese *et al.*, 1999
R137	$HCOO^- + Br_2^- \xrightarrow{O_2} 2Br^- + HO_2 + CO_2$	$4.9 \cdot 10^3$		Jacobi, 1996

Table VII. (Continued)

Reaction no.	Reaction	k_{298}, $M\ s^{-1}$	E_a/R, K	Reference
R138	$HCOO^- + CO_3^- \xrightarrow{O_2} CO_3^{2-} + HO_2 + CO_2$	$1.4 \cdot 10^5$	3300	Zellner *et al.*, 1996
R139	$HAc + OH \xrightarrow{O_2} H_2O + ACO_3 + CO_2$	$1.5 \cdot 10^7$	1330	Thomas, 1965; Chin and Wine, 1994
R140	$Ac^- + OH \xrightarrow{O_2} OH^- + ACO_3 + CO_2$	$1.0 \cdot 10^9$	1800	Fisher and Hamill, 1973; Chin and Wine, 1994
R141	$HAc + SO_4^- \xrightarrow{O_2} SO_4^{2-} + H^+ + ACO_3 + CO_2$	$2.0 \cdot 10^5$		Reese, 1997
R142	$Ac^- + SO_4^- \xrightarrow{O_2} SO_4^{2-} + CH_3O_2 + CO_2$	$2.8 \cdot 10^7$	1210	Reese, 1997; Huie and Clifton, 1990
R143	$HAc + NO_3 \xrightarrow{O_2} NO_3^- + H^+ + ACO_3 + CO_2$	$1.4 \cdot 10^4$	3800	Exner *et al.*, 1994
R144	$Ac^- + NO_3 \xrightarrow{O_2} NO_3^- + CH_3O_2 + CO_2$	$2.9 \cdot 10^6$	3800	Exner *et al.*, 1994
R145	$HAc + Cl_2^- \xrightarrow{O_2} 2Cl^- + H^+ + ACO_3 + CO_2$	1950	4800	Jacobi *et al.*, 1998
R146	$Ac^- + Cl_2^- \xrightarrow{O_2} 2Cl^- + CH_3O_2 + CO_2$	$2.6 \cdot 10^5$	4800	Jacobi *et al.*, 1996
R147	$HAc + Br_2^- \xrightarrow{O_2} 2Br^- + H^+ + ACO_3 + CO_2$	10		Reese *et al.*, 1999
R148	$Ac^- + Br_2^- \xrightarrow{O_2} 2Br^- + CH_3O_2 + CO_2$	100		Jacobi, 1996
R149	$Ac^- + CO_3^- \xrightarrow{O_2} CO_3^{2-} + CH_3O_2 + CO_2$	580		Zellner *et al.*, 1996
R150	$CH_3O_2 + CH_3O_2 \rightarrow CH_3OH + HCHO + O_2$	$1.7 \cdot 10^8$	2200	Herrmann *et al.*, 1999b
R151	$CH_3O_2 + HSO_3^- \rightarrow MHP + SO_3^-$	$5 \cdot 10^5$		Herrmann *et al.*, 1999b
R152	$ETHP + ETHP \rightarrow Prod.$	$1.5 \cdot 10^{8\ c}$	-1500	Herrmann *et al.*, 1999b

[a] n = reaction order – 1.

the analysis for the calculations performed in the present study shows that only the transfer from the gas phase is an effective source (97.4% of the total production flux, i.e., $2.5 \cdot 10^{-8}$ M s^{-1}). The concentration of the HO$_2$ radical in the compared study increases by up to 80% if it is not consumed by copper(I) and iron(II). In CAPRAM2.3 the differences are more extreme: If all TMI reactions are neglected, the HO$_{2(aq)}$ concentration increases from $8.8 \cdot 10^{-11}$ M to $1.6 \cdot 10^{-8}$ M at noon, because the main sinks, i.e., the reactions with copper(I) and copper(II), are missing. In the paper by Matthijsen (1996) for reaction (R18) an averaged reaction rate of $1 \cdot 10^9$ M^{-1} s^{-1} is assumed and for (R20) $k_{20} = 5 \cdot 10^7$ M^{-1} s^{-1} is used. As a result the fluxes are more efficient. During night-time the OH concentration is reduced to about $8.7 \cdot 10^{-15}$ M, while the NO$_3$-concentration increases to $3.4 \cdot 10^{-14}$ M in the continental scenarios. In the marine case the concentration remains at $3 \cdot 10^{-15}$ M (cf. Figure 3).

The only efficient source for the NO$_3$ radical in the aqueous phase is transfer from the gas phase. The other potential source, i.e., the reaction of nitrate with the sulphate radical anion (R97), is negligible at night. Because the main source of gas phase NO$_{3(g)}$ is the reaction of NO$_{2(g)}$ with O$_{3(g)}$, it is obvious, that less NO$_3$ is formed in the unpolluted cases. As can be seen from Table I, the initial concentration of NO$_2$ differs by a factor of 11 between the urban and the marine case. The nitrate radical in the aqueous phase is removed in reactions with the
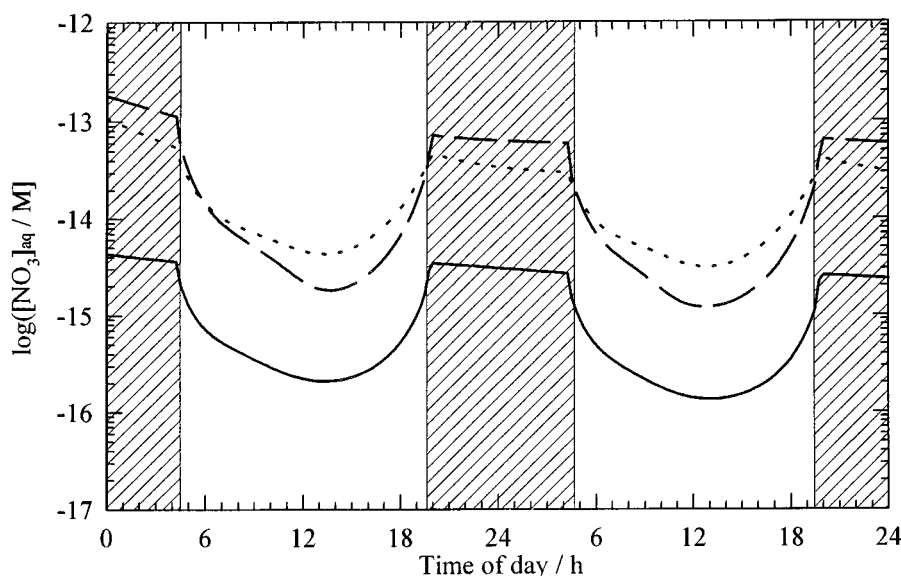
Figure 3. Comparison of model results for $[NO_3]_{aq}$ for urban (......), remote (-----) and marine(———) conditions.

halogenide anions Cl^- and Br^- (R154, R168), which account for more than 90% of the total loss flux $(2.3 \cdot 10^{-10} \text{ M s}^{-1})$.

3.2.2. *Radical Anions*

A plot of the dichloride radical anion concentrations vs time for all three scenarios is shown in Figure 4. The Cl_2^- radical anion is formed in the fast equilibrium (E24), so that the sources for the Cl_2^- correspond to those of the Cl atom. At noon there are two sources for Cl atoms: Firstly, the Cl atom is formed in Reaction (E27) from $ClOH^-$. Since this species is formed in the equilibrium with chloride and OH (E26), the profile of the dichloride radical anion is comparable to that of OH. The second source for chlorine atoms is the reaction of chloride with SO_4^- (R153). Because of elevated NO_3, nighttime $Cl_{(aq)}$ is formed from the NO_3 reaction with chloride during this time. In the urban case, nearly 100% of the chlorine atoms formed are converted to the dichloride radical anion directly, whereas the contribution of the Cl atoms converted in the hydrolysis of the chlorine atom to form $ClOH^-$ is negligible. Further reactions of $ClOH^-$ can be neglected with the only exception of (E28), because this species has a maximum concentration of $9.8 \cdot 10^{-16}$ M, nearly four orders lower than that of Cl_2^-. Generally all Cl formed leads to the formation of Cl_2^- under the conditions considered here.

The maximum concentration of Cl_2^- is reached at noon. In the marine case this concentration is highest, because in this environment the initial concentration of chloride is highest. The main destruction in the marine case is the reaction between Cl_2^- and HO_2/O_2^- (65%) as well as with H_2O_2 (32%). In the urban case, however,
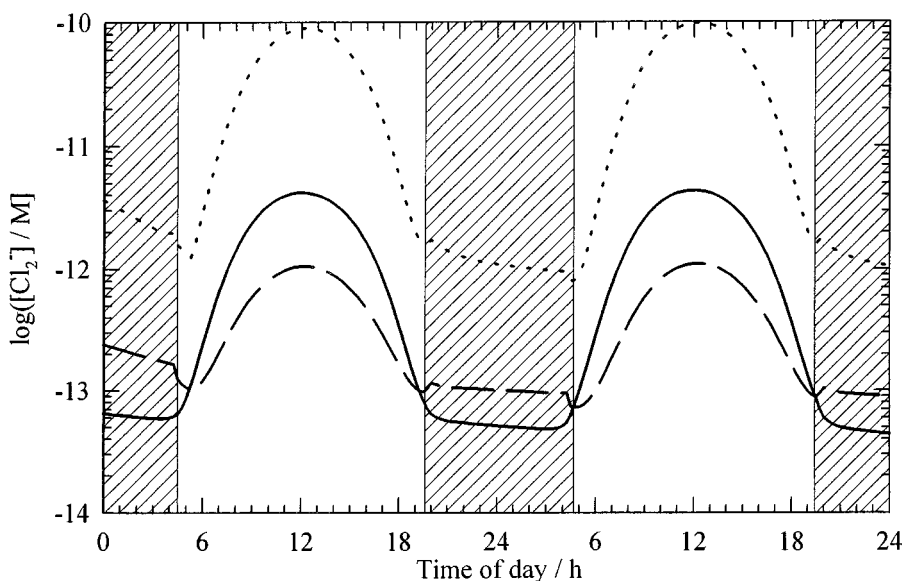
Figure 4. Comparison of model results for [Cl_2^-] for urban (......), remote (-----) and marine(———) conditions.

the destruction of Cl_2^- is dominated by the reactions with Fe^{2+} (50%) and HSO_3^- (37%).

The diurnal variations of the concentration levels of other radical anions, Br_2^-, SO_4^- and CO_3^- are parallel to that of Cl_2^-. They differ only in the maximum concentrations: The maximum of the concentration of the Br_2^- radical anions can be compared with that of the Cl_2^-, because their chemistry is very similar. Its concentration at noon (6.2 · 10^{-11} M) is similar to that of the Cl_2^- radical anion (8.9 · 10^{-11} M). The other two radical anions, the sulphate radical anion, SO_4^-, and the carbonate radical anion CO_3^-, are only present in extremely small concentrations. Both species show a time evolution similar to the dihalogenide radical anions, but their maximum concentration is only 1 · 10^{-14} M, in case of CO_3^- even only 5.5 · 10^{-18} M in the urban case. The production and loss flux of the carbonate radical anion is very small (6.1·10^{-16} M s^{-1}) compared to those of the other radical anions for which they are in the order of 10^{-9} M s^{-1}. For these two radicals their production is mainly influenced by the concentration of OH. At night time they are formed by the reduction of NO_3 via (R52) and (R54).

3.2.3. *Peroxyl Radicals*

Another class of species considered within CAPRAM are the peroxyl radicals in the aqueous phase. The species of interest are the methyl peroxyl radical (MO_2) and the class containing the acetylperoxyl radical (ACO_3) and other C_2 carboxylic peroxyl radicals. The chemistry of the ethyl peroxyl radical in the aqueous phase is

Table VIII. Chlorine chemistry

Reaction no.	Reaction	k_{298}, $M^{-n} s^{-1}$ [a]	E_a/R, K	Reference
R153	$SO_4^- + Cl^- \rightarrow SO_4^{2-} + Cl$	$3.3 \cdot 10^8$	0	Huie and Clifton, 1990; Herrmann *et al.*, 1997
R154	$NO_3 + Cl^- \rightarrow NO_3^- + Cl$	$1.0 \cdot 10^7$	4300	Exner *et al.*, 1992
R155	$Cl_2^- + Cl_2^- \rightarrow Cl_2 + 2Cl^-$	$8.7 \cdot 10^8$		Zellner *et al.*, 1996
R156	$Cl_2^- + Fe^{2+} \rightarrow 2Cl^- + Fe^{3+}$	$1.0 \cdot 10^7$	3030	Thornton and Laurence, 1973
R157	$Cl_2^- + Mn^{2+} \rightarrow 2Cl^- + Mn^{3+}$	$8.5 \cdot 10^6$	4090	Laurence and Thornton, 1973
R158	$Cl_2^- + Cu^+ \rightarrow 2Cl^- + Cu^{2+}$	$1 \cdot 10^7$		$k_{R158} = k_{R156}$
R159	$Cl_2^- + H_2O_2 \rightarrow 2Cl^- + H^+ + HO_2$	$7.0 \cdot 10^5$	3340	Elliot, 1989
R160	$Cl_2^- + MHP \rightarrow 2Cl^- + H^+ + CH_3O_2$	$7.0 \cdot 10^5$	3340	$k_{R160} = k_{R159}$
R161	$Cl_2^- + OH^- \rightarrow 2Cl^- + OH$	$4.0 \cdot 10^6$		Jacobi, 1996
R162	$Cl_2^- + HO_2 \rightarrow 2Cl^- + H^+ + O_2$	$1.3 \cdot 10^{10}$		Jacobi, 1996
R163	$Cl_2^- + O_2^- \rightarrow 2Cl^- + O_2$	$6 \cdot 10^9$		Jacobi, 1996
R164	$Cl_2^- + HSO_3^- \rightarrow 2Cl^- + H^+ + SO_3^-$	$1.7 \cdot 10^8$	400	Jacobi *et al.*, 1996
R165	$Cl_2^- + SO_3^{2-} \rightarrow 2Cl^- + SO_3^-$	$6.2 \cdot 10^7$		Jacobi *et al.*, 1996
R166	$Cl_2 + H_2O \rightarrow H^+ + Cl^- + HOCl$	0.401	7900	Wang and Margerum, 1994

[a] n = reaction order $- 1$.
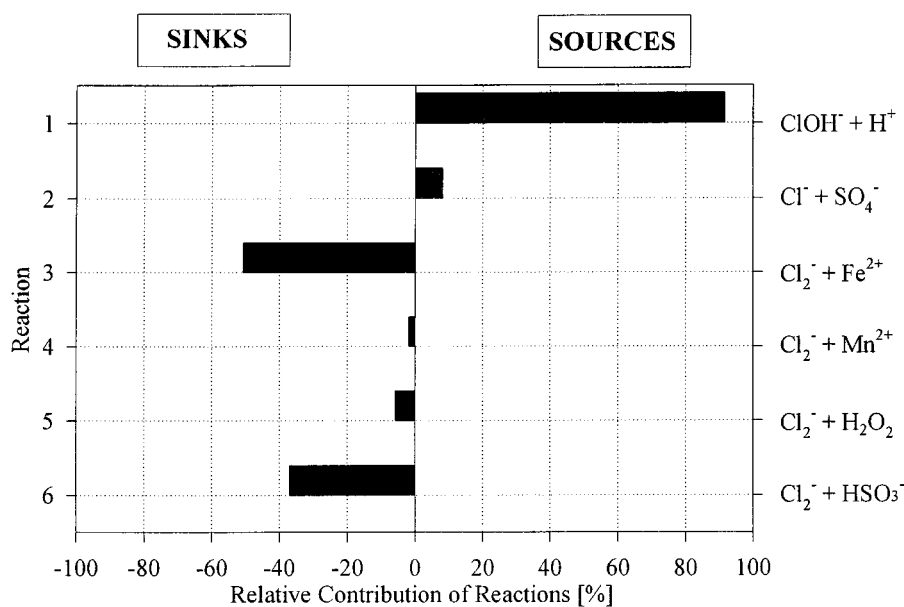
Figure 5. Sinks for $[Cl_2^-]$ and sources for $[Cl \cdot]_{aq}$ for urban conditions, local time: t = 12.00 production flux $[Cl \cdot]_{aq}$: $4.1 \cdot 10^{-8}$ M s^{-1}, loss flux $[Cl_2^-]$: $6.2 \cdot 10^{-9}$ M s^{-1}.
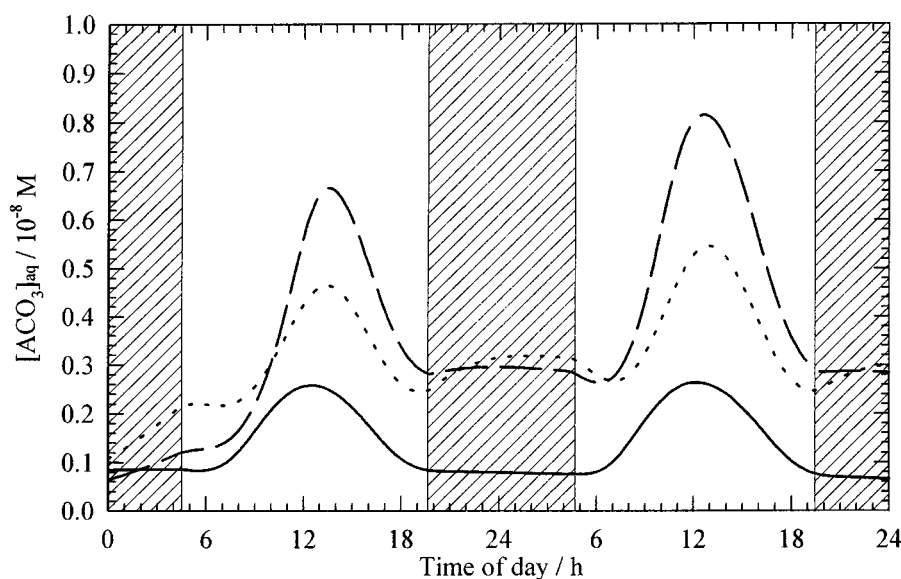
Figure 6. Comparison of model results for [ACO$_3$] for urban (......), remote (-----) and marine(———) conditions (ACO$_3$ = CH$_3$(CO)O$_2$ + O$_2$CH$_2$COOH).

currently restricted to phase transfer followed by its self reaction. To the authors' knowledge, no kinetic data for other reactions such as the cross reaction between the organic peroxyl radicals and HO$_2$/O$_2^-$ are currently available.

In the literature these reactions are assumed as being very slow (von Sonntag, 1987) in the liquid phase. Nevertheless, to estimate the influence of these reactions on the budget of the main radicals test calculations were performed including the reactions between HO$_2$ and CH$_3$O$_2$, ACO$_3$ and ETHP and the reaction of CH$_3$O$_2$ with ACO$_3$. Because of the missing reaction rates the values were taken from the gas phase reactions. All reaction rate constants were in the order of 10^9 M^{-1} s^{-1}. The results from these calculations showed that the OH concentration is not influenced by the reactions added. The HO$_2$ concentration is decreased by about 1%. The diagnosis shows that the reaction with CH$_3$O$_2$ has a contribution of only 3% $(9.2 \cdot 10^{-10}$ M s$^{-1})$ to the total flux. However, the concentration levels of the other peroxyl radicals are decreased significantly (e.g., from $4.3 \cdot 10^{-9}$ M to $1.6 \cdot 10^{-9}$ M in the case of the ACO$_3$ species class at 12:00 of the 2nd day). Due to the current lack of experimental evidence for the occurrence of the RO$_2$/HO$_2$ cross reactions in solution, however, these reactions are neglected.

The diurnal behaviour of the ACO$_3$ species class in solution is shown in Figure 6. During daytime its concentration level reaches $4.3 \cdot 10^{-9}$ M and it is lowered to $3.1 \cdot 10^{-9}$ M during nighttime. This behaviour is influenced by the OH concentration level in the gas phase, because the most important source reaction takes place there. In the aqueous phase ACO$_3$ species are not destroyed, so that the transfer to the gas phase is the only sink. Further reactions of ACO$_3$ are currently not imple-

Table IX. Bromine chemistry

Reaction no.	Reaction	k_{298}, $M^{-n} s^{-1}$ [a]	E_a/R, K	Reference
R167	$SO_4^- + Br^- \rightarrow SO_4^{2-} + Br$	$2.1 \cdot 10^9$		Herrmann *et al.*, 1997
R168	$NO_3 + Br^- \rightarrow NO_3^- + Br$	$3.8 \cdot 10^9$		Zellner *et al.*, 1996
R169	$Br_2^- + Br_2^- \rightarrow Br_2 + 2Br^-$	$1.7 \cdot 10^9$		Reese, 1998
R170	$Br_2^- + Fe^{2+} \rightarrow 2Br^- + Fe^{3+}$	$3.6 \cdot 10^6$	3330	Thornton and Laurence, 1973
R171	$Br_2^- + Mn^{2+} \rightarrow 2Br^- + Mn^{3+}$	$6.3 \cdot 10^6$	4330	Laurence and Thornton, 1973
R172	$Br_2^- + Cu^+ \rightarrow 2Br^- + Cu^{2+}$	$3.6 \cdot 10^6$		$k_{R172} = k_{R170}$
R173	$Br_2^- + H_2O_2 \rightarrow 2Br^- + H^+ + HO_2$	$1.0 \cdot 10^5$		Reese, 1997
R174	$Br_2^- + MHP \rightarrow 2Br^- + H^+ + CH_3O_2$	$1.0 \cdot 10^5$		$k_{R174} = k_{R172}$
R175	$Br_2^- + OH^- \rightarrow 2Br^- + OH$	$1.1 \cdot 10^4$		Jacobi, 1996
R176	$Br_2^- + HO_2 \rightarrow 2Br^- + H^+ + O_2$	$6.5 \cdot 10^9$		Rafi and Sutton, 1965
R177	$Br_2^- + O_2^- \rightarrow 2Br^- + O_2$	$1.7 \cdot 10^8$		Wagner and Strehlow, 1987
R178	$Br_2^- + HSO_3^- \rightarrow 2Br^- + H^+ + SO_3^-$	$5.0 \cdot 10^7$	780	Shoute *et al.*, 1991
R179	$Br_2^- + SO_3^{2-} \rightarrow 2Br^- + SO_3^-$	$3.3 \cdot 10^7$	650	Shoute *et al.*, 1991
R180	$Br_2 + H_2O \rightarrow Br^- + H^+ + HOBr$	1.7	7500	Beckwith *et al.*, 1996

[a] n = reaction order – 1.

Table X. Carbonate chemistry

Reaction no.	Reaction	k_{298}, $M^{-n} s^{-1}$ [a]	E_a/R, K	Reference
R181	$HCO_3^- + OH \rightarrow H_2O + CO_3^-$	$1.7 \cdot 10^7$	1900	Exner, 1990
R182	$CO_3^{2-} + OH \rightarrow OH^- + CO_3^-$	$3.9 \cdot 10^8$	2840	Buxton *et al.*, 1988a,b
R183	$CO_3^{2-} + SO_4^- \rightarrow SO_4^{2-} + CO_3^-$	$4.1 \cdot 10^7$		Estimated
R184	$HCO_3^- + SO_4^- \rightarrow SO_4^{2-} + CO_3^- + H^+$	$2.8 \cdot 10^6$	2090	Huie and Clifton, 1990
R185	$CO_3^{2-} + NO_3 \rightarrow NO_3^- + CO_3^-$	$4.1 \cdot 10^7$		Estimated
R186	$CO_3^{2-} + Cl_2^- \rightarrow 2Cl^- + CO_3^-$	$2.7 \cdot 10^6$		Estimated
R187	$CO_3^{2-} + Br_2^- \rightarrow 2Br^- + CO_3^-$	$1.1 \cdot 10^5$		Huie *et al.*, 1991b
R188	$CO_3^- + CO_3^- \xrightarrow{O_2} 2O_2^- + 2CO_2$	$2.2 \cdot 10^6$		Huie and Clifton, 1990
R189	$CO_3^- + Fe^{2+} \rightarrow CO_3^{2-} + Fe^{3+}$	$2 \cdot 10^7$		Estimated
R190	$CO_3^- + Mn^{2+} \rightarrow CO_3^{2-} + Mn^{3+}$	$1.5 \cdot 10^7$		Cope *et al.*, 1978
R191	$CO_3^- + Cu^+ \rightarrow CO_3^{2-} + Cu^{2+}$	$2 \cdot 10^7$		Estimated
R192	$CO_3^- + H_2O_2 \rightarrow HCO_3^- + HO_2$	$4.3 \cdot 10^5$		Draganic *et al.*, 1991
R193	$CO_3^- + MHP \rightarrow HCO_3^- + CH_3O_2$	$4.3 \cdot 10^5$		$k_{R193} = k_{R192}$
R194	$CO_3^- + HO_2 \rightarrow HCO_3^- + O_2$	$6.5 \cdot 10^8$		$k_{R194} = k_{R195}$
R195	$CO_3^- + O_2^- \rightarrow CO_3^{2-} + O_2$	$6.5 \cdot 10^8$		Eriksen *et al.*, 1985
R196	$CO_3^- + HSO_3^- \rightarrow HCO_3^- + SO_3^-$	$1 \cdot 10^7$		Estimated
R197	$CO_3^- + SO_3^{2-} \rightarrow CO_3^{2-} + SO_3^-$	$5.0 \cdot 10^6$	470	Huie *et al.*, 1991a

[a] n = reaction order – 1.

Table XI. CAPRAM: Aqueous equilibria

Eq. no.	Reactions	K, $M^{a\,z}$	k_{298}, (forward) $M^{-n}\,s^{-1\,z}$	E_a/R, K	Ref.	k_{298} (back) $M^{-n}\,s^{-1\,z}$	E_a/R, K	Ref.
E1	$H_2O \rightleftarrows H^+ + OH^-$	$1.8 \cdot 10^{-16}$	$2.34 \cdot 10^{-5}$	6800	a	$1.3 \cdot 10^{11}$		c
E2	$CO_2 + H_2O \rightleftarrows H_2CO_3$	$7.7 \cdot 10^{-7}$	$4.3 \cdot 10^{-2}$	9250	b	$5.6 \cdot 10^4$	8500	x
E3	$H_2CO_3 \rightleftarrows H^+ + HCO_3^-$	$2 \cdot 10^{-4}$	$1 \cdot 10^7$		c	$5 \cdot 10^{10}$		c
E4	$HCO_3^- \rightleftarrows H^+ + CO_3^{2-}$	$4.69 \cdot 10^{-11}$	2.35	1820	a	$5 \cdot 10^{10}$		c
E5	$HCl \rightleftarrows H^+ + Cl^-$	$1.72 \cdot 10^6$	$8.6 \cdot 10^{16}$	–6890	d	$5 \cdot 10^{10}$		c
E6	$NH_3 + H_2O \rightleftarrows NH_4^+ + OH^-$	$1.77 \cdot 10^{-5}$	$6.02 \cdot 10^5$	560	a	$3.4 \cdot 10^{10}$		c
E7	$HO_2 \rightleftarrows H^+ + O_2^-$	$1.6 \cdot 10^{-5}$	$8.0 \cdot 10^5$	0	e f	$5 \cdot 10^{10}$	0	y
E8	$HNO_3 \rightleftarrows H^+ + NO_3^-$	22	$1.1 \cdot 10^{12}$	–1800	g h	$5 \cdot 10^{10}$		c
E9	$HNO_2 \rightleftarrows H^+ + NO_2^-$	$5.3 \cdot 10^{-4}$	$2.65 \cdot 10^7$	1760	i	$5 \cdot 10^{10}$		c
E10	$HO_2NO_2 \rightleftarrows H^+ + O_2NO_2^-$	$1 \cdot 10^{-5}$	$5 \cdot 10^5$		j	$5 \cdot 10^{10}$		y
E11	$NO_2 + HO_2 \rightleftarrows HO_2NO_2$	$2.2 \cdot 10^9$	$1.0 \cdot 10^7$		k	$4.6 \cdot 10^{-3}$		k
E12	$SO_2 + H_2O \rightleftarrows HSO_3^- + H^+$	$3.13 \cdot 10^{-4}$	$6.27 \cdot 10^4$	–1940	l	$2.0 \cdot 10^8$		c
E13	$HSO_3^- \rightleftarrows SO_3^{2-} + H^+$	$6.22 \cdot 10^{-8}$	3110	–1960	l	$5 \cdot 10^{10}$		c
E14	$HSO_4^- \rightleftarrows SO_4^{2-} + H^+$	$1.02 \cdot 10^{-2}$	$1.02 \cdot 10^9$	–2700	g	$1 \cdot 10^{11}$		c
E15	$HCOOH \rightleftarrows HCOO^- + H^+$	$1.77 \cdot 10^{-4}$	$8.85 \cdot 10^6$	–12	a	$5 \cdot 10^{10}$		c
E16	$HAc \rightleftarrows Ac^- + H^+$	$1.75 \cdot 10^{-5}$	$8.75 \cdot 10^5$	–46	a	$5 \cdot 10^{10}$		c
E17	$Fe^{3+} + H_2O \rightleftarrows [Fe(OH)]^{2+} + H^+$	$1.1 \cdot 10^{-4}$	$4.7 \cdot 10^4$		m	$4.3 \cdot 10^8$		m
E18	$[Fe(OH)]^{2+} + H_2O \rightleftarrows [Fe(OH)_2]^+ + H^+$	$1.4 \cdot 10^{-7}$	$1.1 \cdot 10^3$		n	$8.0 \cdot 10^9$		n
E19	$Fe^{3+} + SO_4^{2-} \rightleftarrows [Fe(SO_4)]^+$	$1.8 \cdot 10^{-2}$	$3.2 \cdot 10^3$		m	$1.8 \cdot 10^5$		m
E20	$HCHO + H_2O \rightleftarrows CH_2(OH)_2$	36	0.18	–4030	o	$5.1 \cdot 10^{-3}$		o
E21	$CH_3CHO + H_2O \rightleftarrows CH_3CH(OH)_2$	$2.46 \cdot 10^{-2}$	$1.4 \cdot 10^{-4}$	–2500	p	$5.69 \cdot 10^{-3}$		p
E22	$CH_2(OH)_2 + HSO_3^- \rightleftarrows HMS^- + H_2O$	$2 \cdot 10^8$	790	2990	q	$3.95 \cdot 10^{-6}$	2990	q
E23	$CH_2(OH)_2 + SO_3^{2-} \rightleftarrows HMS^- + OH^-$	$3.6 \cdot 10^6$	$2.5 \cdot 10^7$	2450	r	$3.95 \cdot 10^{-6}$	5530	q
E24	$Cl + Cl^- \rightleftarrows Cl_2^-$	$1.9 \cdot 10^5$	$2.7 \cdot 10^{10}$		r	$1.4 \cdot 10^5$		t
E25	$Br + Br^- \rightleftarrows Br_2^-$	$6 \cdot 10^5$	$1.2 \cdot 10^{10}$		s	$1.9 \cdot 10^4$		s
E26	$Cl^- + OH \rightleftarrows ClOH^-$	0.7	$4.3 \cdot 10^9$		t	$6.1 \cdot 10^9$		t
E27	$ClOH^- + H^+ \rightleftarrows Cl + H_2O$	$1.6 \cdot 10^7$	$2.1 \cdot 10^{10}$		t	$1.3 \cdot 10^3$		t
E28	$ClOH^- + Cl^- \rightleftarrows Cl_2^- + OH^-$	$2.2 \cdot 10^{-4}$	$1.0 \cdot 10^4$		u	$4.5 \cdot 10^7$		u
E29	$Br^- + OH \rightleftarrows BrOH^-$	333	$1.1 \cdot 10^{10}$		v	$3.3 \cdot 10^7$		v
E30	$BrOH^- + H^+ \rightleftarrows Br + H_2O$	$1.8 \cdot 10^{12}$	$4.4 \cdot 10^{10}$		w	$2.45 \cdot 10^{-2}$		w
E31	$BrOH^- + Br^- \rightleftarrows Br_2^- + OH^-$	70	$1.9 \cdot 10^8$		w	$2.7 \cdot 10^6$		w

[a] Harned and Owen (1958); [b] Welch *et al.* (1969); [c] Graedel and Weschler (1981); [d] Marsh and McElroy (1985); [e] Bielski *et al.* (1985); [f] Baxendale *et al.* (1971); [g] Redlich (1946); [h] Redlich and Hood (1957); [i] Park and Lee (1988); [j] Lammel *et al.* (1990); [k] Warneck and Wurzinger (1988); [l] Beilke and Gravenhorst (1978); [m] Brandt and van Eldik (1995); [n] Hemmes *et al.* (1971); [o] Bell and Evans (1966); [p] Bell *et al.* (1956); [q] Olson and Hoffmann (1989); [r] Jacobi *et al.* (1997); [s] Merényi and Lind (1994); [t] Jayson *et al.* (1973); [u] Grigor'ev *et al.* (1987); [v] Klaning and Wolff (1985); [w] Fornier de Violet (1981); [x] Sirs (1958); [y] estimated; [z] a: stochiometric coefficient, n: reaction order – 1.

mented because of missing laboratory data. With respect to the gas phase, however, transfer from the aqueous phase contributes less than 1% of the total production flux (in the urban case $5.7 \cdot 10^5$ cm^{-3} s^{-1}). In Figure 7 the corresponding evolution for the methyl peroxyl radical (MO$_2$) is shown. The maximum concentration is reached in the marine case ($2 \cdot 10^{-10}$ M). In the other two environments, urban and rural, the concentration increases at daytime only to $1.3 \cdot 10^{-10}$ M and $1.5 \cdot 10^{-10}$ M, respectively. The evolution of MO$_2$ is similar to the one of the OH radical. This
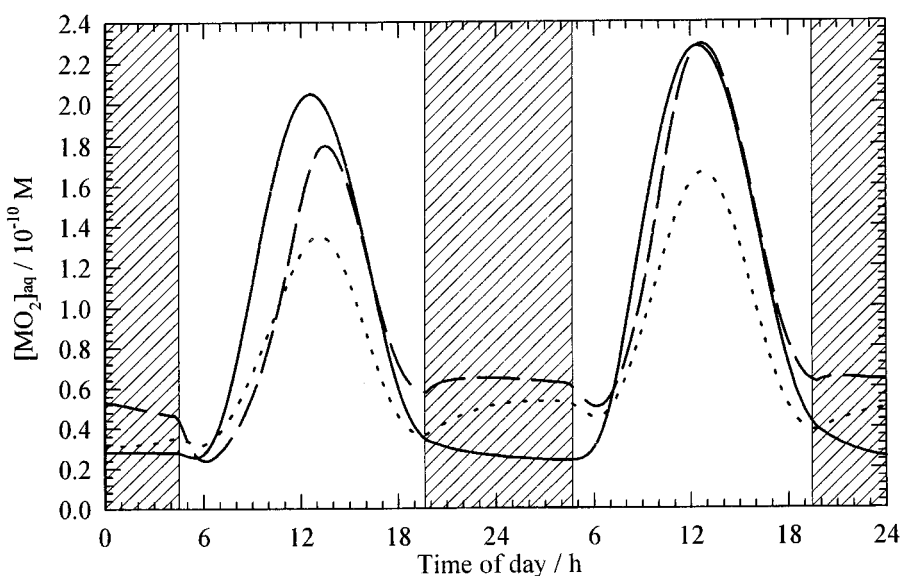
Figure 7. Comparison of model results for [MO_2] for urban (......), remote (-----) and marine(———) conditions ($MO_2 = CH_3O_2$).

can be explained by the main production of the methyl peroxyl radical in the gas phase, which is the reaction between methane and OH and which accounts for 61% of the total production flux ($4.8 \cdot 10^5$ cm^{-3} s^{-1}) in the urban case at noon.

If the curves are compared to those of the OH radical it is evident that the differences are less between the first and second days shown here. In the remote case the maximum concentrations of the OH radical are equal at noon ($1.7 \cdot 10^{-12}$ M) but differences between the levels of the ACO_3 radical exist. Its concentration is increased from $5.7 \cdot 10^{-9}$ M to $8.0 \cdot 10^{-9}$ M. As shown before the most important loss process for OH in solution is its reaction with formaldehyde in its hydrated form. Because of the high concentration ($5.3 \cdot 10^{-6}$ M) this latter species shows no diurnal variation. The most important source for ACO_3 in the aqueous phase are the reactions of acetic acid/acetate with OH (R139, R140). Acetic acid accumulates in both phases from $5.2 \cdot 10^{-7}$ M and $1.1 \cdot 10^9$ cm^{-3} to $1.1 \cdot 10^{-6}$ M and $2.4 \cdot 10^9$ cm^{-3}, respectively, so that the formation flux contributed by (R139) increases.

3.2.4. *Transition Metal Ions (TMI)*

Calculations within the present study were performed with initial concentrations for Mn^{3+}, Fe^{3+} and Cu^+. The underlying physical picture is that upon activation of cloud condensation nuclei containing crustal material, transition metals are dissolved into developing cloud droplets. All TMI are present as soluble species, so that the values can be assumed as total TMI concentrations. In the urban case iron is totally reduced to iron (II) by copper (I). At noon of the second day of the simulation the concentration level of Fe^{2+} reaches $5 \cdot 10^{-6}$ M. The iron(III)-

Table XII. Photolysis rates (aqueous phase), geographical latitude of 51° N

Reaction no.	Reaction	J [s^{-1}]	Range of quantum yield Φ	References
P1	$H_2O_2 + h\nu \rightarrow 2OH$	$7.19 \cdot 10^{-6}$	0.98 ± 0.03 [a]	Zellner *et al.*, 1990
			0.96 ± 0.03 [b]	Zellner *et al.*, 1990
P2	$[Fe(OH)]^{2+} + h\nu \rightarrow Fe^{2+} + OH$	$4.51 \cdot 10^{-3}$	$0.312 \pm 0.03 \ldots 0.074 \pm 0.015$ [c]	Benkelberg and Warneck, 1995
P3	$[Fe(OH)_2]^+ + h\nu \rightarrow Fe^{2+} + OH + OH^-$	$5.77 \cdot 10^{-3}$	$0.255 \ldots 0.07$ [d]	Benkelberg *et al.*, 1991
P4	$[Fe(SO_4)]^+ + h\nu \rightarrow Fe^{2+} + SO_4^-$	$6.43 \cdot 10^{-3}$	$(7.9 \pm 0.34 \ldots 1.56 \pm 0.02) \cdot 10^{-3}$ [c]	Benkelberg and Warneck, 1995
P5	$NO_2^- + h\nu \xrightarrow{H^+} NO + OH$	$2.57 \cdot 10^{-5}$	0.07 ± 0.01 [a]	Zellner *et al.*, 1990
			0.046 ± 0.009 [b]	Zellner *et al.*, 1990
P6	$NO_3^- + h\nu \xrightarrow{H^+} NO_2 + OH$	$4.28 \cdot 10^{-7}$	0.017 ± 0.003	Zellner *et al.*, 1990

[a] $\lambda = 308$ nm, T $= 298$ K; [b] $\lambda = 351$ nm, T $= 298$ K; [c] $\lambda = 280 \ldots 370$ nm; [d] $\lambda = 290 \ldots 365$ nm.
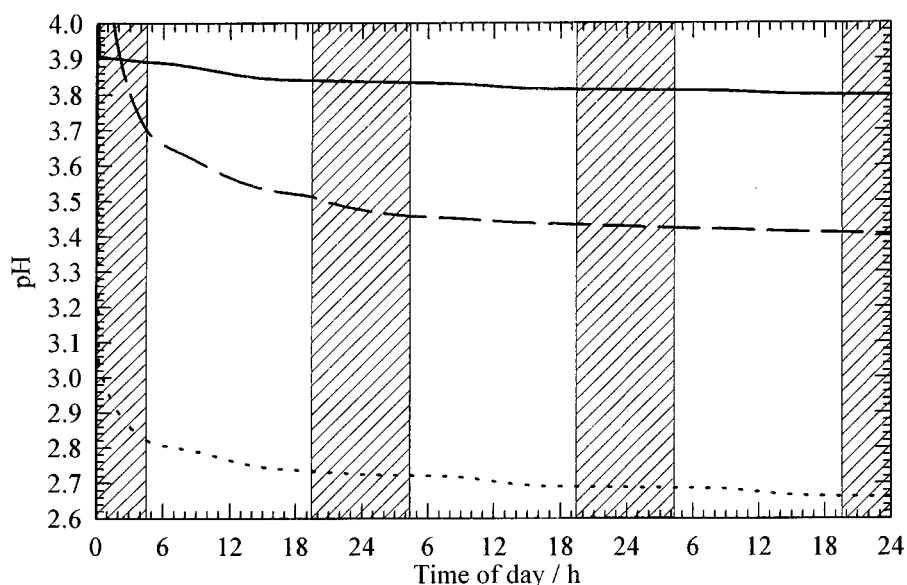
Figure 8. Comparison of model results for the pH value for urban (......), remote (-----) and marine(———) conditions.

monohydroxo-complex, the form of iron(III) with the highest concentration at the given pH value, has a maximum concentration of $1.3 \cdot 10^{-8}$ M only, so that 99.7% of the iron is reduced by copper. The distribution of the manganese is similar: Here the reduced form has a concentration of $[Mn^{2+}] = 4.9 \cdot 10^{-6}$ M, whereas Mn^{3+} is negligible with $3.3 \cdot 10^{-10}$ M at noon. The reduction mainly (90%) takes place by the reaction with hydrogen peroxide (R5). The redox reaction with Fe^{2+} is less important (10%) because of the lower Fe^{2+} concentration compared to H_2O_2 ($8.5 \cdot 10^{-6}$ M). Nearly 60% of the copper in the urban case is oxidised by Fe^{3+} and $Fe(OH)^{2+}$, respectively, so that during day time Cu^{2+} has a concentration of $2.2 \cdot 10^{-7}$ M. The Cu^{2+} ion is then reduced again by HO_2 and therefore it affects the pH value.

In the remote cases the differences in the concentration levels of the TMI are similar to those in the urban case. Whereas, however, 98% of the iron ($4.9 \cdot 10^{-7}$ M) and $\sim$100% of manganese ($2.5 \cdot 10^{-8}$ M) are present in the reduced form, the corresponding fraction for copper is only 29% ($7.5 \cdot 10^{-9}$ M).

In the marine case, Fe^{2+} contributes only 85% of the total iron. The concentration levels of both copper species are nearly equal: only 59% ($5.9 \cdot 10^{-10}$ M) are present in the oxidised form. In the marine case the HO_x concentration is higher so that the fluxes of oxidation and reduction of the copper by HO_2/O_2^- (R17, R18, R20, R21) are nearly equal (oxidation: $6.2 \cdot 10^{-9}$ M s^{-1}, reduction: $6.5 \cdot 10^{-9}$ M s^{-1}). This is in agreement with the highly dynamic coupling of HO_x- and TMI-chemistry as suggested by Matthijsen *et al.* (1996).

3.2.5. *pH Value*

The evolution of the pH value in all three cases over the total simulation time of three days is shown in Figure 8. In the urban case the pH reaches a minimum value of 2.7, whereas in the remote and marine case it is reduced to 3.4 and to 3.8, respectively.

In the urban case pH is determined in the first step by the formation of the iron(III)-monohydroxo-complex in the aqueous phase (E18), because at the given initial pH iron is present as the complex. In the second time step of the calculation (after 900s) soluble gases such as HCl, HCOOH, SO_2 and HNO_3, are transported into the droplet causing an increase of the H^+ concentration. If the system is at steady state the pH value is mainly influenced by the reaction between Cu^{2+} and HO_2 (R20) and not by the dissociation equilibria. The flux of this reaction at noon of the second day amounts to $2.3 \cdot 10^{-8}$ M s^{-1}. In the remote case, the behaviour of the pH is similar but because of the lower initial concentrations of the trace gases (HCl, SO_2, HNO_3) the decrease of the pH is less effective than in the urban case.

In the marine case, the formation of the complex of iron contributes insignificantly to the H^+ concentration, so that the dissolution of SO_2 and the further dissociation to HSO_3^- and SO_3^{2-} becomes more important. In this case the most effective source reaction for H^+ ions is the reduction of Cu^{2+} by HO_2. In the marine scenario, the oxidation of Cu^+ by HO_2 is an important sink for H^+ ions. So, it can be summarised the pH is also controlled by the reactions of HO_2 and Cu^+/Cu^{2+}.

An additional simulation of the pH value was performed with the mechanism of Section 3.2.1, in which TMI chemistry is neglected. Under urban conditions the pH value do not differ significantly (pH = 2.6 at the end of the third day). However, in this case the most important source for the H^+ ions are the reactions of HO_2 with Cl_2^- and Br_2^-. Because of the absence of Cu^{2+} the concentration of HO_2 is enhanced.

3.3. S(IV) → S(VI) CONVERSION

As discussed earlier, several pathways exist in which S(IV) species are oxidised to S(VI). In Figure 14 the most important interconversions are shown for the urban polluted case at noon. Since the SO_3^{2-} concentration in the calculated pH range is negligible, the oxidation starts with HSO_3^-. The direct oxidation is initiated by H_2O_2 and, to a minor extent, by O_3.

Under urban conditions and the initial conditions chosen here (SO_2 = 10 ppb; H_2O_2 = 1 ppb) the reaction path from HSO_3^-/SO_3^{2-} with OH, Cl_2^- and Br_2^- to SO_3^- is more efficient by a factor of 10 compared to the oxidation of S(IV) to S(VI) by H_2O_2 and ozone, respectively (cf. Figure 14). The most significant paths are the reactions with the dihalogenide radical anions and OH. Because the radical anions reach higher concentrations at noon their initiation leads to more effective S(IV)–S(VI) conversion. The resulting sulfite radical anion is quantitatively converted to SO_5^-. In the further reaction steps the importance of the metal ions

for the tropospheric sulphur oxidation is evident: The peroxomonosulfate is fully oxidised by Fe^{2+} and Mn^{2+}, in the reactions (R72) and (R74) producing HSO_5^-. Peroxomonosulfate is an intermediate, which reacts with Fe^{2+} yielding the sulphate radical anion (SO_4^-). During the further oxidation to the sulphate anion, Fe^{2+} plays a minor role with 1% of the loss flux. The main sink for SO_4^- is the reaction with chloride (R153), because the chloride concentration is higher than that of OH^- and, additionally, the reaction rate is increased by nearly one order of magnitude than that of the corresponding reaction of SO_4^- and OH^-.

The reverse reaction of HSO_4^- to SO_4^-

$$X + HSO_4^- \rightarrow HX + SO_4^- \,,$$
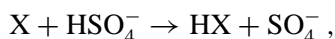
takes place with the X = OH radical during daytime and with X = NO_3 at nighttime. But the contribution of these reactions to the SO_4^- production are nearly negligible: the OH reaction produces about 1% ($4.7 \cdot 10^{-11}$ M s^{-1}) of the sulfate radical anion, the NO_3 reaction even only 0.03% with a flux of $1.4 \cdot 10^{-14}$ M s^{-1}.

The other oxidation pathway from the sulphate radical anion to S(VI) is a two-step reaction, where an iron-sulfato-complex is formed as an intermediate. This pathway may be neglected in further considerations, because the flux is two orders lower than that of the reaction between the sulphate radical anion and chloride. The high concentration of the complex is caused from Reaction (E19), i.e., the equilibrium between Fe^{3+}, SO_4^{2-} and the complex:

$$SO_4^{2-} + Fe^{3+} \rightleftarrows [Fe(SO_4)]^+ \,. \tag{E19}$$

The start of the S(IV) oxidation is similar to the one assumed in the work of Jacob (1986). The main source of SO_3^- is the oxidation of HSO_3^- with radicals. Jacob considers the reaction of HSO_3^- with Cl_2^-, but in his mechanism this reaction does not significantly contribute to SO_3^- production. This is different from the present work, because the rate for this reaction (R164), as measured by Jacobi (1997) and applied here, is nearly one order of magnitude higher than the value estimated by Jacob ($4.6 \cdot 10^7$ M^{-1} s^{-1}). Furthermore, the corresponding reaction with the dibromide radical anion is not included in Jacob's mechanism.

The processes following the formation of SO_5^- are also different when Jacob's model and CAPRAM are compared. Jacob (1986) assumed that reactions with $HCOO^-$, O_2^- and HSO_3^- are responsible for the further reaction to HSO_5^-. The last two of these reactions are also considered in CAPRAM. However, their contribution of the destruction flux is less than $1 \cdot 10^{-3}$%. No kinetic parameters are available for possible reactions of SO_5^- with organics such as $HCOOH/HCOO^-$ which were, accordingly, not considered at this stage. In addition, Jacob's initial mechanism (1986) contains no reactions with TMIs. Although in a later publication (Jacob, 1989) TMIs are included, still no reactions with sulphur containing species were treated. In his work, Jacob outlines the importance of the S(IV) oxidation by H_2O_2. The efficiency of this reaction is dependent on the initial concentration of H_2O_2 and SO_2 which was 3.4 ppb H_2O_2 and 0.1 ppb SO_2 in his work. Because
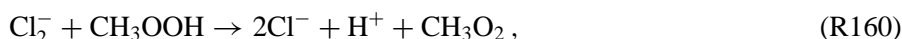
the SO_2 concentration is significantly smaller than the H_2O_2 concentration, this corresponds to an unpolluted scenario. In the present calculations with CAPRAM the initial parameters are chosen for a polluted scenario with 1 ppb H_2O_2 and 10 ppb SO_2. Because of this, in CAPRAM another S(IV) sink, the reaction with O_3, starts contributing to S(IV) oxidation once H_2O_2 is depleted from the gas phase. In fact, the contribution of the S(IV) depletion by H_2O_2 loses in significance because the concentration of $H_2O_{2(aq)}$ at noon of the second day is reduced by one order of magnitude ($8.5 \cdot 10^{-6}$ M) compared to the first time step.

3.4. OXIDATION OF C_1 AND C_2-COMPOUNDS

To the authors' knowledge, CAPRAM is currently the only aqueous phase mechanism, where not only the C_1, but also the C_2 organic species are considered. The oxidation of these species begins with the alcohols, which are transferred from the gas phase. In the liquid phase these species are oxidised to aldehydes and to carboxylic acids. A reaction scheme, outlining mass fluxes and the concentrations at 12:00 (urban case, 2nd day) is shown in Figure 15.

The reaction step from methanol to formaldehyde is dominated by the OH radical reaction (R103). The reactions with the other radicals contributes less than 1%. Further oxidation steps to yield formic acid and CO_2 are exclusively caused by the OH radical. Hydrated formaldehyde, existing in excess to HCHO by a factor of 1000, is in equilibrium with hydroxy methane sulfonate by (E22, E23).

The oxidation of the C_2-species, starting with ethanol, is more complex. The first steps, i.e., the oxidation to acetaldehyde and acetic acid are also dominated by the OH radical. The main sink of acetic acid is its further oxidation to the carboxyl-methyl peroxyl radical. With acetate, the other radicals react in electron transfer reactions, as described in Section 1.2. Less than 1% of the acid reacts with Cl_2^- (R145) to yield CH_3O_2. This pathway represents a link between the C_1 and C_2 organic chemistry. The reaction occurs also with other radicals such as SO_4^-, Br_2^- and NO_3, but the fluxes are very small. The recombination of two methyl peroxyl radicals leads to formaldehyde, but the main fraction of $CH_3O_{2(aq)}$ (70%) is destroyed by HSO_3^- to form methyl hydroperoxide. $CH_3O_{2(aq)}$ may be regenerated by the reaction from the methyl hydroperoxide to the methylperoxyl radical with OH (55%) or Cl_2^- (45%):

$$Cl_2^- + CH_3OOH \rightarrow 2Cl^- + H^+ + CH_3O_2 \,, \tag{R160}$$

$$CH_3OOH + OH \rightarrow CH_3O_2 + H_2O \,. \tag{R32}$$

In the work by Jacob (1986), a similar oxidation chain from formaldehyde to formic acid is described. Conversion from methyl peroxyl radical to methyl hydroperoxide is described with the reaction with HO_2/O_2^- which is not included in CAPRAM, because of missing experimental evidence for this process. However, the importance of the OH radical as an oxidising species is also presented

in this work. In the work by Walcek *et al.* (1997) the oxidation reactions of the organic species are restricted to OH reactions and only the destruction of formic acid to form carbon dioxide by reactions with the Cl_2^- radical anion is additionally considered.

3.5. CONCENTRATION LEVELS OF GAS PHASE SPECIES IN THE ABSENCE AND PRESENCE OF THE AQUEOUS PHASE

The importance of aqueous phase tropospheric processes is demonstrated in the following comparisons of results obtained with separate calculations of the complete CAPRAM and RADM2 mechanisms only. As can be seen from Figure 13, in the urban case the concentrations of both the OH radical and the NO_3 radical in the gas phase are significantly reduced when liquid phase chemistry is included. During daytime the difference between the concentration levels of the OH radical amounts to more than a factor of five. During night-time, however, multiphase processes influence the NO_3 radical in the gas phase even more strongly with the result that the NO_3 concentration levels change from $1.9 \cdot 10^9$ cm^{-3} to $1.4 \cdot 10^6$ cm^{-3}, more than three orders of magnitude.

The difference in concentration of OH and NO_3 in the presence and absence of the liquid phase is mainly due to the phase transfer because both species are effectively removed by the aqueous phase. At noon, the flux of the OH radical is nearly $5.5 \cdot 10^6$ cm^{-3} s^{-1} which is about 58% of the total loss flux of the OH radical at this time. For NO_3 the relative loss into the liquid phase equals about 90% of the total loss flux ($4.3 \cdot 10^4$ cm^{-3} s^{-1}).

The peroxyl radicals show the inverse behaviour to NO_3 and OH radicals during daytime (cf. also Figure 13). Their concentration levels in the gas phase are increased between 5% and 10%, when liquid phase chemistry is included. This effect is explained by the fact that in RADM2 important sinks for both peroxyl radicals exist such as the cross recombination reactions with HO_2 forming peroxyacetic acid (PAA) in the case of the acetyl peroxyl radical and methyl hydrogen peroxide (CH_3OOH) in the case of the methyl peroxyl radical. The HO_2 concentration in the gas phase in the presence of the aqueous phase is reduced from $6 \cdot 10^8$ cm^{-3} to $4.9 \cdot 10^5$ cm^{-3} at noon in the urban case, much stronger than that of RO_2 radicals.

During night time the ratio between the concentrations calculated with and without liquid phase shows the inverse behaviour compared to the daytime. In RADM2 the acetyl peroxyl radical is formed from the reaction between aldehydes (ALD) and NO_3. Because of the phase transfer of the nitrate radical into the droplet the efficiency of this source is reduced in the presence of the liquid phase. The concentration level of the methyl peroxyl radical during night time is somewhat dependent on that of the acetylperoxyl radical because MO_2 is also formed from the recombination of two acetyl peroxyl radicals. It must be noted that the direct phase transfer of the peroxyl radicals is not very important as a source or sink in all cases (at most 5% of the total flux). Differences in concentration levels are rather

caused from the phase transfer of compounds forming or destroying the peroxyl radicals.

A further aspect of CAPRAM calculations refers to tropospheric gas phase ozone. Figure 13 shows also that the absolute difference in the $O_{3(g)}$ concentration under urban conditions after three days amounts to 15 ppb. Under marine conditions the difference is reduced to 1.5 ppb. These values are high in comparison to Walcek $et\ al.$ (1997), who predicts an O_3 loss of less than 2 ppb. It should be taken into account, however, that Walcek $et\ al.$ (1997) have neglected the S(IV) to S(VI) conversion reactions in the liquid phase mechanism. Our CAPRAM analysis shows, that under marine conditions the reaction of HSO_3^- with ozone has a noon flux of $1.7 \cdot 10^{-12}$ M s^{-1} (total flux $4.3 \cdot 10^{-10}$ M s^{-1}), hence establishing an additional ozone loss process.

3.6. CONCENTRATION LEVELS OF AQUEOUS PHASE RADICALS IN A SHORTER CLOUD PERIOD

For the results presented so far it has been assumed to a first approximation, that the cloud considered exists continuously. Although with this assumption the maximum effect of the aqueous phase on the tropospheric chemistry is demonstrated, it may not be considered as being realistic. It has been suggested that cloudy and cloudfree periods alternate in such a way that an air parcel remains in a stratiform cloud for 2–4 hours followed by a cloudfree period which is up to 20 times longer (Lelieveld and Crutzen, 1990).

Based on this picture further calculations were performed with a cloud period of four hours every day. For simplification the liquid water content was set spontaneously to $3 \cdot 10^{-7}$ vol/vol at the beginning of the cloud period. The concentrations at the end of a cloud period are used as the initial concentrations for the next cloud.

In Figure 9 the concentration levels of the OH radical in the aqueous phase for all three different scenarios are shown in comparison to the continuous cloud scenario from Figure 1. It can be seen that in the continental cases (urban and remote) the maximum concentrations are reduced significantly to $4.9 \cdot 10^{-13}$ M and $3.6 \cdot 10^{-13}$ M, respectively, corresponding to a factor of two and three when compared to the concentrations from the previous calculations. In the marine case the concentrations show no large differences. This different behaviour can be explained on the basis of the different reaction pathways for OH in the gas and aqueous phase, which in the latter phase is mainly with organic species. If a cloud does not exist the contribution of the concentration levels in the scenarios is inverse, because the main OH source in the gas phase is the reaction between $O(^1D)$ with water. If the cloud period starts at 14 h not only OH but also all soluble organics are transported into the droplet, so that in the urban case radicals as well as organics are destroyed more effectively than in the marine case, establishing the highest OH concentrations in either phase for the marine scenario.
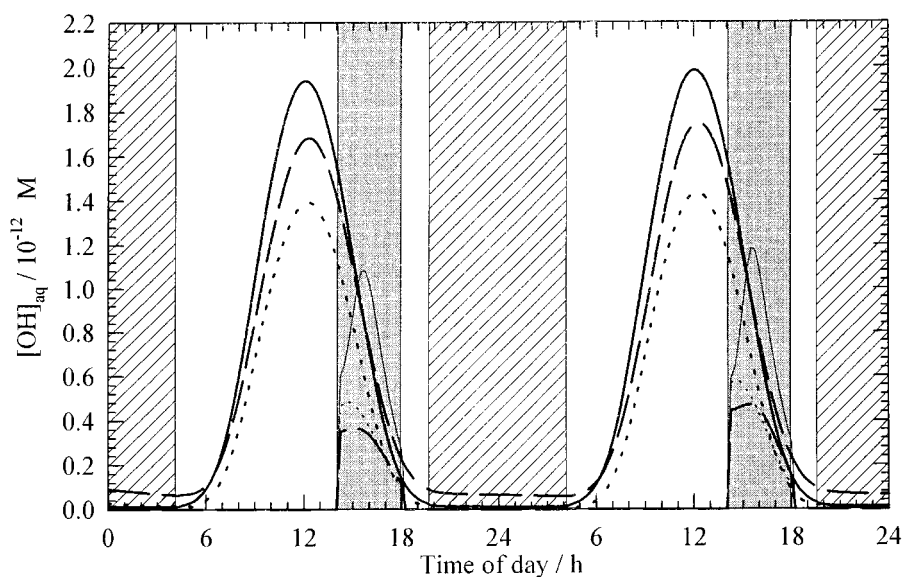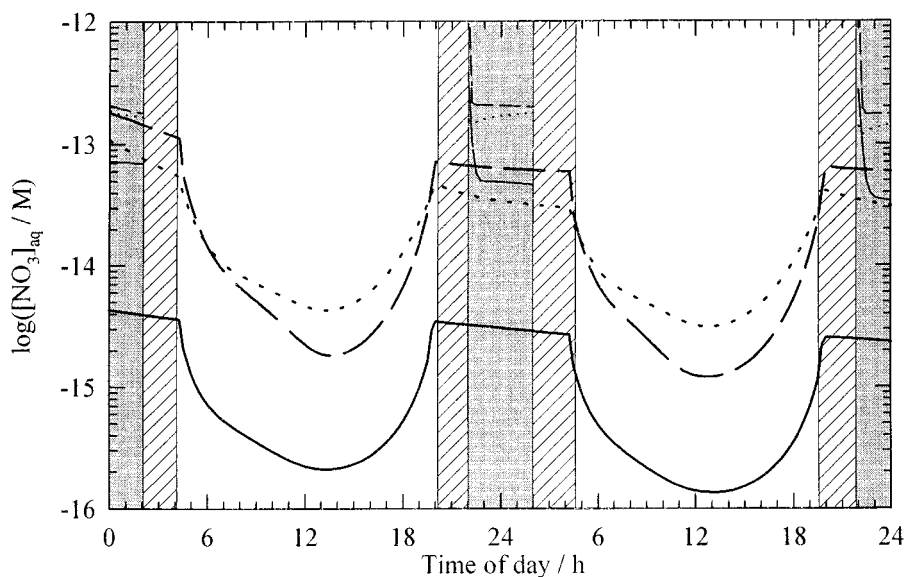
Figure 9. Comparison of model results for $[OH]_{aq}$ for urban (......), remote (-----) and marine(———) conditions with a permanent cloud (bold lines) and with a cloud of 4 h per day.

The reduction of the cloud period can also lead to enhanced radical concentrations in the aqueous phase. In Figure 10 the concentration levels of the NO_3 radical are shown in a cloud period between 22 h and 2 h during night time. As in Figure 3 in the remote case the concentration is highest, and in the marine scenario it is decreased by one order of magnitude. The course of the levels in the remote and marine scenario is striking because after the first time step the concentrations are reduced by a factor of 7 or 4, respectively. The reason for this is that the most important sink reaction is the reaction with HSO_3^- (R43). Because of the higher initial concentration of SO_2 in the urban case, more SO_2 is transported into the aqueous phase forming HSO_3^-. The formation of HSO_3^- is delayed in the other cases, so that in the first step NO_3 is transferred into the droplet and only then the SO_2 concentration leads to sufficient amounts of HSO_3^-.

These examples show that the reduction of the cloud duration period changes the concentration levels for OH and NO_3, however, the differences between the three cases are not changed. The differences, at least partly, are due to the delayed dissolution of the trace gas reactants to reach their original concentration levels in the cloudwater where they act as radical sinks.

3.7. THE INFLUENCE OF THE DROPLET DIAMETER

For the simulations of the cloud chemistry a monodispersed droplet distribution was chosen with a droplet diameter of 1 μm. With this value a very large droplet surface is present enabling as much interactions between both phases as possible.

Figure 10. Comparison of model results for [NO$_3$]$_{aq}$ for urban (......), remote (-----) and marine(———) conditions with a permanent cloud (bold lines) and with a cloud of 4 h per day.

To represent environmental conditions more realisticly, the droplet radius was also changed to 5 and 10 μm for some calculations. The liquid water content is held constant in these considerations so that the total droplet surface is reduced by a factor of 5 and 10, respectively compared to a radius of 1 μm (1.3 · 10^{-11} m$^2_{aq}$ cm$^{-3}_g$). Under these conditions the droplet concentration is 570 cm^{-3} for the 5 μm droplets and only 70 cm^{-3} for the largest droplets considered.

In Figure 11 the different OH concentration levels for urban conditions are shown. It is evident that with the smallest droplets the OH concentration is highest. If the radius is smaller by a factor of five the concentration is reduced by more than a factor of three (4.5 · 10^{-13} M at noon). With the consideration of 10 μm droplets the concentration is reduced by another factor of two to 2.2 · 10^{-13} M. These ratios between droplet radius and concentration clarifies that the OH uptake is dependent on the surface area of the droplets as shown in Section 3.1. With the largest droplets the phase transfer is less important contributing only 6% of the sinks of OH$_{(g)}$. The concentration of OH in the gas phase is consequently enhanced by a factor of 2.6 to 2.6 · 10^6 cm^{-3} compared to the results with 1 μm droplets, whereas the flux from the gas phase into the droplets is reduced by one order of magnitude to 3.3 · 10^5 cm^{-3} s^{-1}.

The different concentrations for the HO$_2$ radical in the aqueous phase are presented in Figure 12. Here the concentrations change only by 20%, from 8.8 · 10^{-11} M in 1 μm droplets to 9.6 · 10^{-11} M in 10 μm droplets and 1 · 10^{-10} M in 5 μm droplets, respectively. This behaviour cannot be found in the gas phase. Whereas in the present of the smallest droplets the concentration is 4.9·10^5 cm^{-3}, it
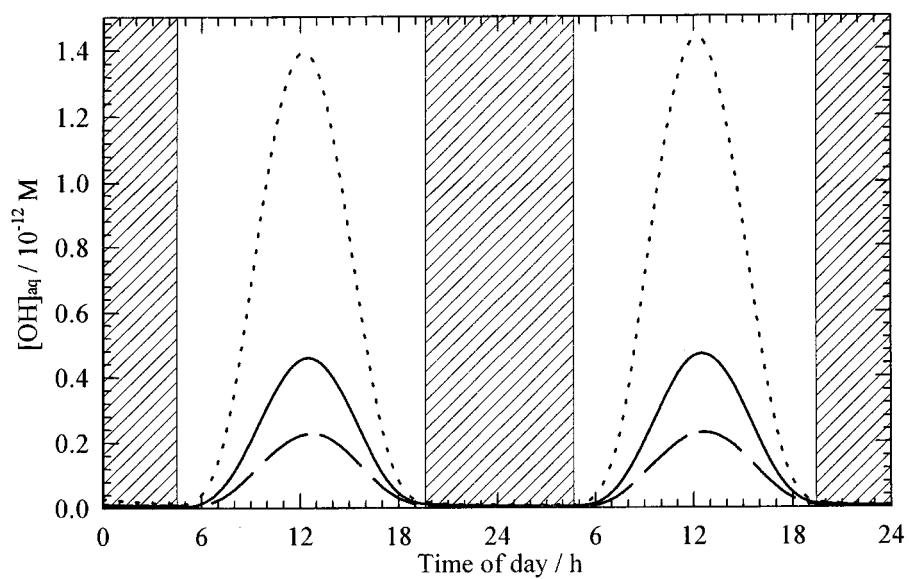
Figure 11. Comparison of model results for $[OH]_{aq}$ for urban conditions with a droplet radius of 1 μm ($\ldots\ldots$), 5 μm (————) and 10 μm (-----).
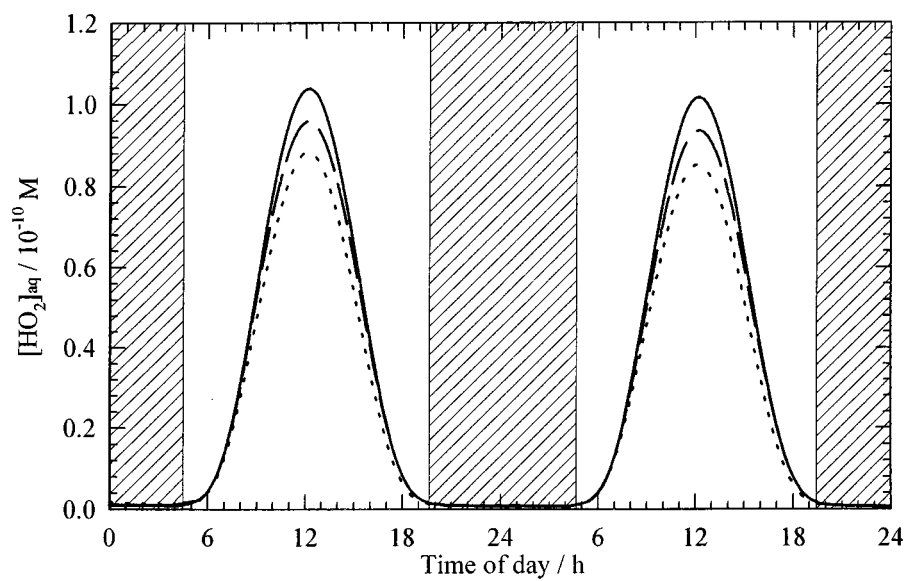
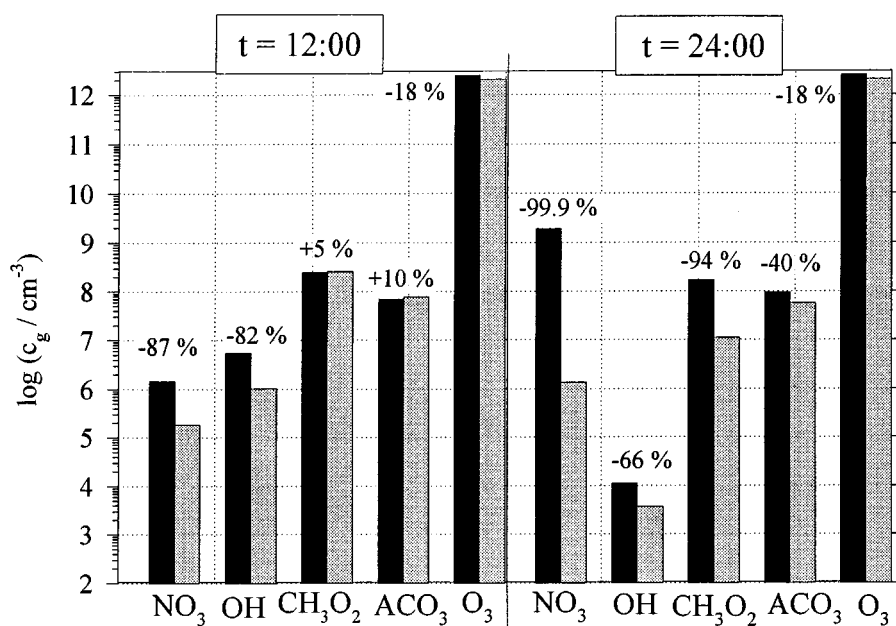*Figure 12.* Comparison of model results for $[HO_2]_{aq}$ for urban conditions with a droplet radius of 1 μm ($\ldots\ldots$), 5 μm (————) and 10 μm (-----).

Figure 13. Comparison of model results for $[OH]_g$, $[NO_3]_g$, $[ACO_3]_g$, $[MO_2]_g$ and $[O_3]_g$ for urban conditions without ■ and with ▨ liquid phase.

increases to $1.2 \cdot 10^7$ cm^{-3} and $4.6 \cdot 10^7$ cm^{-3}, respectively, in the next larger droplet sizes. The concentration of HO_2 in the gas phase corresponds to the OH chemistry. The main source of HO_2 in the gas phase is the reaction between CO and OH. The flux into the 1 μm droplet is $2.4 \cdot 10^6$ cm^{-3} s^{-1} whereas those into the large droplets (5 and 10 μm) are $4.2 \cdot 10^6$ cm^{-3} s^{-1}, equal for 5 and 10 μm droplets. The phase transfer is the main source of $HO_{2(aq)}$ in all droplets. It contributes to 45%, 65% and 70% to the total source strength in 1, 5 and 10 μm droplets, respectively. A diagnosis shows that this is caused by higher concentrations of organics such as $CH_2(OH)_2$, $HCOO^-$ and CH_3OH in the smaller droplets.

4. Summary and Conclusion

In the present work an aqueous phase mechanism, CAPRAM, is described which was combined with the gas phase mechanism RADM2. The calculations were performed for three scenarios, urban, remote and marine differing by initial concentrations. The mass transfer between the phases is described with the resistance model by Schwartz. Furthermore, within the present study a detailed description of the partition of species between both phases was given. The calculations were carried out with a box model describing the aqueous phase as uniform droplets with a radius of 1 μm. However, a variation of the droplet radius (5 and 10 μm) was also considered. The consequences to the concentration levels of some radicals were presented. In addition, shorter cloud periods (4 h per day) were considered
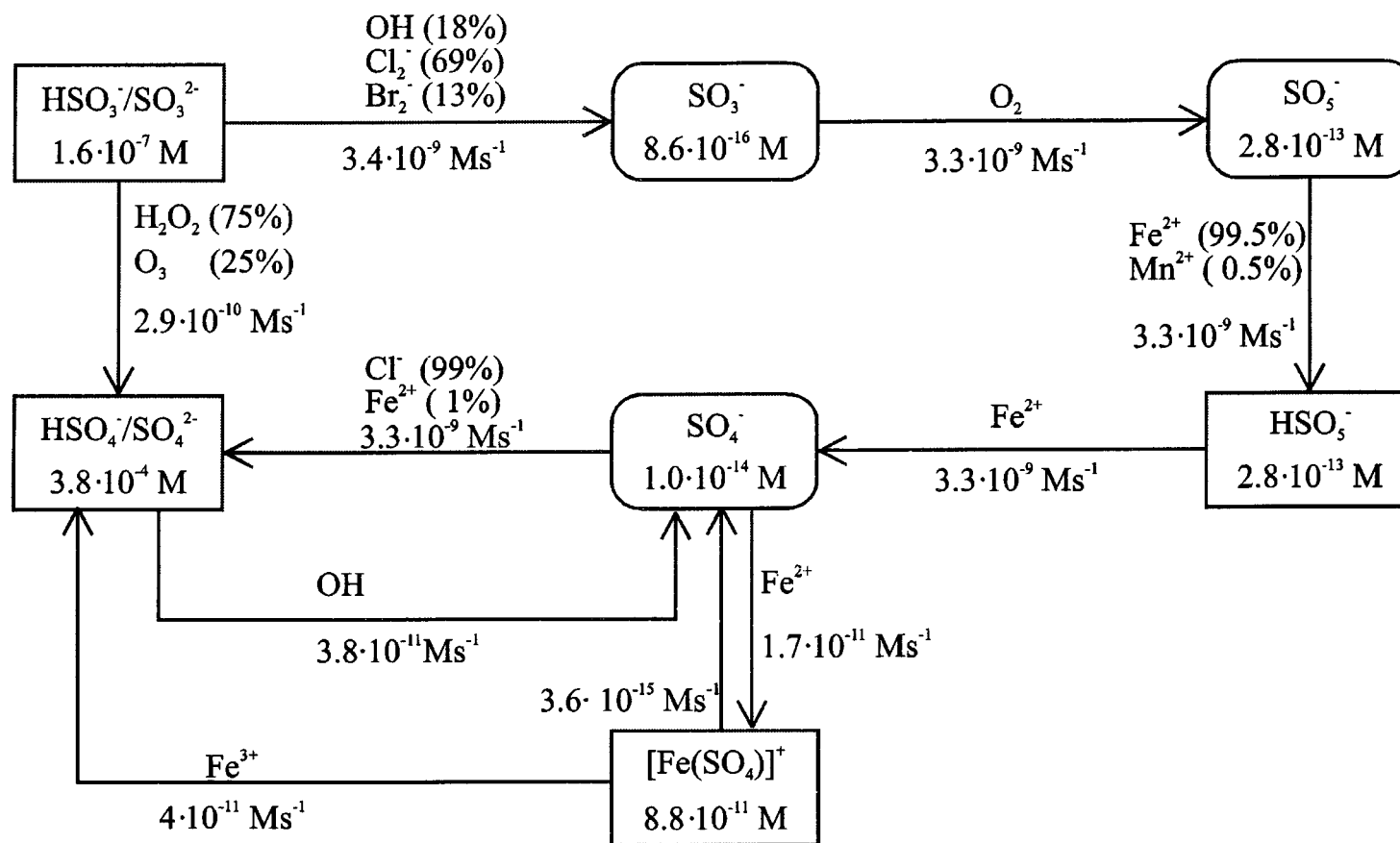
Figure 14. Concentration/flux diagram for oxidation pathways of S(IV) to S(VI) for urban conditions, local time: t = 12:00.
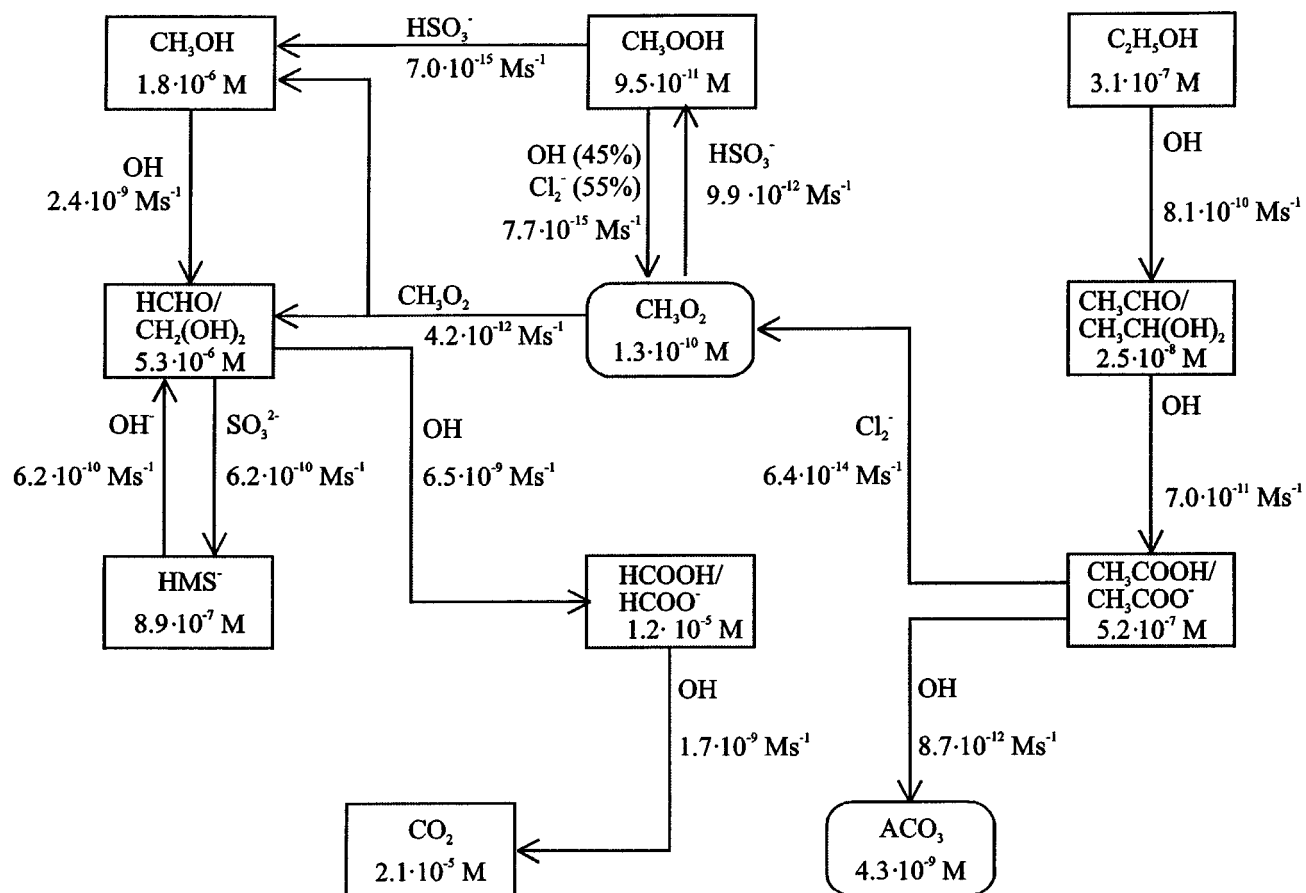
CH$_3$OH
1.8·10^{-6} M

HSO$_3^-$
7.0·10^{-15} Ms^{-1}

CH$_3$OOH
9.5·10^{-11} M

C$_2$H$_5$OH
3.1·10^{-7} M

OH
2.4·10^{-9} Ms^{-1}

OH (45%)
Cl$_2^-$ (55%)
7.7·10^{-15} Ms^{-1}

HSO$_3^-$
9.9·10^{-12} Ms^{-1}

OH
8.1·10^{-10} Ms^{-1}

HCHO/
CH$_2$(OH)$_2$
5.3·10^{-6} M

CH$_3$O$_2$
4.2·10^{-12} Ms^{-1}

CH$_3$O$_2$
1.3·10^{-10} M

CH$_3$CHO/
CH$_3$CH(OH)$_2$
2.5·10^{-8} M

OH

OH$^-$
6.2·10^{-10} Ms^{-1}

SO$_3^{2-}$
6.2·10^{-10} Ms^{-1}

OH
6.5·10^{-9} Ms^{-1}

Cl$_2^-$
6.4·10^{-14} Ms^{-1}

OH
7.0·10^{-11} Ms^{-1}

HMS$^-$
8.9·10^{-7} M

HCOOH/
HCOO$^-$
1.2·10^{-5} M

CH$_3$COOH/
CH$_3$COO$^-$
5.2·10^{-7} M

OH
1.7·10^{-9} Ms^{-1}

OH
8.7·10^{-12} Ms^{-1}

CO$_2$
2.1·10^{-5} M

ACO$_3$
4.3·10^{-9} M

Figure 15. Concentration/flux diagram for oxidation pathways of organic compounds for urban conditions, local time: t = 12:00.

and the differences in the concentration levels compared to the simulation with a permanent cloud of the HO_x radicals and NO_3 were discussed.

The concentration levels of OH, NO_3, radical anions and peroxyl radicals in the aqueous phase are investigated, and the sink and source reactions for these species were analysed. The main source of the OH radical in the aqueous phase is the transfer from the gas phase. The concentration of OH_{aq} reaches its maximum at noon in the marine scenario ($1.9 \cdot 10^{-12}$ M), because organic species, which represent the most effective OH sinks, are less abundant in this scenario. In comparison to the other scenarios the concentration level of the NO_3 radical reaches the maximum under urban conditions at midnight, because it is produced from NO_2 in the gas phase. Comparative calculations made with RADM2 show higher concentrations of both these radicals if only gas phase chemistry is considered.

The behaviour of the methyl peroxyl and the acetyl peroxyl radicals have also been studied. Their concentration levels are influenced by the concentration of $OH_{(g)}$, because both are produced in reactions with OH in the gas phase. For these species the concentration at noon is reduced in calculations with the liquid phase present, because the transfer of the OH radical into the liquid phase causes reduced production of the peroxyl radicals in the gas phase.

In conclusion, it has been shown that within tropospheric aqueous phase particles a wide variety of chemical conversions may occur. Existing mechanisms are extended by the present work and it is shown that aqueous phase chemical conversion may strongly effect the composition of the gas phase. This is not only due to the separation of radical precursors corresponding to their phase ratio. Whether the oxidation capacity of the troposphere is decreased or increased by cloud and/or aerosol chemical processes cannot be stated generally. For such considerations the inventories of trace gases and oxidants have to be analysed for a given regional surrounding. As has been shown here, the existence of the tropospheric aqueous phase does not only lead to the uptake of soluble species but may also result in the active production such as chlorine or bromine molecules and atoms at daytime due to the conversion of OH or at night-time due to the corresponding processes initiated by NO_3.

References

Amels, P., Elias, H., Götz, U., Steinges, U., and Wannowius, K. J., 1996: Kinetic investigation of the stability of peroxonitric acid and of its reaction with sulfur(IV) in aqueous solution, in P. Warneck (ed.), *Heterogeneous and Liquid Phase Processes*, Vol. 2 of *Transport and Chemical Transformation in Pollutants in the Troposphere*, (P. Borell, P. M. Borrell, T. Cvităs, K. Kelly, and W. Seiler, Series Editors), Springer, Berlin, pp. 77–88.

Audiffren, N., Renard, M., Buisson, E., and Chaumerliac, N., 1998: Deviations from the Henry's law equilibrium during cloud events: A numerical approach of the mass transfer between phases and its specific numerical effects, *Atmos. Res.* **49**, 139–161.

Baral, S., Lume-Pereira, C., Janata, E., and Henglein, A., 1986: Chemistry of colloidal manganese oxides. 3. Formation in the reaction of hydroxyl radical with Mn^{2+} ions, *J. Phys. Chem.* **90**, 6025–6028.

Barker, G. C., Fowles, P., and Stringer, B., 1970: Pulse radiolytic inducted transient electrical conductance in liquid solutions of NO_3^-, NO_2^- and $Fe(CN)_6^{3-}$, *Trans. Faraday Soc.* **66**, 1509–1519.

Barlow, S., Buxton, G. V., Murray, S. A., and Salmon, G. A., 1997: Oxidation of hydroxymethanesulfonate initiated by the hydroxyl radical, in P. M. Borrell, P. Borell, T. Cvităs, K. Kelly, and W. Seiler (eds), *Transport and Transformation of Pollutants in the Troposphere*, Vol. 1, Proceedings of EUROTRAC Symposium '96: Computational Mechanics Publications, Southampton, U.K., pp. 361–365.

Baxendale, J. H., Ward, M. D., and Wardman, P., 1971: Heats of formation of HO_2 and OH in aqueous solution, *Trans. Faraday Soc.* **67**, 2532–2537.

Beckwith, R. C., Wang, T. X., and Margerum, D. W., 1996: Equilibrium and kinetics of bromine hydrolysis, *Inorg. Chem.* **35**, 995–1000.

Beilke, S. and Gravenhorst, G., 1978: Heterogeneous SO_2-oxidation in the droplet phase, *Atmos. Environ.* **12**, 231–239.

Bell, R. P., 1966: The reversible hydration of carbonyl compounds, *Adv. Phys. Org. Chem.* **4**, 1–29.

Bell, R. P. and Evans, P. G., 1966: Kinetics of the dehydration of methylene glycol in aqueous solution, *Proc. R. Soc. London A* **291**, 297–323.

Bell, R. P., Rand, M. H., and Wynne-Jones, K. M. A., 1956: Kinetics of the hydration of acetaldehyde, *Trans. Faraday Soc.* **52**, 1093–1102.

Benkelberg, H.-J., Schäfer, A., and Warneck, P., 1991: In K.-H. Becker (ed.), *Air Pollution Research Report 33: Atmospheric Oxidation Processes*, CEC, Brussels, pp. 130–133.

Benkelberg, H.-J. and Warneck, P., 1995: Photodecomposition of iron(III) hydroxo and sulfato complexes in aqueous solution: Wavelength dependence of OH and SO_4^- quantum yields, *J. Phys. Chem.* **99**, 5214–5221.

Berdnikov, V. M., 1973: Catalytic activity of the hydrated copper ion in the decomposition of hydrogen peroxide, *Russ. J. Phys. Chem.* **47**, 1060–1062.

Betterton, E. A., 1992: Henry's law constants of soluble and moderately soluble organic gases: Effects on aqueous phase chemistry, in J. O. Nriagu (ed.), *Gaseous Pollutants: Characterization and Cycling*, Wiley, New York, pp. 1–50.

Betterton, E. A. and Hoffmann, M. R., 1988a: Henry's law constants of some environmentally important ldehydes, *Environ. Sci. Technol.* **22**, 1415–1418.

Betterton, E. A. and Hoffmann, M. R., 1988b: Oxodation of aqueous SO_2 by peroxymonosulfate, *J. Phys. Chem.* **92**, 5962–5965.

Betterton, E. A., Erel, Y., and Hoffmann, M. R., 1988: Aldehyde-bisulfite adducts: Prediction of some of their thermodynamic and kinetic properties, *Environ. Sci. Technol.* 22, 92–99.

Bielski, B. H. J., Cabelli, D. E., Arudi, R. L., and Ross, A. B., 1985: Reactivity of HO_2/O_2^- radicals in aqueous solution, *J. Phys. Chem. Ref. Data* **14**, 1041–1100.

Bongartz, A., Schweighoefer, S., Roose, C., and Schurath, U., 1995: The mass accommodation coefficient of ammonia on water, *J. Atm. Chem.* **20**, 35–58.

Bothe, E., Schuchmann, M. N., Schulte-Frohlinde, D., and von Sonntag, C., 1983: Hydroxyl radical-induced oxidation of ethanol in oxygenated aqueous solutions. A pulse radiolysis and product study, *Z. Naturforsch.* **38b**, 212–219.

Brandt, C. and van Eldik, R., 1995: Transition metal-catalyzed oxidation of sulfur(IV) oxides. Atmospheric relevant processes and mechanisms, *Chem. Rev.* **95**, 119–190.

Buxton, G. V., 1994: Mechanisms for chemical reactions in cloud droplets, in P. M. Borrell, P. Borrell, T. Cvitaš, and W. Seiler (eds), *Transport and Transformation of Pollutants in the Troposphere*, Proceedings of EUROTRAC Symposium '94: SPB Academic Publishing, The Hague, The Netherlands, pp. 978–983.

Buxton, G. V., Greenstock, C. L., Helman, W. P., and Ross, A. B., 1988a: Critical review of rate constants for reactions of hydrated electrons, hydrogen atoms and hydroxyl radicals, (OH, O_2^-) in aqueous solution, *J. Phys. Chem. Ref. Data* **17**, 513–886.

Buxton, G. V., Wood, N. D., and Dyster, S., 1988b: Ionisation constants of OH and HO_2 in aqueous solution up to 200 °C. A pulse radiolytic study, *J. Chem. Soc. Faraday Trans.* **84**, 1113–1121.

Buxton, G. V., Salmon, G. A., and Wood, N. D., 1990: A pulse radiolysis study of the chemistry of oxysulfur radicals in aqueous solution, in G. restelli and G. Angeletti (eds), *Proceedings of the Fifth European Symposium: Physico-Chemical Behaviour of Atmospheric Pullutants*, Kluwer, Dordrecht, pp. 245–250.

Boxton, G. V., McGowan, S., Salmon, G. A., Williams, J. E., and Wood, N. D., 1996a: A study of the spectra and reactivity of oxysulphur-radical anions involved in the chain oxidation of S(IV): A pulse and gamma-radiolysis study, *Atmos. Environ.* **30**, 2483–2493.

Boxton, G. V., Malone, T. N., and Salmon, G. A., 1996b, Pulse radiolysis study of the reaction of SO_5^- with HO_2, *J. Chem. Soc. Faraday Trans.* **92**, 1287–1289.

Buxton, G. V., Malone, T. N., and Salmon, A., 1997: Reaction of SO_4^- with Fe^{2+}, Mn^{2+} and Cu^+ in aqueous solution, *J. Chem. Soc. Faraday Trans.* **93** (16), 2893–2897.

Cabelli, D. E., Bielski, B. H. J., and Holcman, J., 1987: Interaction between copper(II)-arginine complexes and HO_2/O_2^--radicals, a pulse radiolytic study, *J. Am. Chem. Soc.* **109**, 3665–3669.

Chameides, W. L., 1984: The photochemistry of a Remote Marine Straaatiform Cloud, *J. Geophys. Res.* **89**, 4739–4755.

Chawla, O. P. and Fessenden, R. W., 1975: Electron spin resonance and pulse radiolysis studies of some reactions of SO_4^-, *J. Phys. Chem.* **79**, 2693–2700.

Chin, M. and Wine, P. H., 1994: A temperature-dependent competitive kinetics study of the aqueous-phase reactions of OH radicals with formate, formic acid, acetate, acetic acid and hydrated formaldehyde, in G. R. Helz, R. G. Zepp, and D. G. Crosby (eds), *Aquatic and Surface Photochemistry*, Lewis Publishers, Boca Raton, pp. 85–96.

Christensen, H. and Sehested, K., 1981: Pulse radiolysis at high temperatures and high pressures, *Radiat. Phys. Chem.* **18**, 723–231.

Christensen, H., Sehested, K., and Corfitzen, H., 1982: Reactions of hydroxyl radicals with hydrogen peroxide at ambient and elevated temperatures, *J. Phys. Chem.* 86, 1588–1590.

Christensen, H., ehested, K., and Bjergbakke, E., 1989: Radiolysis of reactor water: Reaction of hydroxyl radicals with superoxide (O_2^-), *Water Chem. Nucl. React. Syst.* **5**, 141–144.

Clegg, S. L. and Brimblecombe, P., 1990: Solubility of volatile electolytes in multicomponent solutions with atmospheric applications, *ACS Symposium Series* **416**, 58–73.

Clifton, C. L. and Huie, R. E., 1989: Rate constants for hydrogen abstraction reactions of the sulfate radical SO_4^- alcohols, *Int. J. Chem. Kinet.* **21**, 677–687.

Cope, V. W., Hoffman, M. Z., and Chen, S., 1978: Reactivity of the carbonate radical toward metal complexes in aqueous solution, *J. Phys. Chem.* **82**, 2665–2669.

Damschen, D. E. and Martin, L. R., 1983: Aqueous aerosol oxidation of nitrous acid by O_2, O_3 and H_2O_2, *Atmos. Environ.* **17**, 2005–2011.

Davidovits, M., Hu, J. H., Worsnop, D. R., Zahniser, M. S., and Kolb, C. E., 1995: Entry of gas molecules into liquids, *Faraday Discuss.* **100**, 65–82.

Davies, G., Kirschenbaum, L. J., and Kustin, K., 1968: The kinetics and stoichometry of the reaction between manganese(III) and hydrogen peroxide in acid perchlorate solution, *Inorg. Chem.* **7**, 146–154.

Deister, U. and Warneck, P., 1990: Photooxidation of SO_3^{2-} in aqueous solution, *J. Phys. Chem.* **94**, 2191–2198.

Dentener, F. J. and Crutzen, P. J., 1993: Reaction of N_2O_5 on tropospheric aerosols: Impact on the global distributions of NO_x, O_3 and OH, *J. Geophys. Res.* **98**, 7149–7163.

Diebler, H. and Sutin, N., 1964: The kinetics of some oxidation-reduction reactions involving manganese(III), *J. Phys. Chem.* **68**, 174–180.

Draganic, Z. D., Negron-Mendoza, A., Sehested, K., Vujosevic, S. I., Navarro-Gonzales, R., Albarran-Sanchez, M. G., and Draganic, I. G., 1991: Radiolysis of aqueous solution of ammonium bicarbonate over a large dose range, *Radiat. Phys. Chem.* **38**, 317–321.

Elliot, A. J., 1989: A pulse radiolysis study of the temperature dependence of reactions involving H, OH and e_{aq}^- in aqueous solution, *Radiat. Phys. Chem.* **34**, 753–758.

Elliot, A. J. and Buxton, G. V., 1992: Temperature dependence of the reactions $OH + O_2^-$ and $OH + HO_2$ in water up to $200\,°C$, *J. Chem. Soc. Faraday Trans.* **88**, 2465–2470.

Elliot, A. J. and McCracken, D. R., 1989: Effect of temperature on O^- reactions and equilibria: A pulse radiolytic study, *Radiat. Phys. Chem.* **33**, 69–74.

Elliot, A. J. and Simsons, A. S., 1984: Rate constants for reactions of hydroxyl radicals as a function of temperature, *Radiat. Phys. Chem.* **24**, 229–231.

Eriksen, T. E., Lind, J., and Merenyi, G., 1985: On the acid-base equilibrium of the carbonate radical, *Radiat. Phys. Chem.*, **26**, 197–199.

Exner, M., 1990: Diploma Thesis, Bildung und Reaktionen von Radikalen und Radikalanionen in wäßriger Phase, Georg-August-University Göttingen.

Exner, M., 1992: PhD Thesis, Laserspektrometrische Untersuchungen von Reaktionen des NO_3-Radikals in wäßriger Lösung, Georg-August-University Göttingen.

Exner, M., Herrmann, H., and Zellner, R., 1990: A laser photolysis study of reactions of the carbonate radical anion (CO_3^- in aqueous solution, in K. H. Becker (ed.), *Air Pollution Research Report 33: Atmospheric Oxidation Processes*, Office for official Publications of the European Communities, Luxembourg, pp. 134–138.

Exner, M., Herrmann, H., and Zellner, R., 1992: Laser-based studies of reactions of the nitrate radical in aqueous solution, *Ber. Bunsenges. Phys. Chem.* **96**, 470–477.

Exner, M., Herrmann, H., Michel, J. W., and Zellner, R., 1993: Laser pulse initiated measurements of NO_3 reactions with S(IV) and organic compounds in aqueous solutions, in P. M. Borrell, P. Borrell, T. Cvitaš, and W. Seiler (eds), *Photo-oxidants: Precursors and Products*, Proceedings of EUROTRAC Symposium '92, SPB Academic Publishing, The Hague, The Netherlands, pp. 615–618.

Exner, M., Herrmann, H., and Zellner, R., 1994: Rate constants for the reactions of the NO_3 radical with $HCOOH/HCOO^-$ and CH_3COOH/CH_3COO^- in aqueous solution between 278 and 328 K, *J. Atmos. Chem.* **18**, 359–378.

Fisher, M. M. and Hamill, W. H., 1973: Electronic processes in pulse-irradiated aqueous and alcoholic systems, *J. Phys. Chem.* **77**, 171–177.

Fornier de Violet, Ph., 1981: Polyhalide anions as intermediates in chemistry, *Rev. Chem. Intermed.* **4**, 121–169.

Fuller, E. N., Diffusion coefficients for binary gas systems at low pressures: Empirical correlations, in C. Reid *et al.* (eds), *Properties of Gases and Liquids*, Mc Graw Hill, New York, p. 587.

Gardner, J. A., Watson, L. R., Adewuyi, Y. G., Davidovits, P., Zahniser, M. S., Worsnop, D. R., and Kolb, C. E., 1987: Measurement of the mass accommodation coefficient of $SO_2(g)$ on water droplets, *J. Geophys. Res.* **92**, 10887–10895.

George, C., Ponche, J. L., Mirabel, Ph., Behnke, W., Scheer, V., and Zetzsch, C., 1994: Study of the uptake of N_2O_5 by water and NaCl solutions, *J. Phys. Chem.* **98**, 8780–8784.

Gilbert, B. C., Larkin, J. P., and Norman, R. O. C., 1972: Electron spin resonance studies, part XXXIV. The use of the *aci*-anion from nitromethane as a spin trap for organic radicals in aqueous solution, *J. Chem. soc. Perkin Trans. II*, 1272–1279.

Goldstein, S., Czapski, G., Cohen, H., and Meyerstein, D., 1992: Deamination of β-alanine induced by hydroxyl radicals and monovalent copper ions. A pulse radiolytic study, *Inorg. Chim. Acta* **192**, 87–93.

Graedel, T. E. and Weschler, C. J., 1981: Chemistry within aqueous atmospheric aerosols and raindrops, *Rev. Geophys. Space Phys.* **19**, 505–539.

Graedel, T. E., Mandich, M. L., and Weschler, C. J., 1986: Kinetic model studies of atmospheric droplet chemistry 2. Homogeneous transition metal chemistry in raindrops, *J. Geophys. Res.* **91**, 5205–5221.

Grigor'ev, A. E., Makarov, I. E., and Pikaev, A. K., 1987: Formation of Cl_2^- in the bulk solution during the radiolysis of concentrated aqueous solutions of chlorides, *High Energy Chem.* **21**, 99–102.

Hanson, D., 1992: Measurement of OH and HO_2 radical uptake coefficients on water and sulfuric acid surfaces, *J. Phys. Chem.* **96**, 4979.

Harned, H. S. and Owen, B. B., 1958: *The Physical Chemistry of Electrolytic Solutions*, 3rd edn, Reinhold, New York.

Hart, E. J., Thomas, J. K., and Gordon, S., 1964: A review of the radiation chemistry of single-carbon compounds and some reactions of the hydrated electron in aqueous solution, *Radiat. Res. Suppl.* **4**, 74–88.

Hemmes, P., Rich, L. D., Cole, D. L., and Eyring, E. M., 1971: Kinetics of hydrolysis of ferric ion in dilute aqueous solution, *J. Phys. Chem.* **75**, 929–932.

Herrmann, H., Exner, M. and Zellner, R., 1994: Reactivity trends in reactions of the nitrate radical (NO_3) with inorganic and organic cloudwater constituents, *Geochim. Cosmochim. Acta* **58**, 3239–3244.

Herrmann, H., Reese, A., and Zellner, R., 1995: Time-resolved UV/VIS diode array absorption spectroscopy of SO_x^- ($x = 3, 4, 5$) radical anions in aqueous solution, *J. Mol. Struct.* **348**, 183–186.

Herrmann, H., Jacobi, H.-W., Raabe, G., Reese, A., and Zellner, R., 1996: Laser-spectrocopic laborabory studies of atmospheric aqueous phase free radical chemistry, *Fresenius J. Anal. Chem.* **355**, 343–344.

Herrmann, H., Jacobi, H.-W., Reese, A., and Zellner, R., 1997: Laboratory studies of small radicals and radical anions of interest for tropospheric aqueous phase chemistry: The reactivity of SO_4^-, in P. M. Borrell, T. Cvitaš, K. Kelly, and W. Seiler (eds), *Transport and Transformation of Pollutants in the Troposphere*, Vol. 1, Proceedings of EUROTRAC Symposium '96, Computational Mechanics Publications, Southampton, U.K., pp. 407–411.

Herrmann, H. and Zellner, R., 1998: Reactions of NO_3 radicals in aqueous solution, in Z. B. Alfassi, *N-Centered Radicals*, John Wiley and Sons Ltd.

Herrmann, H., Ervens, B., Nowacki, P., Wolke, R., and Zellner, R., 1999a: A chemical aqueous phase radical mechanism for tropospheric chemistry, *Chemosphere* **38**, 1223–1232.

Herrmann, H., Reese, A., Ervens, B., Wicktor, F., and Zellner, R., 199b: Laboratory and modelling studies of tropospheric multiphase conversions involving some C1 and C2 peroxyl radicals, *Phys. Chem. Earth* **24**, 287–290.

Hindmarsh, A. C., 1980: LSODE and LSODI, two initial value ordinary differential equation solver, *ACM-SIGNUM Newsl.* **15**, 10–11.

Hoffmann, M. R., 1986: On the kinetics and mechanism of oxidation of aquated sulfur dioxide by ozone, *Atmos. Environ.* **20**, 1145–1154.

Hoigné, J., Bader, H., Haag, W. R., and Staehelin, J., 1985: Rate constants of reactions of ozone with organic and inorganic compounds in water- III inorganic compounds and radicals, *Water Res.* **19**, 993–1004.

Holdren, M. W., Spicer, C. W., and Hales, J. M., 1984: Peroxyacetyl nitrate solubility and decomposition rate in acidic water, *Atmos. Environ.* **18**, 1171–1173.

Huie, R. E. and Clifton, C. L., 1990: Temperature dependence of the rate constants for reactions of the sulfate radical, SO_4^-, with anions, *J. Phys. Chem.* **94**, 8561–8567.

Huie, R. E., Shoute, L. C. T., and Neta, P., 1991a: Temperature dependence of the rate constants for reactions of the carbonate with organic and inorganic reductants, *Int. J. Chem. Kin.* **23**, 541–542.

Huie, R. E., Clifton, C. L., and Neta, P., 1991b: Electron transfer reaction rates and equilibria of the carbonate and sulfate radical anions, *Radiat. Phys. Chem.* **38**, 477–481.

Jacob, D. J., 1986: Chemistry of OH in remote clouds and its role in the production of formic acid and peroxymonosulfate, *J. Geophys. Res.*, **91**, 9807–9826.

Jacob, D. J., Gottlieb, E. W., and Prather, M. J., 1989: Chemistry of a polluted cloud boundary layer, *J. Geophys. Res.* **94**, 12975–13002.

Jacobi, H.-W., 1996: Kinetische Untersuchungen und Modellrechnungen zur troposphärischen Chemie von Radikalanionen und Ozon in wäßriger Phase, PhD Thesis, University-GH-Essen, Germany.

Jacobi, H.-W., Herrmann, H., and Zellner, R., 1996: Kinetic investigation of the Cl_2^- radical in the aqueous phase, in Ph. Mirabel (ed.), *Air Pollution Research Report 57: Homogenous and Heterogenous Chemical Processes in the Troposphere*, Office for Official Publications of the European Communities, Luxembourg, pp. 172–176.

Jacobi, H.-W., Herrmann, H., and Zellner, R., 1997: A laser flash photolysis study of the decay of Cl-atoms and Cl_2^--radical anions in aqueous solution at 298 K, *Ber. Bunsenges. Phys. Chem.* **101**, 1909–1913.

Jacobi, H.-W., Wicktor, F., Herrmann, H., and Zellner, R., 1999: A laser flash photolysis kinetic study of the Cl_2^--radical anion with oxygenated hydrocarbons in aqueous solution, *Int. J. Chem. Kin.* **31**, 169–181.

Jayson, G. G., Parson, B. J., and Swallow, A. J., 1973a: Same simple, highly reactive, inorganic chlorine derivatives in aqueous solution, *J. Chem. Soc. Faraday Trans.* **69**, 1597–1607.

Jayson, G. G., Parson, B. J., and Swallow, A. J., 1973b, Oxidation of ferrous ions by per hydroxyl radicals, *J. Chem. Soc. Faraday Trans.* **69**, 236–242.

Jiang, P.-Y., Katsumura, Y., Nagaishi, R., Domae, M., Ishikawa, K., Ishigure, K., and Yoshida, Y., 1992: Pulse radiolysis study of concentrated sulfuric acid solutions, *Chem. Soc. Faraday Trans.* **88**, 1653–1658.

Khan, I. and Brimblecombe, P., 1992: Henry's law constants of low molecular weight (< 130) organic acids, *J. Aerosol Sci.* **23** (Suppl. 1), S897–S900.

Kirchner, W., Welter, F., Bongartz, A., Kames, J., Schweighoefer, S., and Schurath, U., 1990: Trace gas exchange at the air/water interface: Measurements of mass accommodation coefficients, *J. Atmos. Chem.* **10**, 427–449.

Kläning, U. K. and Wolff, T., 1985: Laser flash photolysis of HClO, ClO^-, HBrO and BrO^- in aqueous solution, reactions of Cl- and Br-atoms, *Ber. Bunsenges. Phys. Chem.* **89**, 243–245.

Kläning, U. K., Sehested, K., and Holcman, J., 1985: Standard gibbs free energy of formation of the hydroxyl radical in aqueous solution; rate constants for the reaction $ClO_2^- + O_3 \rightleftarrows O_3^- + ClO_2$, *J. Phys. Chem.* **89**, 760–763.

Kok, G. L., Gitlin, S. N., and Lazrus, A. L., 1986: Kinetics of the formation and decomposition of hydroxymethanesulfonate, *J. Geophys. Res.* **91**, 2801–2804.

Kosak-Channing, L. E. and Helz, G. R., 1983: Solubility of ozone in aqueous solutions of 0–0.6 M Ionic Strength at 5–30 °C, *Environ. Sci. Technol.* **17**, 145–149.

Kozlov, Y. N. and Berdnikov, V. M., 1973: Photodecomposition of hydogen peroxide in the presence of copper ions. IV. Determinations of rate constants of elementary reactions, *Russ. J. Phys. Chem.* **47**, 338–340.

Kuz'min, V. A., 1972: Reactions of the CO_3^- and SiO_3^- radical anions, *High Energy Chem.* **6**, 338–339.

Lammel, G., Perner, D., and Warneck, P., 1990: Decomposition of pernitric acid in aqueous solution, *J. Phys. Chem.* **94**, 6141–6144.

Laurence, G. S. and Thornton, A. T., 1973: Kinetics of oxidation of transition-metal ions by halogen radical anions. Part III, the oxidation of manganese(II) by dibromide and dichloride ions generated by flash photolysis, *J. Chem. Soc. Dalton Trans.*, 1637–1644.

Leibrock, E. and Slemr, J., 1996: Determination of oxygenated hydrocarbons in air by GC/MS, in P. M. Borrell, P. Borrell, Y. Cvitaš, K. Kelly, and W. Seiler (eds), *Transport and Transformation of Pollutants in the Troposphere*, Vol. 1, Proceedings of EUROTRAC Symposium '96, Computational Mechanics Publications, Southampton, U.K., pp. 377–381.

Lelieveld, J. and Crutzen, P. J., 1990: Influences of cloud photochemical processes on tropospheric ozone, *Nature*, **343**, 227–233.

Lelieveld, J. and Crutzen, P. J., 1991: The role of clouds in tropospheric photochemistry, *J. Atmos. Chem.* **12**, 229–268.

Lind, J. A., Lazrus, A. L., and Kok, G. L., 1987, Aqueous phase oxidation of sulfur(IV) by hydrogen peroxide, methylhydroperoxide and peroxyacetic acid, *J. Geophys. Res.* **92**, 4171–4177.

Lind, J. A. and Kok, G. L., 1994: Correction to 'Henry's law determinations for aqueous solutions of hydrogen peroxide, methylhydroperoxide and peroxyacetic acid', *J. Geophys. Res* **99**, 21119.

Logager, T., Sehested, K., and Holcman, J., 1993: Rate constants of the equilibrium reactions $SO_4^{\bullet-}$ + $HNO_3 \rightleftharpoons HSO_4^- + NO_3^{\bullet}$ and $SO_4^{\bullet-} + NO_3^- \rightleftharpoons SO_4^{2-} + NO_3^{\bullet}$, *Radiat. Phys. Chem.* **41**, 539–543.

Loomis, A. G., 1928: *International Critical Tables Vol. III: Solubilities of Gases in Water*, McGraw-Hill, New York, pp. 255–261.

Mackay, D. and Shiu, W. Y., 1981: A critical review of Henry's law constants for chemicals of environmental interest, *J. Phys. Chem. Ref. Data* **10**, 1175–1199.

Marsh, A. R. W. and McElroy, W. J., 1985: The dissociation constant and Henry's law constant of HCl in aqueous solution, *Atmos. Environ.* **19**, 1075–1080.

Maruthamuthu, P. and Neta, P., 1977: Radiolytic chain decomposition of peroxomonophosphoric and peroxomonosulphuric acids, *J. Phys. Chem.* **81**, 937–940.

Matthijsen, J., Builtjes, P. J. H., and Sedlak, D. H., 1995: Cloud model experiments of the effect of iron and copper on tropospheric ozone under marine and continental conditions, *Meteorol. Atmos. Phys.* **57**, 43–60.

McElroy, W. J. and Waygood, S. J., 1990: Kinetics of the reactions of the SO_4^- Radical with SO_4^-, $S_2O_8^{2-}$, H_2O and Fe^{2+}, *J. Chem. Soc. Faraday Trans.* **86**, 2557–2564.

McElroy, W. J., 1997: The interactions of gases with aqueous aerosol particles, central Electr. Gen. Board, Part IV.

Merényi G. and Lind, J., 1994: Reaction mechanism of hydrogen abstraction by the bromine atom in water, *J. Am. Chem. Soc.* **116**, 7872–7876.

Mirabel, P., 1996: Investigations of the uptake rate of some atmospheric trace gases, RINOXA Final Report.

Möller, D. and Mauersberger, G., 1992: Cloud chemistry effects on tropospheric photo-oxidants in polluted atmosphere – model results, *J. Atmos. Chem.* **14**, 153–165.

Möller, D. and Mauersberger, G., 1995: Aqueous phase chemical reaction system used in cloud chemistry modelling, in A. Flossmann, T. Cvitaš, D. Möller, and G. Mauersberger (eds), *Clouds: Models and Mechanisms*, ISS, Garmisch-Partenkirchen, Germany, pp. 77–93.

National Bureau of Standards, 1971: JANAF thermodynamic tables, 2nd edn, NSDRS-NBS 37, U.S. Dept. of Commerce, Washington, D.C.

Neta, P. and Huie, R. E., 1986: Rate constants for reactions of NO_3 radicals in aqueous solution, *J. Phys. Chem.* **90**, 4644–4648.

Norman, R. O. C., Storey, P. M., and West, P. R., 1970: Electron spin resonance studies. Part XXV. Reactions of the sulphate radical anion with organic compounds, *J. Chem. Soc. B.*, 1087–1095.

Nowacki, P., 1998: Modeling of size-resolved multi-phase chemical processes in clouds under polluted atmospheric conditions, PhD Thesis in preparation, BTU Cottbus.

Olson, T. M. and Hoffmann, M. R., 1989: Hydroxyalkylsulfonate formation: Its role as a S(IV) reservoir in atmospheric water droplets, *Atmos. Environ.* **23**, 985–997.

O'Sullivan, D. W., Lee, M., Noone, B. C., and Heikes, B. G., 1996: Henry's law constant determinations for hydrogen peroxide, ethyl hydroperoxide and peroxyacetic acid, *J. Phys. Chem.* **100**, 3241–3247.

Park, J.-Y. and Lee, Y. N., 1988: Solubility and decomposition kinetics of nitrous acid in aqueous solution, *J. Phys. Chem.* **92**, 6294–6302.

Pick-Kaplan, M. and Rabani, J., 1976: Pulse radiolytic studies of aqueous $Mn(ClO_4)_2$ solutions, *J. Phys. Chem.* **80**, 1840–1843.

von Piechowski, M., Nauser, T., Hoignè, J., and Bühler, R. E., 1993: O_2^- Decay catalysed by Cu^{2+} and Cu^+ ions in aqueous solutions: A pulse radiolysis study for atmospheric chemistry, *Ber. Bunsenges. Phys. Chem.* **97**, 762–771.

Pikaev, A. K., Sibirskaya, G. K., Shirshov, E. M., Glazunov, P. Y., and Spitsyn, V. I., 1974: Pulsed radiolysis of concentrated aqueous solutions of nitric acid, *Dokl. Phys. Chem., Proc. Acad. Sci. U.S.S.R.*, **215**, 328–331.

Ponche, J. L., George, C., and Mirabel, P., 1993: Mass transfer at the air/water interface: Mass accommodation coefficients of SO_2, HNO_3, NO_2, *J. Atmos. Chem.* **16**, 1–21.

Raabe, G., 1996: *Eine laserphotolytische Studie zur Kinetik der Reaktionen des NO_3-Radikals in wäßriger Lösung*, Cuvillier, Göttingen, Germany.

Rafi, A. and Sutton, H. C., 1965: Radiolysis of aerted solutions of potassium bromide, *Trans. Faraday Soc.* **61**, 877–890.

Redlich, O., 1946: The dissociation of strong electrolytes, *Chem. Rev.* **39**, 333–356.

Redlich, O. and Hood, G. C., 1957: Ionic interaction, dissociation and molecular structure, *Faraday Discuss.* **24**, 87–93.

Reese, A., 1992: Diploma Thesis, Untersuchungen zur Spektroskopie und Kinetik der Radikalanionen SO_x^- ($x =3, 4, 5$) in wäßriger Lösung, University Essen, Germany.

Reese, A., 1997: PhD Thesis, UV/VIS-spektrometrische und kinetische Untersuchungen von Radikalen und Radikalanionen in wäßriger Lösung, University Essen, Germany.

Reese, A., Herrmann, H., and Zellner, R., 1997: Kinetics and spectroscopy of organic peroxyl radicals (RO_2) in aqueous solution, in P. M. Borrell, P. Borrell, T. Cvitaš, K. Kelly, and W. Seiler (eds), *Transport and Transformation of Pollutants in the Troposphere*, Vol. 1, Proceedings of EUROTRAC Symposium '96, Computational Mechanics Publications, Southhampton, U.K., pp. 377–381.

Reese, A., Herrmann, H., and Zellner, R., 1999: Kinetic and spectroscopic investigations of the Br_2^- radical in aqueous solution, in P. M. Borrell and P. Borrell (eds), Proceedings of the EUROTRAC-2 '98 Symposium, WIT Press, Southampton, pp. 714–718.

Rettich, T. R., 1978: Some photochemical reactions of aqueous nitric acid, *Diss. Abstr. Int. B* **38**, 5968.

Röth, E.-P., 1992: A fast algorithm to calculate the photonflux in optically dense media for use in photochemical models, *Ber. Bunsenges. Phys. Chem.* **96**, 417–420.

Rohrer, F. and Brüning, D., 1992: Surface NO and NO_2 mixing ratios measured between 30°N and 30°S in the Atlantic region, *J. Atmos. Chem.* **15**, 253–267.

Rudich, Y., Talukdar, R. K., Ravishankara, A. R., and Fox, R. W., 1996: Reactive uptake of NO_3 on pure water and ionic solutions, *J. Geophys. Res.* **101**, 21023–21031.

Ruggaber, A., Dlugi, R., Bott, A., Forkel, R., Herrmann, H., and Jacobi, H.-W., 1997: Modelling of radiation quantities and photolysis frequencies in the aqueous phase in the troposhere, *Atmos. Environ.* **31**, 3137–3150.

Rush, J. D. and Bielski, B. H. J., 1985: Pulse radiolytic studies of the reactions of HO_2/O_2^- with Fe(II)/FE(III) ions. The reactivity of HO_2/O_2^- with ferric ions and its implication on the occurrence of the Haber-Weiss-reaction **89**, 5062–5066.

Sander, R. and Crutzen, P. J., 1996: Model study indicating halogen activation and ozone destruction in polluted air masses transported to the sea, *J. Geophys. Res.* **101**, 9121–9138.

Saxena, P. and Hildemann, L. M., 1996: Water-soluble organics in atmospheric particles: A critical review of the literature and application of thermodynamics to identify candidate compounds, *J. Atmos. Chem.* **24**, 57–109.

Schuchmann, M. N. and von Sonntag, C., 1988: The rapid hydration of the acetyl radical. A pulse radiolysis study of acetaldehyde in aqueous solution, *J. Am. Soc.* **110**, 5698–5701.

Schwartz, S. E., 1986: Mass transport considerations pertinent to aqueous phase reactions of gases in liquid water clouds, in W. Jaeschke (ed.), *Chemistry of Multiphase Atmospheric Systems*, NATO ASI Series, Vol. 6, Springer, Berlin, pp. 415–471.

Schwartz, S. E. and White, W. H., 1983: Kinetics of reactive dissolution of nitrogen oxides into aqueous solution, *Adv. Environ. Sci. Technol.* **12**, 1–115.

Schwarz, H. A. and Bielski, B. H. J., 1986: Reactions of HO_2 and O_2^- with iodine and bromine and the I_2^- and I atom reduction potentials, *J. Phys. Chem.* **90**, 1445–1448.

Schweitzer, F., Magi, L., George, C., and Mirabel, P., 1998: Uptake rate measurements of methane-sulfonic acid and glyoxal by aqueous droplets, *J. Phys. Chem.* **102**, 593–600.

Sedlak, D. L. and Hoigné, J., 1993: The role of copper and oxalate in the redox cycling of iron in atmospheric waters, *Atmos. Environ.* **27A**, 2173–2185.

Sehested, K., Holcman, J., and Hart, T. J., 1983: *J. Phys. Chem.* **87**, 1951–1954.

Sehested, K., Logager, T., Holcman, J., and Nielsen, O. J., 1994: Formation and reactions of the NO_3 radical in aqueous solution, in P. M. Borrell, P. Borrell, T. Cvitaš, and W. Seiler (eds), *Transport and Transformation of Pollutants in the Troposphere*, Proceedings of EUROTRAC Symposium '94, SPB Academic Publishing, The Hague, The Netherlands, pp. 999–1004.

Shoute, L. C. T., Alfassi, Z. B., Neta, P., and Huie, R. E., 1991: Temperature Dependence of the rate constants for reaction of dihalide and azide radicals with inorganic reductances, *J. Phys. Chem.* **95**, 3238–3242.

Sirs, J. A., 1958, Electronic stopped flow measurements of rapid reactions in solution. Part 2. Glass electrode pH measurements, *Trans. Faraday Soc.* **54**, 207–212.

von Sonntag, C., 1987: *The Chemical Basis of Radiation Biology*, Taylor & Francis.

Stanbury, D. M., 1989, Reduction potentials involving inorganic free radicals in aqueous solution, *Adv. Inorg. Chem.* **33**, 69–138.

Stockwell, W. R., Middleton, P., Chang, J. S., and Tang, X., 1990: The second generation regional acid deposition model. Chemical mechanism for regional air quality modeling, *J. Geophys. Res.* **95**, 16343–16367.

Stockwell, W. R., Kirchner, F., Kuhn, M., and Seefeld, S., 1997: A new mechanism for regional atmospheric chemistry modeling, *J. Geophys. Res.* **102** (D22), 25847–25879.

Tang, Y., Thorn, R. P., Mauldin III, R. L., and Wine, P. H., 1988: Kinetics and spectroscopy of the SO_4^- radical in aqueous solution, *J. Photochem. Photobiol. A* **44**, 243–258.

Thomas, J. K., 1965: Rates of reaction of the hydroxyl radical, *Trans. Faraday Soc.* **61**, 702–707.

Thomas, K., Volz-Thomas, A., Mihelcic, D., Smit, H. G. J., and Kley D., 1998: On the exchange of NO_3 radicals with aqueous solutions: Solubility and sticking coefficient, *J. Atmos. Chem.* **29**, 17–43.

Thornton, A. T. and Laurence, G. S., 1973: Kinetics of oxidation of transition-metal ions by halogen radical anions. I. The oxidation of iron(II) by dibromide and dichloride ions generated by flash photolysis, *J. Chem. Soc. Dalton Trans.*, 804–813.

Wagner, I. and Strehlow, H., 1987: On the flash photolysis of bromide ions in aqueous solution, *Ber. Bunsenges. Phys. Chem.* **91**, 1317–1321.

Wagner, I., Strehlow, H., and Busse, G., 1980: Flash photolysis of nitrate ions in aqueous solution, *Z. Phys. Chem* **123**, 1–33.

Walling, C. and Goosen, A., 1973: Mechanism of the ferric ion catalyzed decomposition of hydrogen peroxide. Effect of organic substrates, *J. Am. Chem. Soc.* **95** (9), 2987–2991.

Walling, C., 1975: Fenton's reagent revisited, *Acc. Chem. Res.* **8**, 125–131.

Walcek, C. J., Yuan, H. H., and Stockwell, W. R., 1997: The influence of aqueous-phase chemical reactions on ozone formation in polluted and nonpolluted clouds, *Atmos. Environ.* **31** (8), 1221–1237.

Wang, T. X. and Margerum, D. W., 1994: Kinetics of reversible chlorine hydrolysis: Temperature dependence and general-acid/base-assisted mechanisms, *Inorg. Chem.* **33**, 1050–1055.

Warneck, P. (ed)., 1996: *Heterogeneous and Liquid-Phase Processes*, Springer Verlag, Berlin, Germany.

Warneck, P. and Wurzinger, C., 1988: Product quantum yields for the 305 nm photodecomposition of NO_3^- in aqueous solution, *J. Phys. Chem.* **92**, 6278–6283.

Weinstein-Lloyd, J. and Schwartz, S. E., 1991: Low-intensity radiolysis study of free-radical reactions in cloudwater: H_2O_2 production and destruction, *Environ. Sci. Technol.* **25**, 791–800.

Welch, M. J., Lifton, J. F., and Seck, J. A., 1969: Tracer studies with radioactive Oxygen-15. Exchange between carbon dioxide and water, *J. Phys. Chem.* **73**, 3351–3356.

Weschler, C. J., Mandich, M. L., and Graedel, T. E., 1986: Speciation, photosensitivity and reactions of transition metal ions in atmospheric droplets, *J. Geophys. Res.* **91**, 5189-5204.

Wicktor, F., Reese, A., Herrmann, H., and Zellner, R., 1996: Lasergestützte kinetische und spektroskopische Untersuchungen des Br_2^--Radikalanions in wäßriger Lösung, GDCh Umwelt und Chemie, Umwelttagung 1996.

Wilhelm, E., Battino, R., and Wilcock, R. J., 1977: Low-pressure solubility of gases in liquid water, *Chem. Rev.* **77**, 219–262.

Wolke, R. and Knoth, O., 1966: Numerical solution of air pollution models: Aqueous chemistry, *Zeitschrift für Angewandte Mathematik und Mechanik*, Special Issues: ICIAM95, Issue 5: Applied Sciences, especially Mechanics, 551–552.

Zehavi, D. and Rabani, J., 1972: The oxidation of aqueous bromide ions by hydroxyl radicals. A pulse radiolysis investigation, *J. Phys. Chem.* **76**, 312–319.

Zellner, R., Exner, M., and Herrmann, H., 1990: Absolute OH quantum yields in the laser photolysis of nitrate, nitrite and dissolved H_2O_2 at 308 and 351 nm in the temperature range of 278–353 K, *J. Atmos. Chem.* **10**, 411–425.

Zellner, R., Herrmann, H., Exner, M., Jacobi, H.-W., Raabe, G., and Reese, A., 1994: Bildung und Reaktionen von Oxidantien in flüssiger Phase, Final Report, University-GH-Essen, Förderkennzeichen FK 07EU7801.

Zellner, R. and Herrmann, H., 1995: Free radical chemistry of the aqueous atmospheric phase, in R. J. H. Clark and R. E. Hester (eds), *Advances in Spectroscopy, Spectroscopy in Environmental Science*, Wiley, London, Vol. 3, pp. 381–451.

Zellner, R., Herrmann, H., Exner, M., Jacobi, H.-W., Raabe, G., and Reese, A., 1996: Formation and Reactions of Oxidants in the Aqueous Phase, in P. Warneck (ed.), *Heterogeneous and Liquid Phase Processes*, Springer, Berlin, pp. 146–152.

Ziajka, J., Beer, F., and Warneck, P., 1994: Iron-catalysed oxidation of bisulphite aqueous solution: Evidence for a free radical chain mechanism, *Atmos. Environ.* **28**, 2549–2552.

Zimmermann, J. and Poppe, D., 1996: A supplement for the RADM2 chemical mechanism: The photooxidation of isoprene, *Atmos. Environ.* **30**, 1255–1269.